POLITECNICO MILANO 1863

SCUOLA DI INGEGNERIA INDUSTRIALE E DELL'INFORMAZIONE

Executive Summary of the Thesis

Generating stochastic mobility and charging profiles with high technological detail for Electric Vehicle applications

Laurea Magistrale in Energy Engineering - Ingegneria Energetica

Author: Matilde Petris - Lorenzo Villa

Advisor: Prof. Emanuela Colombo

Co-advisor: Francesco Davide Sanvito

Academic year: 2020-2021

1. Introduction

In July 2021 the European Commission presented a new package of proposals called *Fit for 55* highlighting updated strategies to reach the ambitious goal of carbon neutrality by 2050.In particular, the transport sector is at the core of European policies as it accounts itself for 25% of all green house gases emissions.

To reach this goal, the direct electrification of road vehicles can contribute to curb GHG emissions. Such paradigmatic change should be supported by the integration of transport and electricity sectors. Such sector coupling, by means of smart charging strategies such as Vehicle to Grid, can provide the energy systems with the flexibility required by high variable renewable energy penetration scenarios. In order to design the most effective integrated solutions the planning phase is required. Such phase is supported by energy system modelling tools that require time resolved mobility and charging profiles to allow a thorough integration between the demand and supply sides. Yet, providing mobility and charging profiles to energy system modelling framework allows to investigate which strategies or scenarios are more beneficial for the grid, alleviating the surge of electricity demand due to transport electrification. The generation of mobility and charging profiles usually requires empirical data that is rarely available which resolution and spatial coverage might be very limited. Simulation tools are suitable to generate a wide variety of both mobility and charging profiles starting from publicly available datasets. The goal of this work is to revise the major tools available in the scientific literature and test the effect of implementing a refined vehicle consumption model on a selected framework output. The tool will be tested on other structural improvements in order to increase its accuracy.

2. Literature review

A review of the state-of-art of mobility profile generation tools is performed to assess and improve the modelling detail of the consumption estimation methods. Two kind of approaches have been followed in developing mobility time-series models: (i) processing large real-world transport datasets to simulate user behaviour as series of events; (ii) creating curves with bottom-up stochastic simulators starting from aggregated mobility data.

The first approach mostly uses processes based on the Markov chain theory to replicate highly-resolved chains of events requiring abundance of trip records, and generating output with high time and geographical resolution. This extremely data-rich procedure hinders scaling adaptation, limiting the application to countries for which datasets are not available. Fisher *et al.* [2] adopted an inhomogeneous Markov chain approach to model user daily travels. These are derived from a German institution database aiming to produce electric vehicle charging profiles. The same data source is the basis on which Gaete-Morales *et al.* [3] built an open-source tool for generating stochastic mobility profiles. The model, called *Emobpy*, generates trips by means of Monte Carlo simulations. The modelling framework is able to estimate trip consumption thanks to a vehicle dynamic simulator applied to customised driving cycles that are, in turn, derived from the World-wide harmonized Light duty Test Cycle (WLTC).

The second approach focuses on reproducing randomness of user habits, but losing the activity-rich sequence of mobility events. Average trip features are randomized and allocated to users according to general time habits. Decoupling behavioural modelling from event chains allows to extend the methodology to countries with little data availability. RAMP-mobility, introduced in Mangipinto *et al.* [4], grounds on a stochastic core engine to generate Europe-wide mobility and charging profiles. Stochastic bottom-up generation of profiles starts from randomized average trip features assigned to user-specific time windows, from which consumption is estimated with an empirical correlation. A thermal correction, function of the external temperature, is applied to vehicle consumption, and charging profiles are produced from mobility curves considering customizable charging probabilities and strategies. This model is selected for its wide applicability, since it requires general mobility input data. Moreover, it is released open-source and it has been developed by SESAM group of Politecnico di Milano. An in-depth analysis pointed out some limitations in terms of vehicle consumption representation and the sole applicability to electric powertrains. In addition to that, some amendments are applied to better characterize the mobility patterns. Moreover, the validation is extended to different case studies in order to corroborate the validity of absolute value outputs going beyond the already validated dimensionless profiles. Finally, the modelling framework will be tested in terms of effects of increasing the spatial resolution and the detail of vehicle representation.

Existing vehicle dynamic models show similarities in regard to the vehicle dynamics module, differing mainly for the thermal load estimation. The traction power required in each time-step to perform a trip is computed considering equations accounting for aerodynamic losses, rolling resistance, road grade and inertia forces. Vehicle Consumption Assessment Module (VCAM) [5] is the selected model to improve the technological detail of RAMP-mobility and accurately characterize its vehicle consumption representation. VCAM is an open-source high quality model, developed by SESAM group of Politecnico di Milano. The framework is able to simulate both electric vehicles and internal combustion engine vehicles consumption, by considering input driving cycles. For this reason, the refinement of trip-specific consumption in RAMP-mobility requires the generation of customised driving cycles (DCs) to describe the driving session, given the input variables: trip duration and average speed. These can be computed through the synthesis of specific DCs from large trip recordings using Markov chain methods, or starting from a reference driving cycle and adapting its sections to customised trips. This second methodology is chosen to develop a new Driving Cycle Generator tool.

3. Methodology

3.1. Driving Cycles Generator

A specific tool to generate driving cycles (DCs) is developed to create realistic driving patterns given two input parameters: *average speed* and *trip duration*. The methodology followed starts from the World-wide harmonized Light duty Test Cycle (WLTC) in *Figure 1*, and through a cut and paste of the reference cycle sections generates custom DCs. The produced profiles are generated in one of the following driving environments: *Urban*, *Urban-ExtraUrban* and *Urban-Highway*. The different types are simulated according to input velocity and average speed of the reference urban section through

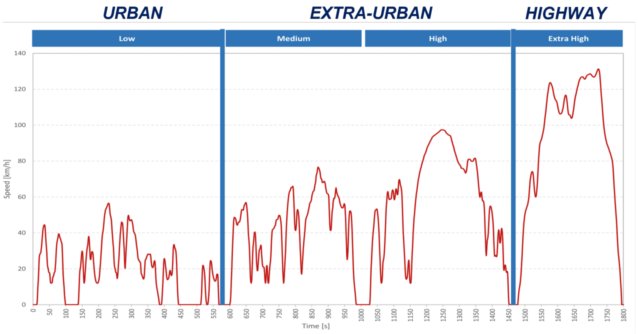

Figure 1: WLTC reference driving cycle divided into three sections: *Urban*, *ExtraUrban* and *Highway*.

the *Urban Share* reported in *Equation 1*. An overview of the methodology followed is reported in *Figure 2*, highlighting the insertion of initial and final urban in all DCs to simulate smooth driving behaviors. Transitions are added to limit deceleration values at the end of each section, and profile rescaling is applied to match the input average speed.

$$US = \frac{\overline{v} - \overline{v}_{extraurban}}{\overline{v}_{urban} - \overline{v}_{extraurban}} \quad (1)$$

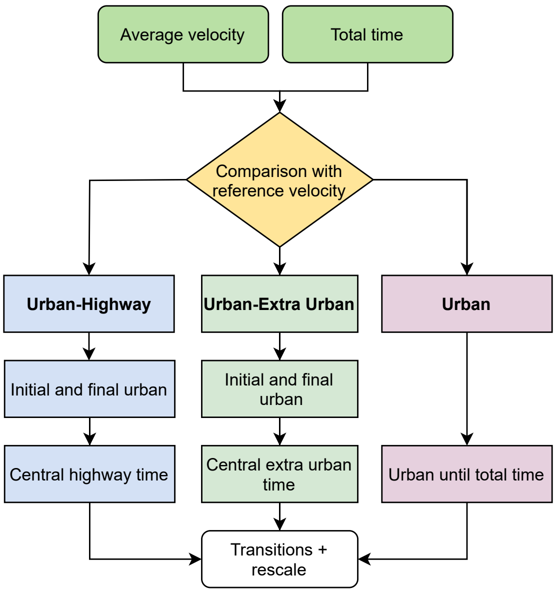

Figure 2: Conceptual scheme of the Driving Cycle Generator tool functioning.

Examples of the produced driving cycles are reported in *Figure 3* where the different *Urban Shares* affect the length of initial and final sections. An exception is highlighted in the last driving cycle where a different approach is adopted for the central highway section to avoid unrealistic start-and-stops. Velocity values are selected according to a transition probability matrix derived from the *WLTC extra-high* section, and which contains, for each value of velocity, the probability to have another value in the following time step; this process recalls the one used in Markov chains.

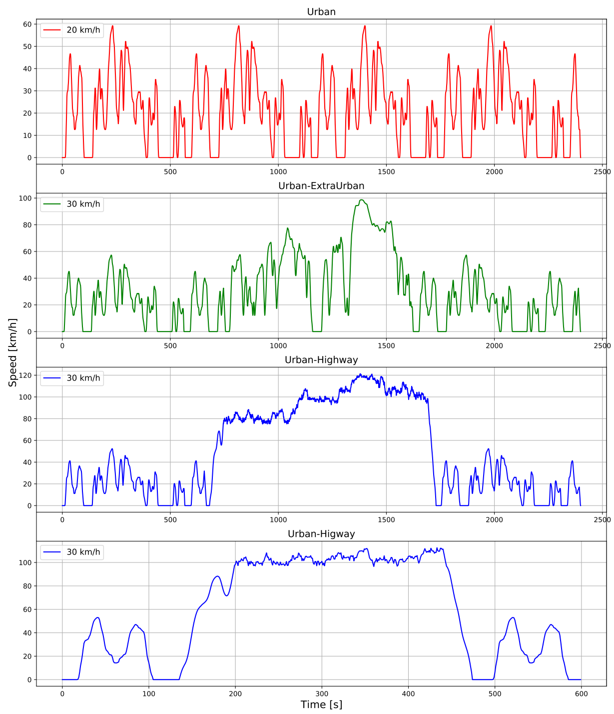

Figure 3: All possibilities of driving cycles generated.

The generated driving cycles have features which make them realistic. Firstly, they are characterized by soft starting and ending sections; secondly have final velocity always set to 0 km/h; then the highway environment has never unrealistic start-and-stops, and lastly the acceleration and deceleration are controlled and limited to 2 m/s^2.

3.2. RAMP-mobility improvements

RAMP-mobility is composed of two modules: *mobility* and *charging*. The examination of the first one pointed out a simplified estimation of vehicle consumption compared to the approach found in the literature. This work is focused on the implementation of a trip specific consumption, and on the substitution of the empirical correlation with a vehicle dynamic simulator as consumption model. RAMP-mobility defines trips in time domain, hence to apply the trip specificity an average trip speed is associated through the introduction of empirical distributions, assessed from a trip records database. Therefore, each trip is linked to a specific driving cycle generated with the developed tool using the same couple of key features: *duration* and *average speed*. Once the trip modelling is improved, the associated driving cycle is simulated in VCAM, and an average consumption value is obtained. The coding implementation is optimized adopting double-entry consumption tables, previously computed, from which RAMP-mobility selects values of average power at given couples of parameters.

Since minor inconsistencies were found in the model, other two structural corrections are introduced: functioning windows complementary definition, and skipped distance recovery. Functioning windows are time frames in which mobility events occur, and are divided in *Main* and *Free Time* to highlight daily main hours for trip occurrence. Only *Free Time* windows extremes are defined applying the input variability, while *Main* windows are mirrored; this correction prevents voids and overlapping periods. Distance recovery is introduced to solve incoherence between average daily distance given as input and simulated one. This is caused by the stochastic occasional use variable, that models the contingency of driving in a day. The mechanism introduced reassigns not-driven distance of *Free Time* windows to *Main* periods respecting the total average distance.

For what concern *charging* module strong modelling uncertainties, hard to be tackled, are detected in the implementation of charging probabilities, which aim to model the infrastructure availability and the user plug-in decision. The infrastructure availability is modelled with a piecewise function, which is improved in this work adding weekend specific time parameters. An additional output is added in RAMP-mobility *charging* module, to determine connection time-series, which are fundamental to analyze the potential of V2G technology.

4. Case studies

The impact of the improvements have been assessed applying the model to two case studies: *Italy*, for which the majority of mobility data are updated, and *The Netherlands*, for which default data are slightly adjusted. New regional data sources from Istat are used to shape Italian mobility. Most relevant upgrades are the lower daily average distance and the six-segment vehicle fleet representation. The processing of a commuting trip register produces the duration-velocity relationships used to link trip features; this new input is also extended to other European countries. Three steps are applied to show the effect of each improvement: *Mobility behaviour* in which functioning windows definition and distance recovery are introduced; *Trip-specific consumption* that implements the trip linkage with DC; and *Vehicle consumption model* applying VCAM to each DC.

5. Results

The results for Italy, introducing the described improvements, are compared in terms of average mobility profiles and transport energy demand. In *Figure 5*, the impact on the demand for each day type is reported highlighting an overall increase of 30% with respect to *Reference* case. This rise is caused by the distance recovery mechanism and is mitigated by the new consumption evaluation method, which is proved to slightly reduce the power demand. The less evident effect on weekends, visible also on mobility profiles in *Figure 4*, is a consequence of a lower distance recovery, caused by different occasional use values. The reduction of energy demand is however compensated by higher profile peaks for weekdays. The introduction of trip specificity not coupled with an appropriate consumption model, produces a further 60% increment, proving that transport demand is highly sensible to the consumption evaluation method.

Analyzing the number of users simultaneously connected to the grid derived from the improved charging module, user charging behaviour is an important limit for the V2G implementation reducing the available storage, while the impact of a varied infrastructure availability during the day is less evident. However, infrastructure availability has to be carefully modelled since it causes charging coincidence and creates spikes in the profiles. This analysis has been carried out without changes of the Italian infrastructure availability and of the behavioural function, thus

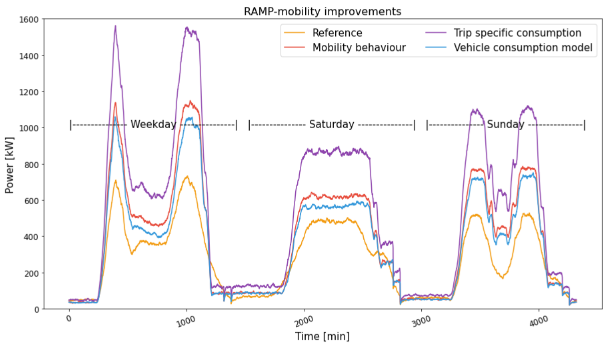

Figure 4: Profile comparison of all the implemented cases.

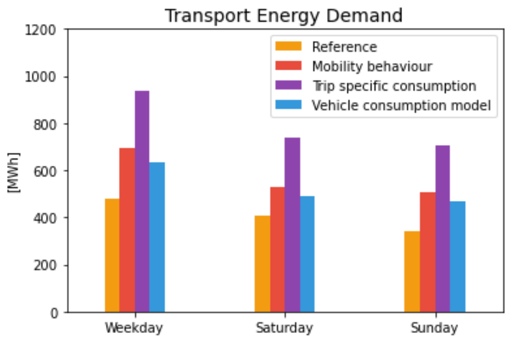

Figure 5: Comparing total transport demand of all the implemented cases.

the accuracy of this conclusion is limited and could be further investigated.

6. Model quality assessment and sensitivity

The updated RAMP-mobility has been assessed to evaluate its quality in both mobility and charging modules.

6.1. Mobility module

Measured mobility profiles are not available hence the accuracy of this output is assessed considering aggregated data. The first approach, followed for European countries, refers to annual vehicle kilometers derived from Eurostat databases of passenger kilometers. A range of distance is determined considering extreme values of car occupancy rate, and the results reported in *Figure 6* are in the selected range for most countries. The second approach, used for Italian mobility, adapts RAMP-mobility to model conventional vehicles from which the annual liters of petroleum consumed are computed. This value is compared with measured one de-

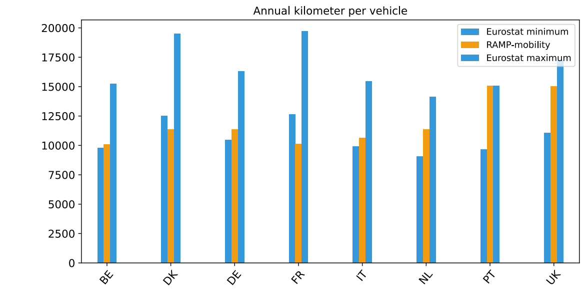

Figure 6: RAMP-mobility annual vehicle kilometers for selected countries and the *Eurostat* minimum and maximum values.

rived from oil bulletins, and a good accuracy is reached with national relative error of 12%.

6.2. Charging module

The charging module has been assessed with *ElaadNL* measured data for The Netherlands, collecting information regarding charging transactions. The collected data have been processed by Beltramo *et al.* [1] to generate the yearly charging profile. RAMP-mobility input data have been corrected accordingly, to simulate conditions similar to the context of empirical data. The quantitative parameters selected to estimate the accuracy of the model are two statistical values: the *Normalized Root Mean Square Error (NRMSE)* and the average *Load Factor (LF)*, defined in *Equations 2* and *3*. The NRMSE is used to evaluate the difference point by point between simulated and measured data, and is applied to both the charging time-series and the load duration curve. The average LF represent the variability inside the charging demand between daily peak power consumption and daily average one, highlighting the differences in profile shape. It is computed for both profiles considering an hourly-resampled time-series to smooth possible short steep peaks, and the comparison is assessed in terms of relative error.

$$NRMSE = \frac{\sqrt{\frac{\sum_{x}^{N_t}(P_{model}(x)-P_{measured}(x))^2}{N_t}}}{P_{measured,max} - P_{measured,min}} \quad (2)$$

$$\overline{LF} = \sum_{d=1}^{365} \frac{P_{average}(d)}{P_{peak}(d)} \cdot \frac{1}{365} \quad (3)$$

Different cases have been analyzed in relation

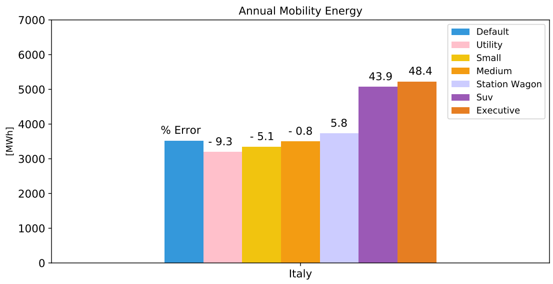

Figure 7: Annual mobility energy for the simulated cases for Italy.

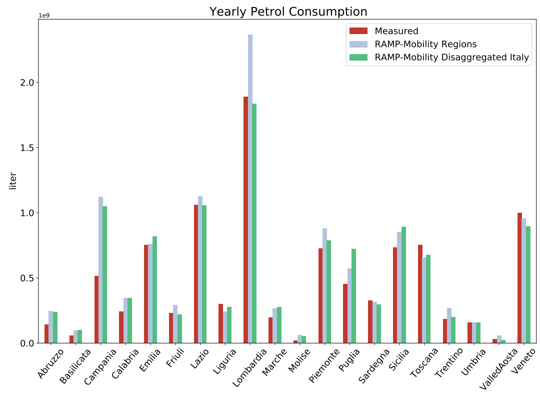

Figure 8: Comparison of annual petrol consumption.

to the charging probability parameters, introducing the improvement concerning the specific *Weekend* function. These parameters have been tuned to reach better results concerning the validation metric, which have then been compared with those reported by Mangipinto *et al.* [4], finding similar NRMSE, and a 10% decrease of the LF error. A sensitivity analysis is performed using the same metric to assess the impact of variability parameters. Only weekend occasional use modify the profiles due to the incomplete distance recovery.

7. Model testing

Further analysis aiming to test input data dependence and modelling resolution are performed to provide additional insights for future works. The most impacting data is the driving distance, that causes an important variation of demand if changed. A six-segments vehicle fleet characterization has been tested, and two conclusions have been drawn. Firstly, only two reference classes are needed to represent the whole country fleet since consumption of different segments are clustered into two groups as displayed in *Figure 7*. Secondly, with the actual vehicle share the impact of larger vehicles is negligible and the adoption of a single-segment fleet causes marginal errors lower than 5% if a *Medium* reference vehicle is selected.

The availability of regional datasets is finally exploited to test the effect of a higher geographical resolution. Italian regions are simulated and compared with annual regional petrol consumption values; the same approach is followed distributing the demand of the country simulation according to population weights. The single region approach leads to a higher error around 19%, compared to 11% for the national simulation, mainly due to *Lombardia* and *Campania* as showed in *Figure 8*. In conclusion, the worst overall accuracy and the higher computational effort result in a limited utility of the regional characterization.

8. Conclusions

The updated RAMP-mobility developed with this work solves some inconsistencies of the original framework as the definition of functioning windows and the inconsistency between input and output average daily distance. Therefore, a more accurate and realistic model is created, and the coupling with the consumption model VCAM allows to increase its technological level of detail. The global impact of these variations produces an annual transport energy demand 30% higher than the *Reference* case, thus the consumption estimation has to be carefully modelled seen the influence on the aggregated mobility profiles.

Input data has been proven to have great leverage on RAMP-mobility output, thus finding reliable sources and refining their processing enriches the quality of the results. This could be object of further investigation for other European countries, together with the charging module as some limits have been found during its analysis. Efforts to improve charging probabilities are necessary in future works seen the high level of uncertainty in their definition, and a country detailing should be considered, adopting a common method to determine these values.

References

[1] Agnese Beltramo, Andreea Julea, Nazir Refa, Yannis Drossinos, Christian Thiel, and Sylvain Quoilin. *Using electric vehicles as flexible resource in power systems: a case study in the Netherlands. International Conference on the European Energy Market, EEM*, July 2017.

[2] David Fischer, Alexander Harbrecht, Arne Surmann, and Russell McKenna. *Electric vehicles' impacts on residential electric local profiles – A stochastic modelling approach considering socio-economic, behavioural and spatial factors. Applied Energy*, 233-234:644–658, January 2019.

[3] Carlos Gaete-Morales, Hendrik Kramer, Wolf-Peter Schill, and Alexander Zerrahn. *An open tool for creating battery-electric vehicle time series from empirical data – emobpy. Scientific Data*, April 2020.

[4] Andrea Mangipinto, Francesco Lombardi, Francesco Sanvito, Sylvain Quoilin, Matija Pavičević, and Emanuela Colombo. *RAMP-mobility: time series of electric vehicle consumption and charging strategies for all European countries.* doi: 10.13140/RG.2.2.29560.26880, 2020. *Unpublished.*

[5] Francesco Sanvito, Michele Ferraro, Riccardo Mereu, and Emanuela Colombo. *Improving electric vehicle consumption representation in energy system modelling: the impact of temperature in all European countries.* doi: 10.13140/RG.2.2.26325.35046, October 2020. *Unpublished.*

POLITECNICO
MILANO 1863

SCUOLA DI INGEGNERIA INDUSTRIALE
E DELL'INFORMAZIONE

Generating stochastic mobility and charging profiles with high technological detail for Electric Vehicle applications

Master of Science Thesis in
Energy Engineering - Ingegneria Energetica

Authors: **Matilde Petris**

Lorenzo Villa

Students ID: 10530300 - 10527480
Advisor: Prof. Emanuela Colombo
Co-advisors: Ing. Francesco Davide Sanvito
Academic Year: 2020 - 2021

Abstract

In the context of decarbonization strategies, the electrification of the transport sector is crucial to reach the announced European goals in the framework of the European Green Deal. Sector coupling is considered a solution to reduce emissions and to provide the flexibility required by an energy system characterized by high share of renewable energy sources. To accurately consider the transport sector load, profiles describing its influence on the energy system are needed. However, seen the limited accessibility of measured data concerning electric vehicles load curves, simulated hourly demand profiles are crucial. In particular, realistic curves with high temporal and spatial modelling resolution are required to plan grid capacity expansion and to optimize the energy dispatching. Therefore, the open-source RAMP-mobility model, which simulates mobility and charging profiles for 28 European countries, has been analyzed in detail and improvements have been proposed to increase the technological detail of the modelling structure. The key enhancement introduced is the coupling with the vehicle dynamic simulator, VCAM, for the estimation of trip-specific consumption. The development of a Driving Cycle Generator tool is required to characterize trips with realistic driving patterns, obtained from WLTC reference cycle. The updated RAMP-mobility model is compared with different set of measured data to test both mobility and charging modules. A better degree of accuracy is reached, with a higher precision of produced results with respect to the original model. Modelling insights are deduced highlighting the importance of vehicle consumption estimation, which varies considerably the annual transport demand. Moreover, regional characterization and vehicle fleet detailing do not affect the transport demand, hence to an increased model complexity does not correspond variation of result. In conclusion, the updated model produces a grid connection time-series which is used to assess the impact of user behavior on Vehicle to Grid (V2G) technologies.

Keywords: Electric vehicles, Mobility time-series, Charging time-series, Energy system modelling, Driving cycles, Vehicle consumption models.

Sommario

Nel contesto delle strategie di decarbonizzazione, l'elettrificazione del settore dei trasporti è essenziale visti gli obbiettivi annunciati dall'Unione Europea con il Green Deal. L' interconnessione dei settori economici è considerata una soluzione per ridurre le emissioni e creare la flessibilità richiesta in un settore energetico caratterizzato in ampia parte da rinnovabili. Per poter considerare l'impatto dei trasporti è necessario determinare profili di carico che ne descrivano l'interazione con il sistema energetico. Tuttavia, vista la limitata disponibilità di dati empirici, è fondamentale avere modelli per simulare la domanda oraria di un insieme di veicoli elettrici. In particolare sono necessari consumi realistici ad alta risoluzione temporale per pianificare lo sviluppo della rete e ottimizzare la distribuzione dell'energia. Pertanto il modello *open-source* RAMP-mobility, capace di simulare la domanda di mobilità e di ricarica di una flotta di veicoli elettrici in 28 paesi Europei, è stato analizzato e migliorato per aumentarne il dettaglio tecnologico. L'avanzamento principale introdotto in questa tesi è l'utilizzo di un modello di simulazione dinamica del veicolo, VCAM, per stimare il consumo energetico di ogni spostamento. Per rappresentare realisticamente gli spostamenti, è stato sviluppato uno strumento per la creazione di percorsi di guida specifici a partire dal driving cycle di riferimento WLTC. La nuova versione di RAMP-mobility è stata confrontata con dati empirici per valutarne le capacità di rappresentazione della domanda di mobilità e di ricarica. È stata raggiunta una migliore accuratezza, e i risultati prodotti hanno dimostrato una maggior precisione rispetto alla versione originale del modello. Conclusioni di tipo modellistico sono state tratte dalle simulazioni effettuate evidenziando che il maggior dettaglio tecnologico di consumo ha un impatto significativo sulla domanda di mobilità. Caratterizzare regionalmente il modello e rappresentare più nel dettaglio i veicoli di una nazione non variano la domanda di mobilità, pertanto al modello più complesso non corrisponde una variazione dei risultati. Infine è stato prodotto un ulteriore profilo che descrive le connessioni alla rete elettrica, necessario per valutare l'impatto del comportamento degli utenti sulla tecnologia V2G.

Parole chiave: Veicoli elettrici, Profili di mobilità, Profili di ricarica, Modellazione di sistemi energetici, Driving cycles, Modelli di consumo per veicoli.

Contents

Introduction

The context of this work is the transport sector, in particular the electric mobility seen its fast growing. Measured databases for European countries on electric vehicle mobility demand are not available, as this technology is still in an early adoption phase. For this reason, tools able to describe how the driving population behaves in different European countries are of major importance.

With this thesis work the authors aim to improve the modelling accuracy of the transport sector, allowing the estimation of more precise electric vehicles load profiles. The selected open-source model is RAMP-mobility, which is characterized by high temporal detail for 28 European countries. It relies on traditional mobility data, time-related user habits, population and vehicle fleet composition. The input data refers to traditional mobility, since these are more representative of the whole drivers behaviour compared to electric mobility data. Therefore, the electric vehicles drivers' are assumed to behave similarly to those of conventional ones. The produced output consists of mobility demand time-series, simulating the power supplied to the EV battery, and the related charging demand based on customizable parameters concerning the charging process.

Load curves describing electric vehicles charging demand are of major importance for energy system models to analyze the impact of transport on the power sector. The coupling of transport sector to the one of energy is important to allow its decarbonization, as it accounts for a large share of European greenhouse gases emissions. Additionally, significant advantages could be derived from this integration in terms of further flexibility offered to the grid through smart charging strategies and Vehicle to Grid (V2G) technologies. Grid connection time-series is added as output of the charging process to assess the impact of charging probabilities on grid flexibility operations.

The structure of this work is here reported:

- *Chapter 1* describes the European context focusing on the transport sector and its coupling with the energy sector.
- *Chapter 2* provides a literature review of electric vehicles load profiles modelling and vehicle consumption models to assess how other works deal with vehicle consumption estimation, and which improvements could be introduced in RAMP-mobility.
- *Chapter 3* presents the methodology followed to upgrade RAMP-mobility structure and to develop a new tool for *real-world* driving cycles generation necessary to improve the technological detail of RAMP-mobility consumption model.
- *Chapter 4* presents two case studies describing the data adopted to apply RAMP-mobility simulating Italy and The Netherlands.
- *Chapter 5* is dedicated to the presentation of the results. Firstly, examples of the driving cycles generated with the tool are illustrated. Then, the step-by-step implementation of the improvements to RAMP-mobility is showed for Italy and The Netherlands, comparing steps in terms of mobility time-series and energy demand. Finally the charging results for the grid connection analysis are reported.
- *Chapter 6* presents the methodology and the results of the model quality assessment of the updated RAMP-mobility, for both mobility and charging profiles.
- *Chapter 7* assess the impact of input data changes on mobility profile and annual energy demand, with particular attention to the detail of the vehicle fleet composition, and lastly the effect of increased geographical resolution is analyzed.
- *Chapter 8* concludes the work highlighting the main outcomes and discussing the possible future developments of the research.

An overview of the entire work is reported in *Figure 1* highlighting the main steps followed.

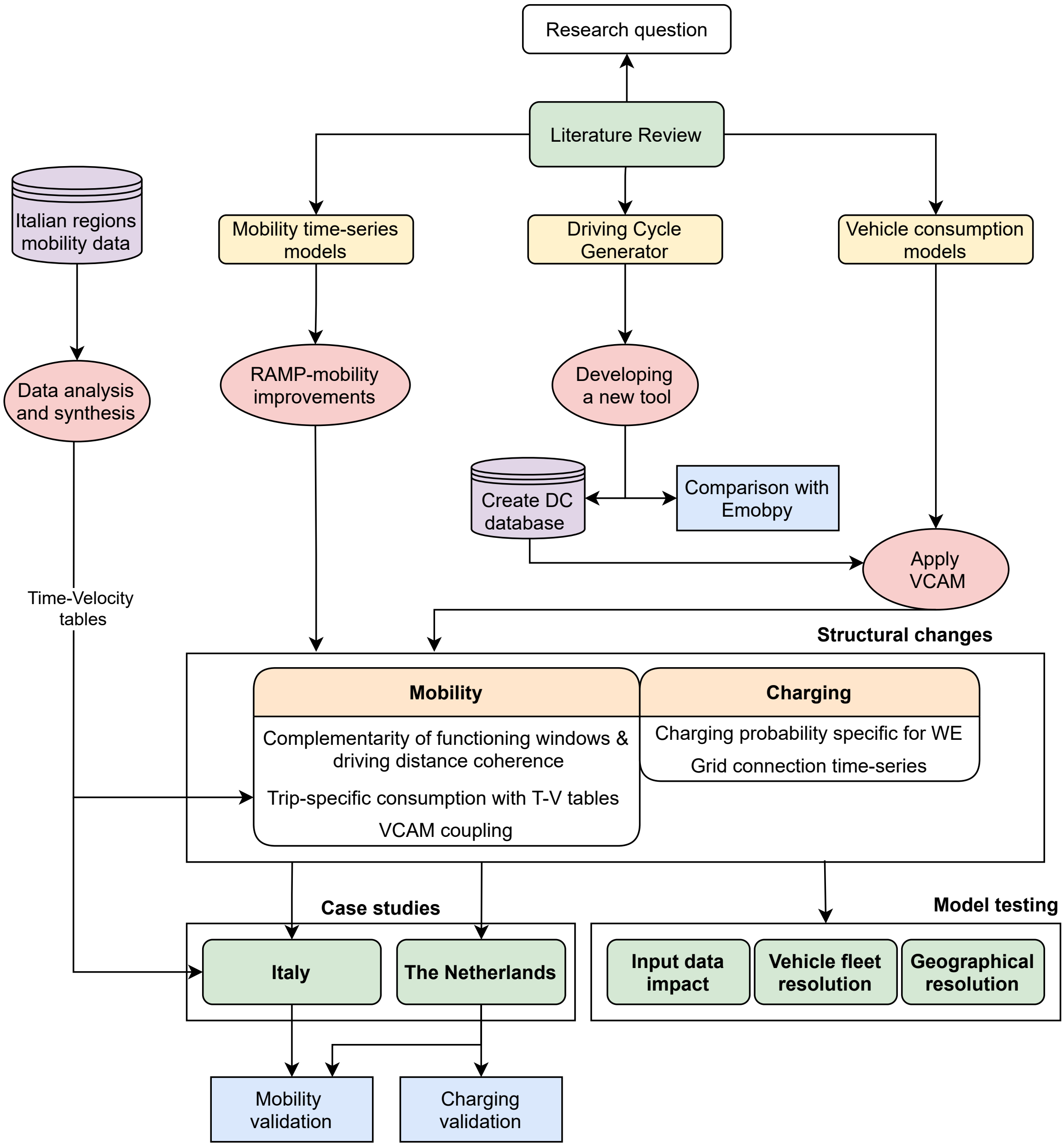

Figure 1: Scheme of the thesis structure.

1 | The Context

1.1. The transport sector in the European framework

In July 2021 the European Commission presented a new package of proposals called *Fit for 55* containing the strategies to make the European *Green Deal* a reality and achieving the goal of world's first climate-neutral continent by 2050. During the presentation speech, the President of the European Commission Ursula von der Leyen, as already declared in 2019 with the *Green Deal* [7], stressed out the commitment to reach a decarbonized economy:

> *"The fossil fuel economy has reached its limits. We want to leave the next generation a healthy planet as well as good jobs and growth that does not hurt our nature. The European Green Deal is our growth strategy that is moving towards a decarbonised economy."* [8]

In particular, the transport sector is at the core of European policies since alone it accounts for 25% of all EU greenhouse gasses (GHG) emissions, second only to power generation [6]. The *Fit for 55* includes different measures to tackle directly the transport sector and its rising emissions. In this package of proposal the introduction of a new emission trading system specific for this sector is highlighted and the ambitious target of reducing the emissions of new cars by 55% in 2030 and 100% by 2035, compared to 2021 values, is set. Consequently, all new cars in 2035 will be zero-emission and electric mobility offers a significant contribution in this direction. This radical change will require an important expansion of the charging infrastructure in the coming years to ensure that electric vehicles reach the same flexibility of use of fuel-powered ones. This expansion will bring huge business opportunities, but also critical technical challenges. [8]

Focusing on passenger cars, they are responsible for about 12% of all GHG emissions in the European Union, meaning that switching sales of new vehicles to fully electric ones is crucial to meet the decarbonization targets for the transport sector. Looking at sales trends, EVs are gaining market shares faster than previously expected, reaching in Europe the 10.5% of new sales and dropping the average CO_2 emission of new cars by 12%. [34] This soaring will allow car-makers to drop their production costs by exploiting scale effects and developing dedicated platforms optimized for BEVs production. According to a *BloombergNEF* study [4], all vehicle segments will reach price parity by 2026; even considering the worst raw material price scenarios, the projections are shifted onward of no more than two years, leading to an affordable electric mobility well before than policy requirements. The economic driver is even more impacting if the total costs of ownership are considered. EVs have indeed much lower operating costs, leading to benefits for drivers with higher annual mileage, that can anticipate the forecasted transition based on price parity considerations. In this context important car-makers such as *Volvo*, *Ford Europe* and *General Motors* have already pledged to phase out internal combustion engines by 2035, followed by *Volkswagen* and *Peugeot* willing to end investments in conventional vehicles and the development of new models. [35]

1.2. Transport sector coupling

Seen the major role of the transport sector in GHG emissions, its coupling is fundamental to allow the reduction of pollutants. This means demand electrification and production of clean alternative fuels, as green hydrogen or more generally e-fuels, connecting the transport sector to renewable energy sources. Considering electric vehicles, the expected increase of EVs market share in the coming years points out the need to satisfy the consequent increase in electricity demand through renewable energy sources (RES) to reduce the CO_2 emissions, thus promoting the phase out of conventional power plants. However, RES supply is affected by intermittent renewable resources which increase the difficulties in managing grid stability and cause challenges in keeping the balance between electricity demand and supply. Traditionally this equilibrium is controlled with a portfolio of different power plants, which provide the required flexibility through frequency control of electric machines, that is more complex to be managed with RES generators and not economically viable. Therefore, with the increase of renewable share, new kind of flexibility measures based on fast storage solutions are needed to avoid mismatches between demand and supply and consequent blackouts. [23]

As mentioned, electric vehicles diffusion lead to the increase of electricity demand, but can also be beneficial for the electric grid by providing a large storage capacity. This could be used to increase the flexibility of the system enhancing the so-called Vehicle to Grid (V2G) concept. Vehicles are parked most of their time for about 10 hours a day, while the charging window is limited to a much shorter time, hence offering significant elasticity in decoupling the transport demand from the electricity one. Smart charging strategies could exploit this flexibility maximizing the storage potential and providing services like local energy balance, frequency control and reserve power to the Transmission System Operator (TSO) that controls the grid. To take advantage of this technology suitable equipments are necessary, as telemetry and two-way communications, together with a massive number of aggregated users to achieve the required scale [23]. V2G technologies allow for bi-directional energy exchange between vehicle batteries and the grid, which can be managed in relation to renewable power generation, and significantly reduce the level of curtailment [32]. Despite these advantages, V2G operations through fast charging and discharging events could create degradation problems on EVs batteries, hence introducing the need of a trade-off between flexibility services offered to the system and battery lifetime. [37]

To understand how electric vehicles and the power grid could be coupled together through V2G technology and smart charging strategies, an accurate representation of mobility profiles and the related charging demand is required. Starting from real input data and through a precise estimation of vehicles consumption, the mobility pattern of a user sample can be modelled. Knowing the mobility demand it is possible to manage the charging events for flexibility purposes providing the TSO with the services previously mentioned. It is important to stress out the attention on the user travel pattern which has to be kept independent from these operations, hence exploiting batteries flexibility without affecting user behavior.

This thesis work fits in the context described above and aims to improve existing modelling tools by increasing output accuracy and technical aspects. These tools consider user habits and mobility statistics, to generate driving patterns from which grid connection time-series, consumption profiles and charging demand are determined. These time-series are fundamental inputs for energy system models, which are used for capacity planning and operational optimization. Therefore, producing more detailed and realistic profiles of EVs electricity demand could help in designing new infrastructure, as well as in evaluating the potentialities of smart control technologies to define future strategies for the energy sector.

2 | Literature Review

The overall objective of this work is to design a tool which considers human driving habits to produce mobility and charging time-series with high technological detail and with accurate vehicle consumption estimations. Therefore, through variation of input parameters more accurate scenarios can be simulated. The selected starting model is RAMP-mobility which includes all the required features, relies on easily accessible data, is able to simulate 28 European countries, and has been developed by SESAM group of Politecnico di Milano. A review of the models available in literature is performed to assess strengths and weaknesses of the approaches used in other modelling works, and to find possible improvements for the selected model. Firstly, models for electric vehicles mobility profile are reviewed, with a focus on RAMP-mobility [25]. Secondly, vehicle consumption models are analyzed with particular attention to Vehicle Consumption Assessment Model (VCAM). As last step, the coupling of mobility profiles and vehicle consumption models is assessed considering the methodologies found in the literature.

2.1. State of the art: mobility time series models

Various models can be found in the literature modelling the impact of electric vehicles mobility and the related charging demand, mainly relying on stochastic processes able to reproduce EVs users behaviour. In this section the review is focused on models producing mobility time-series.

2.1.1. Overview of existing models

One of the first models elaborated back in 2013 by the Joint Research Center (JRC) [31], aimed to build a database of load profiles for EVs in six European countries, taking data from the behaviour of conventional car drivers. The driving patterns are collected through sample travel surveys obtaining a 5-minute temporal interval series which describe the car status: *driving* or *parked*. Another element taken from surveys is the average speed of the trip associated to each driving period. The amount of electricity consumed during driving periods is estimated as function of the EV type and the aforementioned travel speed. A speed-dependent quadratic function specific for three different vehicle types classified as *Small*, *Medium*, and *Large*, is used to calculate the power consumption based on the vehicle speed. The correlation between velocity and power elaborated by the JRC is represented in *Figure 2.1*, where the different types of vehicles are highlighted. This consumption model based on an empirical correlation is the same introduced in RAMP-mobility described in *Section 2.1.2*.

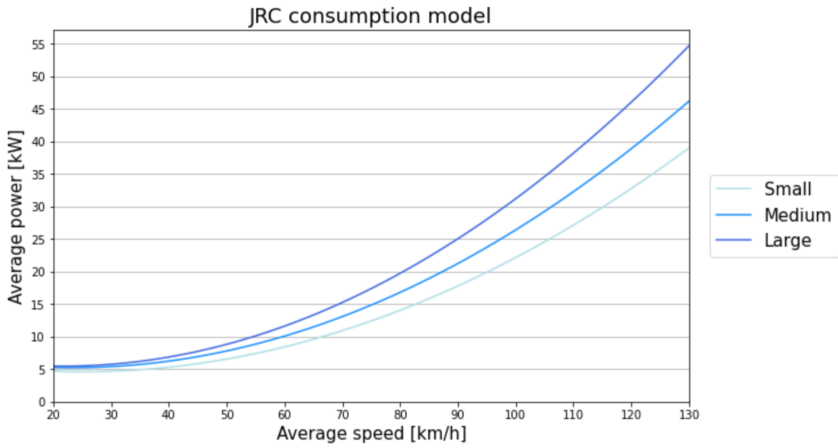

Figure 2.1: Estimated quadratic speed-dependent energy consumption curves. [31]

Once the energy consumption is defined the electricity requested from the grid during parking periods is estimated under certain assumptions. These are related to: home charging always available, reduced recharge rate when close to the full capacity, and minimum threshold of 30 minutes to identify parking periods in which charging is possible.

Another approach commonly used in literature is the Markov-chain. Fischer *et al.* [10] in 2018 implemented a stochastic bottom-up model to assess EVs load profiles with the innovative consideration of socio-economical, technical and spatial factors which influence the charging electricity demand and behaviour. The work has been developed starting from the analysis of a large dataset on mobility behaviour in Germany, *Mobilität in Deutschland (MID)* [28]. An in-homogeneous Markov chain is used to sample a series of car trip destinations in relation to factors as the car driver occupation, the day of the week and the time of the day. The travel destinations are classified as inside town, outside town, workplace and home. The related trip distance, together with driving duration and parking time, are estimated trough a probability distribution obtained from the huge MID dataset which collects 70000 car trips. Socio-economic considerations are used to estimate the number of cars per households, the first daily departure time and parking duration when at workplace. Knowing trip kilometers, driving time and parking length, the presence at a charger can be estimated and the related electricity demand is calculated. It is important to highlight that high detail on demographic aspects is considered in this model using a logistic function which introduces the driver sensitivity towards battery State of Charge (SOC), reported in *Figure 2.2*.

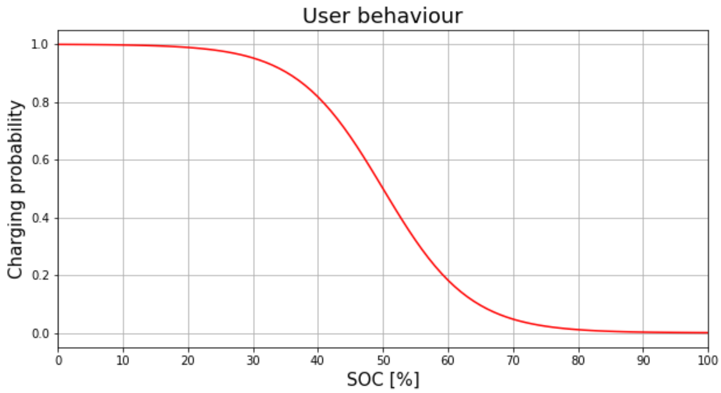

Figure 2.2: User behaviour logistic function introduced by Fisher *et al.* [10].

Assessing the energy consumption of transportation in the United States of America (USA) is the goal of Muratori *et al.* [29]. The method used to generate a realistic picture of the transportation demand is based on a behavioural model, built following a Markov chain approach applied to time use data from *The American Time Use Survey (ATUS)*. Starting from this dataset and focusing on three different states (*home, work, away*), the transition probabilities have been assessed and used to model the Markov chain-based activity pattern generator. Once driving diaries are obtained for each user, the mobility patterns are divided between commuting to work and trips for leisure. To characterize the home-work commuting trips, a distribution of typical mileage from a statistical data report is used, while for leisure times the trip duration is estimated as a random fraction of the away-state window length. The coupling of the time behavioural model and the statistics about trips produces the driving pattern key parameters used to generate a realistic velocity profile for each trip, named driving cycle. Trips are characterized either by duration, for leisure purposes, either by distance, for work commuting, and a specific driving cycle is generated for each trip. A vehicle dynamic simulator model computes the consumption of the trips that occurs in the user driving diary. The population is externally determined and differentiated between worker/non-worker, and male/female.

Two open-source python models focused on EVs energy consumption have been recently published and regularly updated: *Vehicle Energy Consumption in Python (VencoPy)* and *Emobpy*. They both assess charging profiles for EV fleets with assigned characteristics starting from national travel surveys and trips datasets. Their current versions are based on the aforementioned German national survey MID. Starting from large amount of travel data *VencoPy* filters and rearrange the collected trips to obtain person-specific travel diaries, while *Emobpy* generates stochastic day tours applying Monte Carlo simulations to the probability distributions obtained from the dataset. Their common feature is the need of large amount of mobility-specific data to assess the transport demand, leading to country specific applications.

The *VencoPy* tool presented in Wulff *et al.* [39] exploits the whole potential of highly detailed mobility survey results, which can guarantee high temporal and geographical resolution. The mobility demand is assessed firstly with an analysis of the dataset, that filters and cleans the information of each reported trip. Afterword, all the trips are reformatted in hourly profiles and merged into personal daily travel diaries, according to distance driven and trip purposes. The time between two trips is considered for the charging availability, while the SOC of the vehicle is computed assuming a constant kilometer-specific electricity consumption. At the end of the mobility section two databases are generated collecting the mileage travel diaries and the type of parking derived from the travel purpose. The tool is further developed to address the estimation of the available flexibility given by different charging strategies and scenarios. The main limit is the specificity of the required trip dataset, which is hardly found for countries different from Germany.

The stochastic open-source model *Emobpy* [11] grounds on empirical mobility statistics from MID, vehicle specifications and customizable assumptions as inputs. Inputs and outputs for *Emobpy*, and the sequence of generated time series is reported in *Figure 2.3*. The output results are four time series and major attention is given to the mobility demand profile:

- Vehicle mobility contains the location of vehicles and the distance travelled at each time step. This time series has a spatial characterization considering six different trip destinations: workplace, home, shopping, leisure, errands and escort. Other data related to trip departure hours, minimum and maximum time at a given location, trips per day and trip characteristics are considered, all information specific for driver types: commuter or non-commuter. To ensure variability of profiles, a Monte Carlo approach is used.
- Driving electricity consumption time series provides information on the electricity taken from the battery while driving. This requires inputs as vehicle specific characteristics, ambient temperature and driving cycles, which are the main parameters

used to describe drivers' behaviour. This part will be analyzed more in detail in *Section 2.2* dealing with vehicle consumption models.

- The third time series is the grid availability which provides information whether a vehicle is connected to the grid in a time step and with which power. Charging power capacities and charging infrastructure are the main inputs and the variability is obtained through a Monte Carlo approach.
- Grid electricity demand is the last time series containing the information on the electricity needed from the grid at each time step. Different charging strategies can be simulated or even customized by the user.

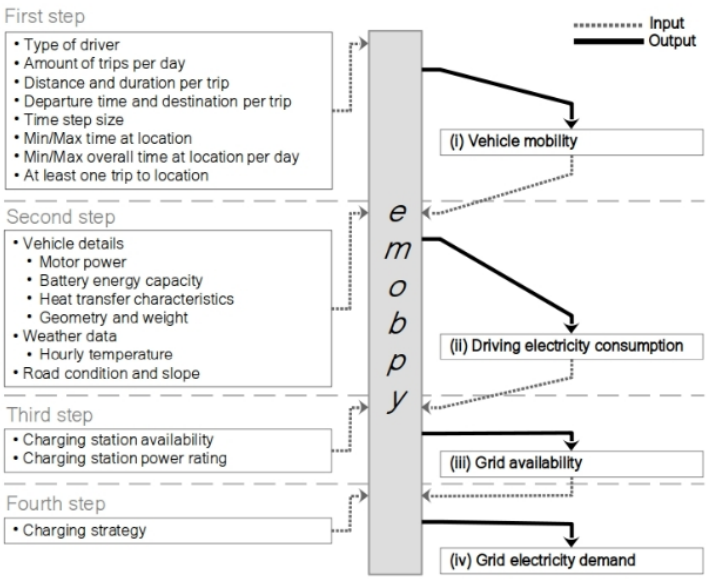

Figure 2.3: Inputs and outputs and the sequence of generating the four time-series. [11]

This model presents important improvements related to spatial characterization, detailed user behaviour, accurate vehicle consumption, temperature effects on electricity consumption profiles and the possibility of customization. However, limits can be found in its validation, which is not clearly presented, and in the data used which are specific for German mobility.

Both *Emobpy* and *VencoPy* require huge datasets describing the mobility to create the chain of states which are country specific, hence limiting the use of the model in other countries where specific data are hard to gather. For this reason, a different approach is adopted in RAMP-mobility model relying on easily accessible data as population composition, vehicles share and aggregated mobility statistics.

2.1.2. RAMP-mobility

RAMP-mobility [25] is an open-source model accessible at the following GitHub repository: https://github.com/RAMP-project/RAMP-mobility. This model builds on a previous work for stochastic load simulations developed by the SESAM group, RAMP [22], able to generate demand profiles based on simple time-of-use information specific for different user types in 28 European countries. In RAMP-mobility additional information is considered as vehicle fleet composition and driving specific parameters. It is made of two subsequent simulation models reported in *Figure 2.4*: the mobility pattern and the charging profile. The mobility pattern generates profiles for each user with one-minute resolution, which are used as input for the second simulation that produces the corresponding charging demand. This is function of other parameters as the charging strategy adopted and the information about the charging infrastructure.

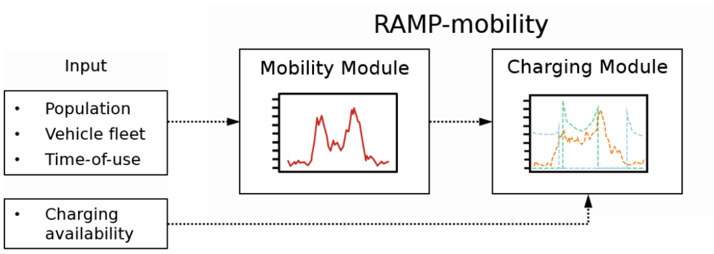

Figure 2.4: Conceptual scheme of the overall model structure composed by two separated modules. [25]

To obtain the mobility pattern simulation, different inputs are considered. The country-specific population share divided into three users' categories *(Workers, Students, Inactive)* is used to split the 2500 representative total users simulated for each country. The individuals in each user class are then split into three electric vehicles segments, which differ for the size *(Small, Medium, Large)*, to represent the vehicle fleet of the country. To each vehicle type a different battery capacity and driving consumption curve are associated as presented in the JRC report [31]. Driving consumption parameters are used to compute vehicles consumption as a function of the trip velocity, which is afterwords corrected through a multiplication coefficient to consider outdoor temperature effects on heating and cooling contributions.

A key input for time-series generation are the *functioning windows*, which are the time frames in which mobility events can occur. Two types are defined for each user: *Main* and *Free Time* functioning windows. In the first type main daily trips occurs, whereas in the second one occasional trips are considered. Each user is characterized by these two functioning windows. *Students* and *Workers* have two *Main* functioning windows, to mirror morning and evening commuting to work or study place, and three *Free Time* windows covering the remaining hours of the day. *Inactive* users have instead one *Main* window since no time slot is preferred for the daily mobility, and two *Free Time* windows in the early morning and late evening. Each user has associated two different *Appliances* to model the different behaviour in main and free time hours. All these data are derived from JRC mobility surveys [1] and *Eurostat* data series. As last step, user behaviour is differentiated for day type *Weekday, Saturday, Sunday*, and festivity days which are modelled as Sundays. On weekends and festivities *Workers* and *Students* behave as *Inactive* users for what concern functioning windows definition and daily travel needs. Stochastic randomization is associated to the total daily distance, the average velocity, functioning windows start/end and the power consumption.

Considering travel specific data, the total daily distance specific for country and day is given as input; it is then divided per type of functioning window through the *percentage usage* computed from the typical hourly distribution of trips given as input. The average trip velocity defined for user, day and country is used to compute the total daily time of travel, which is the termination condition of RAMP-mobility's algorithm. The average velocity is a representative value obtained from the trip's average distance and time, used to shift the iteration limit into the time domain to be coherent with the original structure of RAMP. New trips are simulated until the total travelled time for each user is reached. Another parameter used to determine whether the user takes the car or not in a functioning window, is the *occasional use* which simulates the probability of making at least one trip in a day. The algorithm iterates for every user producing sequences of trips until the termination condition is satisfied. At each time-step in which the trip is simulated, an average value of power consumption is assigned in relation to the car size through a simplified equation derived from JRC travel surveys [31]. The workflow of the mobility pattern simulation module is represented in *Figure 2.5* where the aforementioned elements are highlighted.

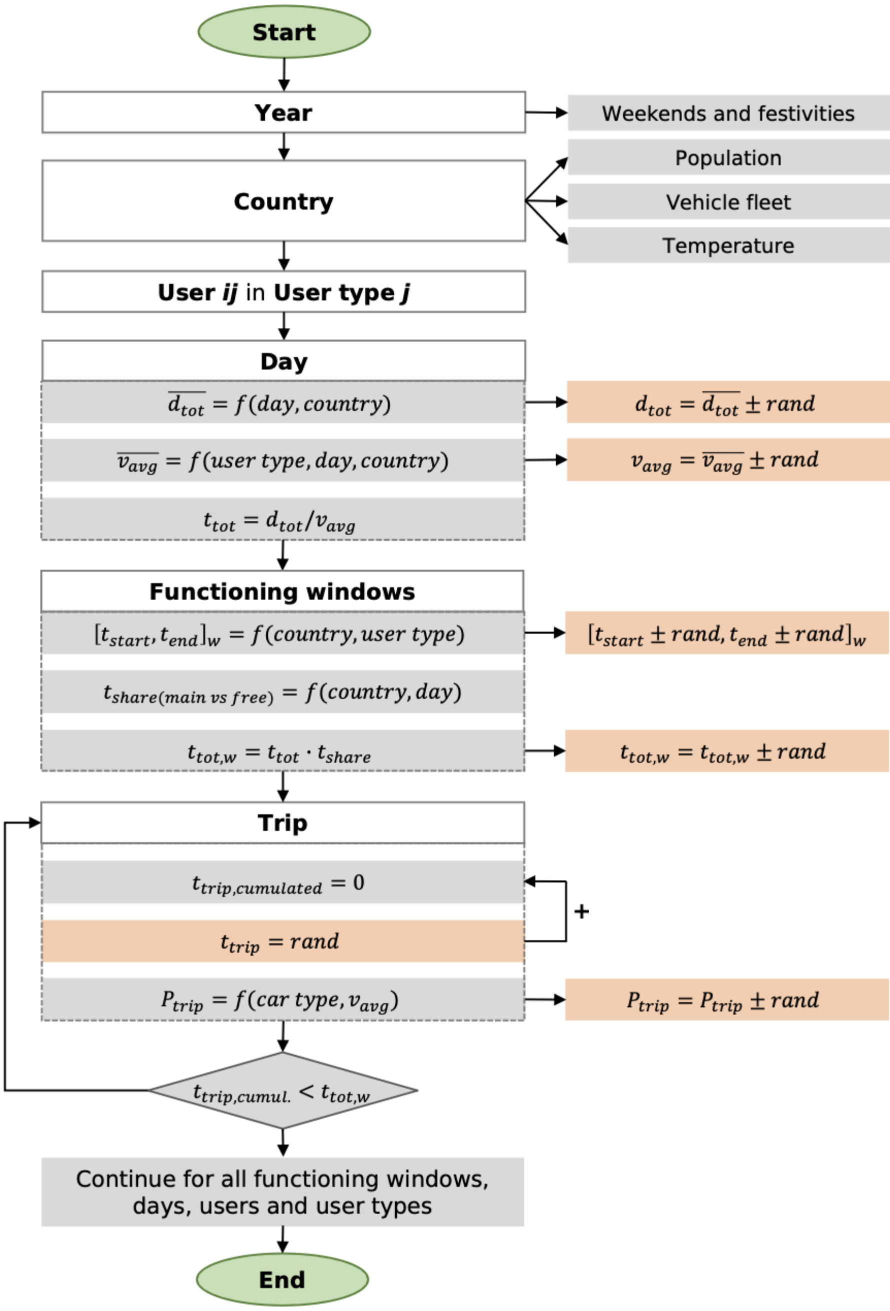

Figure 2.5: Conceptual scheme of the mobility module workflow. [25]

Once the mobility demand time series is defined, the model allows for three different charging strategies to compute the charging load demand:

- **Uncontrolled charging**. Users can charge as soon as possible and with no power limits. As the trip ends and a charging point is available, the charging event begins. The probability of finding a charging infrastructure has two different options: a constant probability value of finding the infrastructure at each parking and a piecewise probability function which reduces the probability in the main hours of the day. If the infrastructure is available, the type of charging station is chosen according to the probability distribution of the charging point type. The charging event lasts until the maximum state of charge is reached which is set to 80% to preserve battery lifetime.
- **Night charging**. Users prefer to charge during night hours to limit the overload during day peaks. If a parking time is in the night-hours the vehicle is charged otherwise this does not happen unless there is not enough energy for the following trip. Moreover, the charging event does not occur at maximum power but at the minimum value which allows to have the battery fully charged in the morning.
- **VRES charging**. Users charge when there is an excess of renewable energy production hence shifting the charging event in the hours in which the residual load, which is the difference between load demand and renewable generation, is negative.

Together with the charging probability function and charging points availability, which can be customized by the user, optionally user behaviour function, showed in *Figure 2.2*, can be activated to correlate the plug-in probability to the SOC of the car when parked as presented by Fischer *et al.* [10]

2.2. State of the art: vehicle consumption models

In this section the review is focused on how different models estimate the vehicles consumption. Most of vehicle dynamic simulators are similar since the fundamental equations needed to compute the power required for a given driving cycle are determined by the physical model of the vehicle. In the literature what makes the difference between the models is the level of detail at which the analysis is performed. If and how the consumption of auxiliaries, such as Heating Ventilation and Air Conditioning (HVAC) systems, is included, and how the dependence on ambient variables, air temperature and density, is considered which can have a major role especially for battery electric vehicles. Some examples of these models are here briefly described.

2.2.1. Overview of existing models

Muratori *et al.* [29] in the model developed to compute the transport energy consumption in the USA, adopted a backward dynamic simulator built in Simulink-MATLAB environment, to simulate the vehicle dynamics and compute the consumption associated to specific driving cycles. The model is based on the computation of the instant power required at the wheels to perform the driving pattern considering road grade, air drag force and a rolling resistance coefficient linearly dependent on road inclination. The simulator can be operated with different types of vehicles (BEV, ICEV, HEV, PHEV) and their main characteristics have been chosen as representative for each class. A specific optimization strategy is implemented to optimize the fuel consumption of HEV and PHEV. For the models with an electric motor the regenerative breaking is also considered and for BEVs a lower limit on SOC is imposed to 20%: if the SOC reaches this value the vehicle is supposed to be stopped and cannot complete the driving cycle. The model computes the instant consumption with a one-second resolution, for both gasoline and electricity required to the vehicle for the imposed driving pattern.

A hybrid physical-empirical model is developed by Deschenes *et al.* [5] to estimate the energy consumption of the EV fleet of a Canadian taxi company, and to optimize the operation through precise predictions. The hybrid approach followed considers the specific taxi driving constraints, that a pure physical model cannot grasp. The physical model is based on the computation of the energy required to perform a trip with a simplified equation that accounts for road grade, rolling resistance and aerodynamic losses. The energy demand is then corrected by an empirical multi-linear regression model, which was trained on the data of the taxi fleet. The correction factor is meant to introduce the dependence on ambient temperature and auxiliaries' consumption. Since a lot of different kind of data were available for each vehicle, the authors also performed other regression analysis to assess the possibility of improvements of the forecasts accuracy. The outcome of the study reveals that adding linear regression on fleet data can improve up to 61% the precision of the forecast comparing to the basic physical model, but it requires large dataset for the analysis.

The approach followed by Gaete-Morales *et al.* [11] to estimate the driving electricity consumption starts from the creation of custom driving cycles which simulate the user driving pattern. How these driving cycles are obtained is the focus of *Section 2.3.2*. Having the series of velocities for each trip, the energy consumed is computed considering for each time step the power values at the battery level: it can provide energy to the vehicle as it discharges, or receive energy being charged through regenerative braking. To compute the battery load, different contributions are considered: (i) motor input power required to overcome the tractive effort which is determined considering rolling resistance, climbing force, aerodynamic losses, and inertia force; (ii) generator output power which represents the energy recovered through breaking; (iii) auxiliary power for accessories and (iv) thermal power needed to keep the vehicle cabin temperature at a certain comfort value. Focusing on the thermal component, it is computed through a heat balance model which considers all the possible heat transfer mechanisms occurring in the cabin as the sensible heat of passengers, the heat transfer through walls, the enthalpy of outside air and the enthalpy of discharged air to outside. The result is the heat provided by the device to keep the target temperature from which the cooling or heating power is obtained considering the coefficient of performance (COP) of the device. This estimation of the power to heat or cool the vehicle cabin through the heat balance is physically detailed and represents the main difference with the model used in this work.

2.2.2. VCAM

The open-source python tool Vehicle Consumption Assessment Model (VCAM) [33], developed by SESAM group, is a lumped parameter model which assess the fuel consumption of light-duty vehicles by implementing a physical model of the vehicle, and computing the energy requirement to perform a given driving cycle. The tool can simulate three different power-trains, ICEV, BEV and PHEV, and different types of vehicles can be modelled by inserting some key performance parameters.

The model is split into three sections: vehicle longitudinal dynamics, power-train efficiency and auxiliary systems. The first section is based on a power balance that computes the traction power required in each time-step summing up four different contributions: aerodynamic friction, rolling resistance, climbing resistance and mass inertia. The auxiliaries consumption includes a constant value for electrical appliances and an electric consumption due to the HVAC system, which is computed as the ratio between the required thermal power and a coefficient of performance. The required thermal power is computed depending on the external temperature following the function used by Lajunen [21]. The COP depends on the ambient temperature and on the type of HVAC module of the vehicle. Two different configurations have been modelled: Air Conditioning and Positive Temperature Coefficient heater (AC+PTC), and Heat Pump with backup Positive Temperature Coefficient heater (HP+PTC). During heating condition, the thermal load for ICEV and PHEV is assumed to be satisfied with waste heat recovery from the engine, and a minor additional power is considered only to run fans. An additional power computed as function of the external temperature is included in the balance for BEVs due to the consumption related to the Battery Thermal Management System (BTMS).

ICEV fuel consumption is computed considering an engine efficiency function of the load and a constant fuel loss for the time spent in idling mode. For BEVs instead the electricity discharged from the battery is computed considering a constant discharge efficiency and including the regenerative breaking energy computed considering the maximum torque limitation and the upper limit to the SOC of the battery. Operation of PHEV is modelled as a combination of two different strategies and the choice depends on the state of charge of the battery: charge depleting mode and charge sustaining mode. The first strategy is adopted until the SOC reaches a minimum threshold and aims to maximize the electric mode. The charge sustaining strategy instead drives the car mostly relying on the conventional engine, using the battery only for recovery purposes and leading to cyclic SOC behaviour. The model includes some standard reference driving cycles as well as the input files for modelling some specific vehicles, a great advantage is the possibility to custom driving cycles and simulate specific vehicles.

2.3. State of the art: driving cycles generation

In this section the driving cycles, fundamental to estimate the energy consumed by different types of vehicles, are explored. DCs represent driving velocities patterns of car drivers and are necessaries inputs for the model previously described.

There are different ways in which DCs can be obtained. The first approach is used when large datasets on real-world driving behaviour are available and can be synthesized to get reference driving cycles. These DCs are usually used to check the compliance of vehicle pollutant emissions with respect to the applicable emissions limits, and to establish the reference vehicle fuel consumption and CO_2 performances. Reference driving cycles can be found in different world areas and are specific for the drivers behaviour of that region. An attempt to design a harmonized driving cycle representative of the worldwide light duty vehicle driving behaviour, is the World-wide harmonized Light duty Test Cycle (WLTC) obtained from data collected in Europe, Japan, India, Korea, and USA combined with suitable weighting factors [36]. Markov chain approach is another method found in the literature to produce DCs when huge datasets are available, by converting the real driving data into Transition Probability Matrix (TPM) used in a Markovian process. The second approach goes in the opposite direction and adapts standard DCs to parameters as velocity and time to obtain customized ones. The goal is to get realistic driving cycles for specific trip parameters keeping the general features of a reference cycle.

2.3.1. Driving cycles creation through Markov chain

Customized DCs can be generated by Markovian stochastic tools based on historical data as presented by Muratori *et al.* [29]. The driving profile generator described in the paper creates a stochastic driving pattern starting from a single characterization parameter, duration or distance, and adopting literature available TPM. A transition probability matrix is a matrix of states defined by actual velocity, in which each cell contains the probability of stepping from the actual value of velocity to another one. Adopting a Monte Carlo method to pick random sequences of speed values leads to the buildup of the random driving pattern for the desired duration. Firstly, the generator needs to link the single parameter to a second one to fully characterize the trip, for this implementation a duration-distance probability distribution is used. A single driving cycle is composed by the three sections *Urban, Highway, Urban*, and their proportion is randomly estimated according to the highway ratio, a parameter computed from the trip characteristics. Urban and highway sections are generated from different TPMs that reflects the different driving conditions and are derived from Gong *et al.* [13]. The model produces custom driving cycles with shapes similar to the ones used to generate the TPMs, which are assumed by the authors as realistic driving behaviours.

Markovian processes are also used by Yang *et al.* [40] as a tool to obtain representative *real-world* driving cycles from huge drive patterns datasets. The authors performed data analysis on a database of real driving patterns by clustering them and producing transition probability matrices. Some candidate driving cycles with the desired length are then generated with Monte Carlo simulations. Finally, the accuracy of the DCs is evaluated, by identifying twelve assessment criteria to select the most representative for the starting dataset.

2.3.2. Adapting standard driving cycle to reference parameters

When specific datasets are not available and the goal is to obtain a realistic driving cycle with specific trip parameters, the method to be followed is the rearrangement of a reference driving cycle to produce similar ones with the desired overall characteristics.

In the model developed by Gaete-Morales *et al.* [11], custom DC to compute the driving electricity consumption profiles are obtained from the WLTC. In this test cycle four sub-classes are present each representative of different driving patterns (*Low-speed, Medium-speed, High-speed, Extra-High-speed*), and all sub-classes can be characterized by an average velocity. Given the trip average velocity coming from the first time-series of the model, the tool first selects the sub-class with the closest average velocity, and then the driving cycle sub-class is rescaled to create a custom driving cycle with the average velocity of the trip to be simulated. Since WLTC sub-sections have a finite duration, the custom driving cycle is replicated until the total time of the trip is reached. However, this way of proceeding produces driving cycles which are unlikely a realistic representation of driving pattern. Firstly, acceleration and deceleration could reach values which are unfeasible for most of the vehicles; secondly, the generated trip rarely ends with a 0 km/h velocity. Lastly, the repetition of the same pattern for the entire driving cycle produces unrealistic driving behaviours.

Another approach overcoming this problem is presented by Gruosso [14]. The starting point is the *ARTEMIS* reference driving cycle [2], which includes three real world driving cycles derived from European driving data: *Urban, Rural* and *Motorway*. Three fundamentals information of every car driver is considered: departure and arrival locations, trip duration and trip distance. Knowing these variables a recombination of *ARTEMIS* segments is made considering the trip locations. If start and end happen in a city, the custom driving cycle is all urban, whereas if locations differ in typology, a mixture of *Urban* and *Rural* or *Urban* and *Motorway* is made. To size the share assigned to urban and rural/motorway, average speeds of *ARTEMIS* driving cycles are considered.

3 | Methodology

In this chapter, the methodology followed to improve the technological detail of the stochastic model RAMP-mobility, described in detail in *Section 2.1.2*, and to obtain more accurate mobility and charging profiles, fundamental for energy system modelling, is presented. This is possible through the link with vehicle dynamic simulator, able to compute physically based consumption estimations, and with other improvements introduced both at the level of the stochastic process, which is the core of the model, and of the charging. The goal of this work is to assess the impact of introducing a more accurate vehicle consumption model and determine how the output is affected. To couple the simulator with RAMP-mobility, driving cycles are required and a new specific tool is developed aiming to solve some limits found in the reviewed models related to the characteristics of produced driving cycles.

3.1. Driving Cycles generator

The first idea followed to improve the modelling of vehicle consumption, inspired by the methodology adopted by Gaete-Morales *et al.* [11], is to link each generated trip to a specific *real-world* driving cycle, thus increasing the technical resolution of RAMP-mobility. To achieve this purpose a tool able to create realistic driving cycles from specific trip features, as average *speed* and *duration*, is required. Different approaches are adopted in literature, as described in *Section 2.3*, to create *real-world* driving cycles. The method showed in *Section 2.3.2*, based on adapting a reference driving cycle to specific parameters is chosen, since enough detailed for the scope of consumption modelling and no empirical databases are available. The development of a new tool is required to overcome the limits of the method adopted by Gaete-Morales *et al.* [11] highlighted in the previous chapter.

3.1.1. Construction

Reference driving cycle

The World-wide harmonized Light duty Test Cycle (WLTC), which is the standard *real-world* cycle for emission and consumption measurements, is selected as reference cycle to create the Driving Cycle Generator tool.

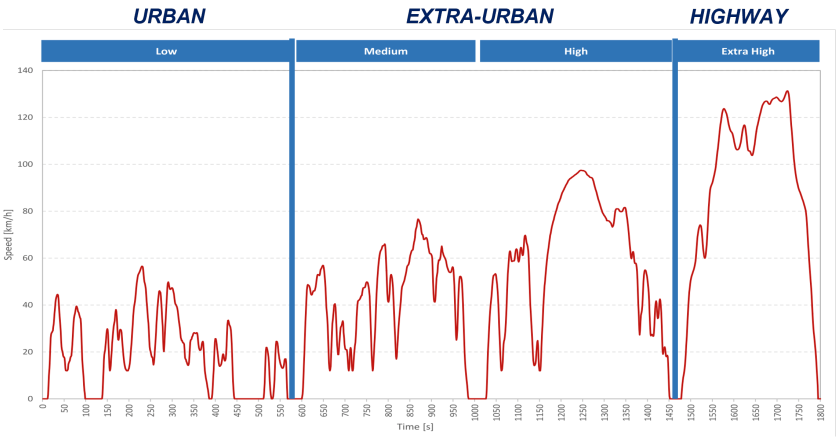

Figure 3.1: World-wide harmonized Light duty Test Cycle (WLTC): reference driving cycle for the generator tool.

Three sub-cycles have been identified from the reference WLTC cycle according to their average speed; each section should replicate the driving mode respectively in *Urban*, *ExtraUrban* and *Highway* environments. Formally the WLTC is made of four parts, *Low, Medium, High,* and *Extra-High*, which aim to model driving conditions at different speeds [*Figure 3.1*]. Since the generator considers only three classes, the *Medium* and the *High* sections have been considered together to represent the driving condition of extra-urban non-highway roads, called *ExtraUrban*. The methodology used to obtain realistic velocity profiles by combining these three sub-cycles is here exposed.

Urban Share definition

The custom driving cycles are generated from the WLTC through a recombination of its sections depending on the given input parameters: the *average speed* and the *duration*. Starting from the couple of values, the generator firstly assesses which of the three driving environments is supposed to be driven, choosing between *Urban*, *Urban-ExtraUrban* or *Urban-Highway*. In relation to the input values, one of the three options is selected according to the Urban Share (US) variable. The US is function of the average target speed, the average *Urban* and *ExtraUrban* velocities as express in *Equation 3.1*.

$$US = \frac{\overline{v} - \overline{v}_{extraurban}}{\overline{v}_{urban} - \overline{v}_{extraurban}}. \tag{3.1}$$

This variable is used to size the share of DC in the urban environment with respect to the extra-urban one. Two threshold values have been selected creating three different situations:

- *Urban Share higher than 0.9:* the type of driving cycle is *Urban* (even if the given average speed is higher than the *Urban* one, this to avoid too short *ExtraUrban* sections which are not realistic)
- *Urban Share between 0 and 0.9:* the driving cycle is a mix of *Urban* and *ExtraUrban*
- *Urban Share lower than 0:* the driving cycle is in *Urban-Highway* conditions and the US is updated considering the average speed of the *Highway* section instead of the *ExtraUrban* one.

An urban section is present in all the possible cases to model the initial transition from the start event to the cruise phase, and the ending transition before the trip ends. Once the US is defined, the total urban time of the custom DC can be computed with a minimum limit set to 220 seconds to always have a representative urban section. In the full *Urban* case, this time will correspond to the total time of the driving cycle and the *Urban* section of the WLTC is repeated until the total time is reached. For the other two cases instead, the urban time computed is divided and allocated half at the beginning and half at the end of the driving cycle to simulate a smooth start and end of the trip. The length of the central part is determined in a complementary way to satisfy the input duration; this section is reserved to *ExtraUrban* or *Highway* segments in relation to the target average speed, and the WLTC reference section is repeated until the total non-urban time is reached, as for the urban section.

Transition definition and rescaling

To connect the different sections and avoid time steps with strong decelerations, a soft linkage is made thanks to transitions. These are seconds needed to bring the velocity of the last time step down to zero with realistic values of deceleration. To compute the transition time a conservative value of deceleration is set to $0.1g$ since from the analysis of the WLTC maximum acceleration are around $0.17g$, while deceleration are in the range of $-0.15g$. Transitions are time steps added to sections in which the last velocity is higher than 0 km/h. Consequently, subsequent section's time is reduced of the transition duration. For what concern the last urban section, its transition time is removed from the initial section since it has been verified that at the beginning enough values at 0 km/h are present and can be omitted if needed. In this way the custom driving cycle has smooth passages between sections with controlled deceleration and the final speed value will always be brought down to 0 km/h. As last step, since transitions are added and average velocities of the different reference sections are changed, the final driving cycle is rescaled to reach the input average speed through a scaling factor.

A final check is made on the scaling factor since, if the rescaling has a high value, the acceleration or deceleration could be higher than 2 m/s^2. This is considered the maximum accepted value, since the WLTC values are just below this limit. If the scale factor threshold value is reached the driving cycle is recomputed through the *Probabilistic Highway* approach, presented in the following paragraph, and the initial and final urban sections are eliminated. This is made when the average input velocity is too high to avoid sections with low average velocities, as the *Urban* ones, which cause an increase in the scaling factor to reach the target speed.

Probabilistic Highway

A particular situation is verified when the total input time allows to have more than one WLTC *Highway* sections repeated. With the process illustrated above the custom driving cycle will be composed by initial and final *Urban* and by a central *Highway* section which is repeated, meaning that there would be stop instants and sharp velocity decrease during the highway driving mode. This is considered as an unrealistic condition and overcame with a different methodology. In this condition, where the number of *Highway* sections to be inserted is more or equal to one, the creation of the driving cycle follows the procedure of the *Probabilistic Highway*. A procedure inspired by the Markov chain technique, used in literature to synthesize *real-world* driving cycle from empirical database [*Section 2.3.1*], is implemented. Initial and final *Urban* are always present, while the central section has starting and ending parts of the WLTC *Highway* until the speed of 81 km/h. The remaining time required to satisfy the total input duration is filled with a probabilistic section. A velocity sequence specific for the highway environment is generated from a Transition Probability Matrix, which is an additional input required by the generator tool and should be created analyzing a typical highway driving behaviour. A TPM represents the probability, given a value of velocity, to have a certain other value in the following time step. This has been obtained from the analysis of velocities states of the WLTC *Extra-High* section. This stochastic profile replicates the highway driving pattern avoiding unrealistic stop-and-go events. Transition is present also in this case linking the last probabilistic instant with the final section to avoid steep deceleration.

The developed Driving Cycle Generator tool is able to produce realistic driving cycles from the couple of key trip features, average *speed* and *duration*, by defining probable driving environments and associating to each section of the trip a characteristic repeated sub-cycle, derived from the reference driving cycle. In addition to the trip parameters, the tool requires as input the standard driving cycle WLTC and a TPM for the highway driving profile. The entire process followed for the creation of driving cycles is deterministic with the exception of long highway trips and is briefly presented in *Figure 3.2*. A database of custom driving cycles with 1 km/h as velocity meshing gap, and 5 min as time one is generated following the aforementioned methodology, and is used as input for the VCAM model to estimate the power consumption associated to each couple of key parameters.

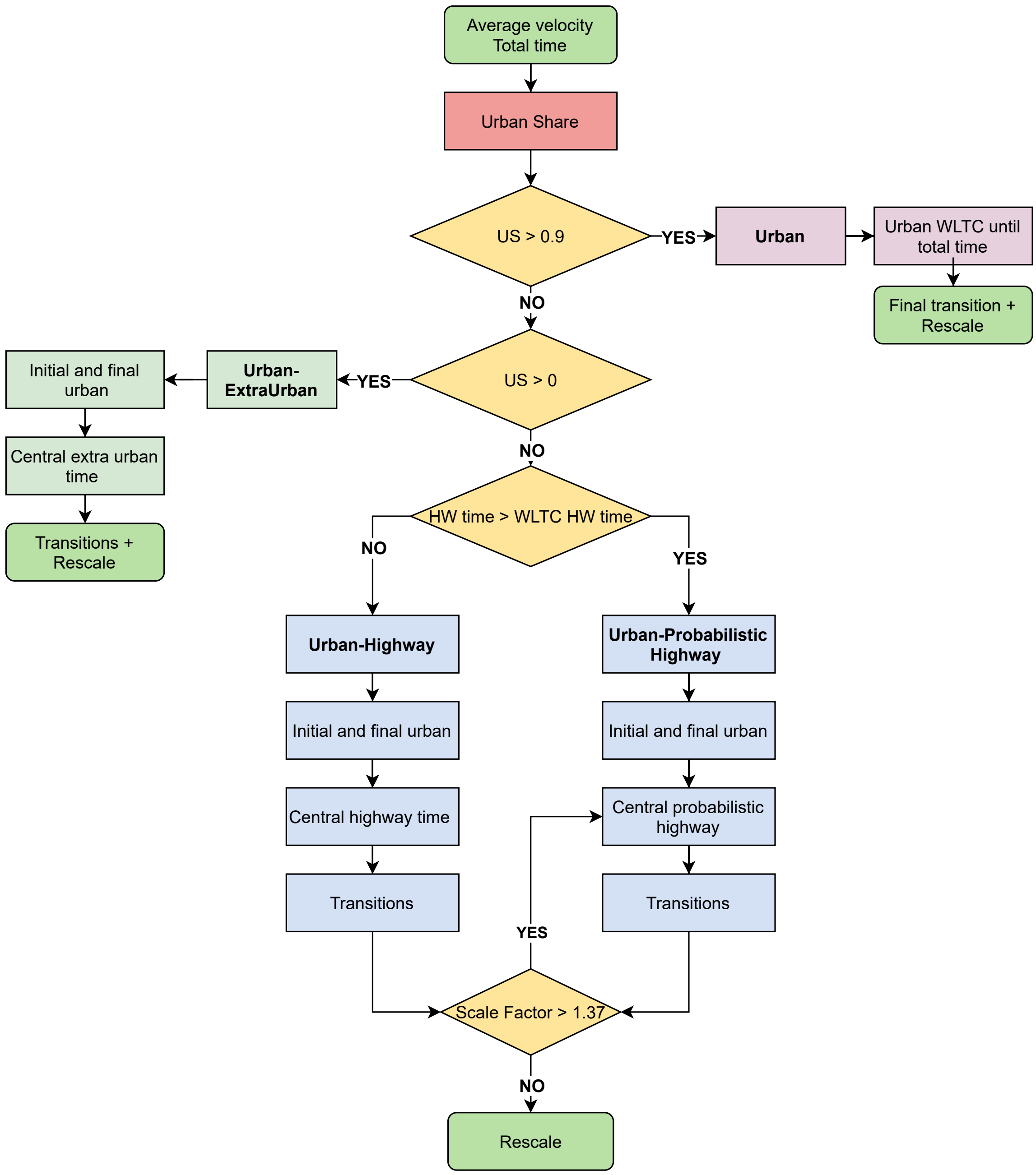

Figure 3.2: Conceptual scheme of the Driving Cycle Generator tool functioning.

3.1.2. Comparison with *Emobpy* generator

To evaluate the goodness of the driving cycle generator, a comparison with the driving cycles generated with *Emobpy* methodology is performed. The method developed by Gaete-Morales *et al.* [11] and described in *Section 2.3.2*, is similar to the one adopted in this thesis, since they are both based on a recombination of the reference WLTC. However, some critical issues have been found for specific values of speed, for which the *Emobpy* generator requires large rescaling hence causing much higher accelerations compared to the reference cycle. The solution developed in this work aims to limit this problem and create more realistic driving patterns.

The comparison with *Emobpy* methodology is performed creating a set of critical driving cycle with both generators and evaluating their realism with a metric of significant indicators. The DCs chosen are the ones with average speed closer to the limit of each class, because these driving cycles are those that need to be rescaled more. Three limit cases are considered for *Emobpy*, since the four WLTC sub-sections are used (*Low-Speed, Medium-Speed, High-Speed, Extra-High-Speed*); and two for the generator of this thesis, since three main types of cycles are created (*Urban, Urban-ExtraUrban, Urban-Highway*). A standard value of time duration is used for all driving cycles since it does not affect the metric. The chosen indicators are: maximum speed, maximum acceleration/deceleration and driving share in accelerating, decelerating, and idling mode. The results are compared between each other considering the WLTC parameters as reference and the relative percentage error is used to evaluate the two driving cycles generators.

3.2. RAMP-mobility improvements

In this section, the methodology adopted to improve some modelling aspects of RAMP-mobility, which emerged from the study of the model as weak points, is described. Two main directions have been followed: (i) improving the stochastic process with some progresses concerning the internal coherence of the model itself and with more accurate vehicle consumption estimations to simulate a more realistic demand; (ii) developing the charging process through more specific charging probabilities and introducing the analysis of connected vehicles.

3.2.1. Structural mobility improvements

The limits found in the study of the original model structure are related to three different aspects: the definition of mobility behaviour, the specificity of vehicle consumption, and the vehicle consumption model adopted.

Mobility behaviour

This class of improvements aim to solve two limits found in the model analysis related to functioning windows and simulated driving distance.

Complementary functioning windows

Functioning windows extremes definition is subject to an input random parameter which is used to vary the start and end for each simulated *Appliance*. In the original model independent stochasticity is applied to both types of windows, *Main* and *Free Time*, and when defining input functioning windows a time frame is reserved between the end of each *Free Time* and the start of each following *Main* to avoid possible overlaps related to this variability. However, the independent variation cannot avoid empty time gaps and possible overlaps, hence, to solve this problem, the solution here proposed allows to define *Main* functioning windows as complementary to *Free Time* sections. In this way the stochasticity is applied only to one type of functioning window, *Free Time* one, and the *Main* is obtained from the remaining time gaps. In *Figure 3.3* it is possible to understand how the functioning windows for *Worker* and *Inactive* users are originally defined, and how the just presented approach vary the windows extremes. To allow this definition *Appliance* list, which is filled with firstly the one for *Main* windows and secondly the *Free Time* ones, is reversed in the order to allow primarily the definition of *Free Time* duration subject to input variability. The decision of starting from *Free Time* windows and not from *Main* ones is a consequence of the following improvement introduced.

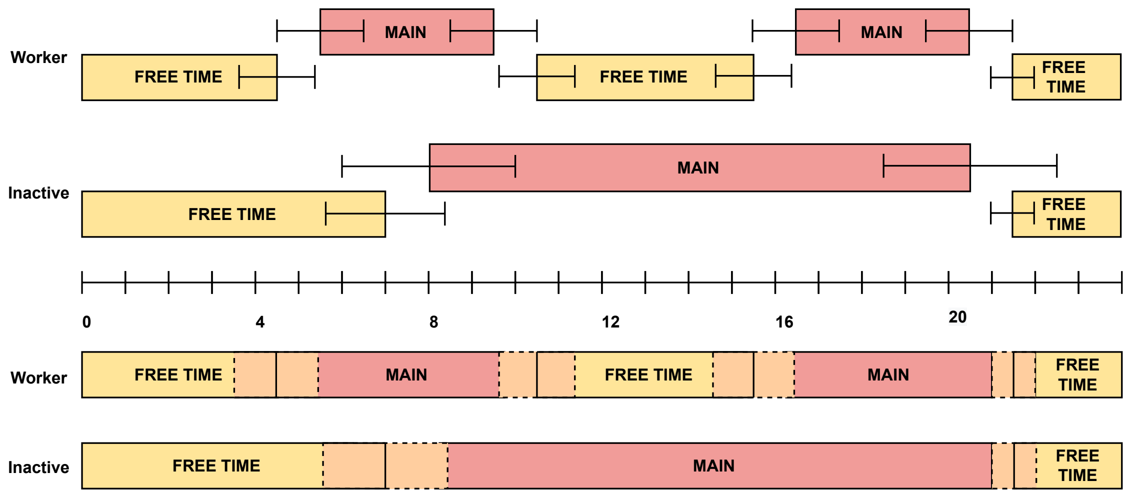

Figure 3.3: Functioning windows definition: above the original overlapping approach, below the complementary one.

Another change is introduced to improve the modelling of *Free Time* windows. A lower probability of picking a night time-frame is added in the case of three *Free Time* windows, to model the difference between this type of windows. A lower probability of early-morning and late-night trips is set, compared to mid-day ones.

Distance recovery

The second important limit of the model is related to the coherence between input daily distance, which describe the average distance per day specific for user type, and the effective distance travelled by each user. Even if RAMP-mobility is not developed with the goal of producing realistic driving trips, and for this reason it requires only few average data, it is important to check that the overall mobility demand generated reproduce the given input data. Analyzing the characteristics of the generated trips and computing the total driving distance for each user, a lack of consistency was found since lower distances with respect to input values were simulated. The cause of this problem is found in the *occasional use*, which aims to model the possibility of not using at all the car in a functioning window. This possibility lowers the average driving distance compared to the input one, which is instead supposed to be the average distance of the overall population.

To solve this issue, without deleting the realism of the *occasional use* parameter, that is crucial to shape the mobility profile, a solution based on the recovering of not-driven distance in the functioning windows affected by this variable is proposed. Since the *occasional* *use* parameter is intended to model the intermittency of usage mostly in leisure time, the distance skipped by a user in a *Free Time* window is reassigned to its correspondent *Main*. In this way the total user average distance remains the same given as input, while only the proportion between kilometers driven in the two different windows may be different from the input value. This solution works until no intermittency of usage is inserted in *Main* windows, but this is not the case of weekends in which is considered a probability of not using the car in peak hours. For this reason, and due to random variability on the input distance, the average driving distance is not exactly the one inserted. The implementation of this correction requires some relevant modification in the stochastic process, since the order in which the *Appliances* are run must be inverted, as anticipated in the previous paragraph. Additionally, a local variable is introduced to temporarily memorize the not-driven distance and reassign these kilometers to the following *Appliance*. For this reason, a new attribute *kind* is inserted to describe the type of *Appliance*, necessary to understand if the skipped distance needs to be recovered or not.

Trip specific consumption

After having solved some internal intrinsic limits of RAMP-mobility, the vehicle consumption estimation has been analyzed. In its default version the model computes the average consumption assigned to each time-step of the trips, using an average daily speed generated independently on the trips. The link between daily velocity and power consumption is represented by the JRC equation, which characterizes the vehicle consumption for three size of cars. Since the goal of this thesis work is to improve the accuracy of the output mobility and charging profiles, a more realistic modelling of the consumption is introduced. The first step in this direction is the adoption of an average value of consumption specific for each trip instead of a daily average value. To reach this goal, a mean trip velocity is required given the length of the trip, which can then be characterized by two parameters: *duration* and *speed*. Consequently, an empirically generated probability distribution, to link trip duration to a typical travel velocity, is necessary. Once the average parameters of the trip are fixed, it can be linked to a driving cycle produced with the *real-world* Driving Cycle Generator described in *Section 3.1*. A database of driving cycles has been created with the generator for couples of duration and average speed, creating a matrix of speed and duration classes, with step of 1 km/h and 5 min. Consequently, each simulated trip is associated to the closest driving cycle in terms of these two key parameters. The average consumption value for each driving cycle is computed applying the JRC correlation, described by Pasaoglu *et al.* [31], to each time-step, and an average of the time-series is computed to represent the DC consumption.

To simplify the implementation in RAMP-mobility, the consumption for each couple *duration* and *speed* is pre-computed, and consumption tables, in which at a given couple of speed and time a mean consumption values is linked, is inserted as input to the model. These tables are generated for each set of parameters of the JRC equation, modelling *Small, Medium* and *Large* vehicles. Additionally, an analysis to assess the dependence of the average values of consumption on the trip parameters is performed, aiming to identify possible simplifications of the input tables; from the same analysis, the variability on power values is estimated, and the input value is updated to 5%. A graphical illustration of how the consumption tables are used in the stochastic process is presented in *Figure 3.4*. A check is introduced to verify whether the driving cycle is feasible for the simulated vehicle segment, otherwise the trip is discarded and the generation process is repeated. A DC is labelled as *Infeasible* when the power required from the battery exceeds the vehicle maximum for at least a time instant (*see [33] for more details*).

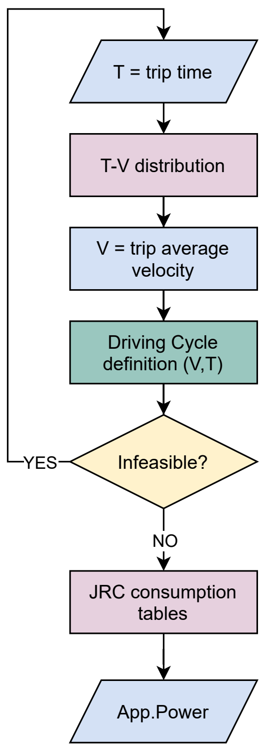

Figure 3.4: Conceptual scheme of the trip specific consumption model implemented.

Vehicle consumption model

A step forward is made with the implementation of a new consumption model which increases the accuracy of the estimation and improves the quality of the model. As in

Section 3.2.1, the consumption is trip-specific requiring a correlation between trip duration and velocity, and the Driving Cycle Generator is used to realistically describe the driving pattern. The vehicle dynamic simulator VCAM is introduced to determine the average consumption associated to specific driving cycles. This model has been selected since it considers the effect of external temperature, simulates the consumption of different types of power-trains, and its quality has been verified [33]. An analysis of the thermal component has been carried out comparing this model with *Emobpy* framework, described in the literature review (*Chapter 2*), to assess the possibility of thermal module refinement. The results, reported in *Appendix A*, did not brought to significant improvements to VCAM model, hence it is introduced in its original structure. This last step completes the characterization of the trip-specific consumption model, exploiting the detailed description of the travel as a driving cycle, and simulating the dynamic behaviour of a vehicle along the generated path. The overall effect on RAMP-mobility is the shift from a duration-only trip depiction and a daily simplified consumption, to a per second definition of driving behaviour and a physically based consumption model.

As for the previous step, consumption tables are adopted using the VCAM model. Each driving cycle has been simulated for all the vehicle segments, and the average consumption for the selected trip has been stored in the tables. With this kind of implementation from the computational point of view there is no difference between this step and the previous one. An analysis on the produced tables similar to the one described in the previous step is made to verify the dependence on the trip characteristic parameters. Similarly, the variability on power is reduced from 10% to 5%.

Another minor change is required to properly model the thermal demand of the vehicle HVAC system, highly dependent on the external temperature. RAMP-mobility already models the variation of the load with the external temperature through a correction factor. A similar method is adopted to reproduce VCAM thermal model: the consumption stored in the tables does not include the thermal demand, which is added after the stochastic process. This additional consumption is computed through a cubic function obtained from the VCAM simulation of the thermal power demand with different values of external temperature. The implemented function for BEVs assumes an Heating Ventilation and Air Conditioning (HVAC) system composed of Heat Pump and Positive Temperature Coefficient heater (HP+PTC), which is adopted for all the reference vehicles.

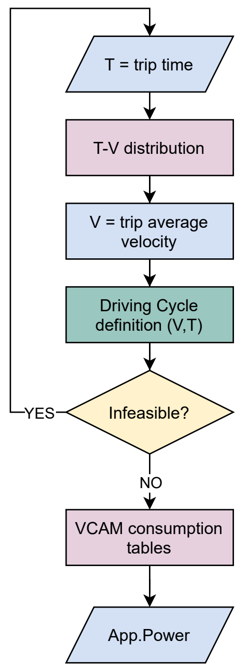

Figure 3.5: Conceptual scheme of the trip specific consumption model implemented with VCAM introduction.

A graphical illustration, as the one presented for the previous step, of how the newly introduced consumption tables are used is illustrated in *Figure 3.5*. This way of implementing VCAM allows to create a parallel version of RAMP-mobility for the simulation of gasoline powered vehicles, which will be used in the model quality assessment in *Chapter 6*. The only variations required are in the consumption tables, which are computed using VCAM with ICEV, and in the thermal additional consumption function, which depends on the type of drive-train.

3.2.2. Structural charging improvements

In this section the focus is moved from the mobility simulation to the charging process. Once the mobility demand is generated, this profile is used as input to estimate the charging curve. As already described in *Section 2.1.2*, three different charging strategy could be used. In all of them, to model the charging infrastructure probability two options are available: daily constant probability or a piecewise function used to differentiate the possibility to find a charging point during the day. This second choice is implemented since it is more likely to have free EVs chargers at home either as private or as public point present in residential areas. However, seen the absence of spatial characterization in the model, to approximate this differentiation, an higher probability in the early morning and in the late evening is considered. This is related to the higher probability of being at home during these periods and the result is presented in *Figure 3.6*.

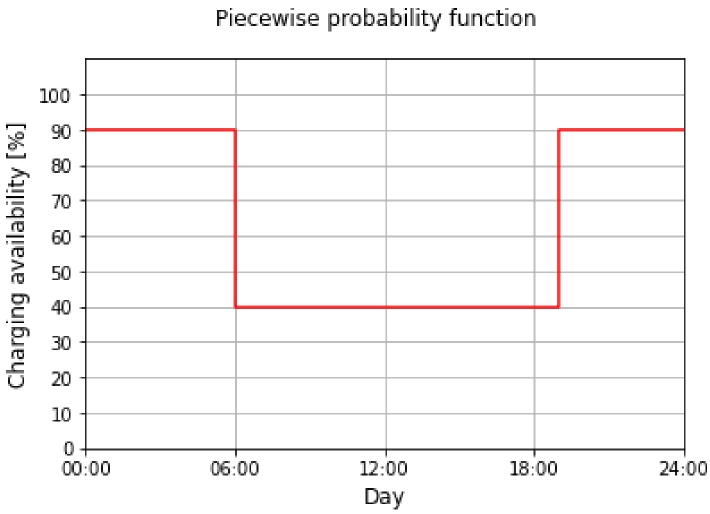

Figure 3.6: Piecewise probability function for charging infrastructure.

An improvement of this characterization is considered to better describe weekends charging events. A piecewise function specific for Saturdays and Sundays is introduced with the lower mid-day probability of finding a charging point applied for a shorter time window. This is used to describe the different charging behaviour which is expected on weekend and for which more time is spent at home in the morning and in the evening. These two functions will be fundamental in the validation of the charging profiles in *Chapter 6* and will be object of a sensitivity analysis seen their high level of uncertainty.

Additionally to the charging infrastructure probability, also the user behaviour decision to charge could be activated in the default RAMP-mobility version. This is modelled considering the *user behaviour* function, reported in *Equation 3.2* and proposed by Fischer *et al.* [10]. This equation correlates a probability of charging to the actual State of Charge, and tries to model the user decision of plug-in.

$$Ch_{prob} = 1 - \frac{1}{1 + e^{-K \times (SOC - SOC_{per})}} \quad \text{with } K = 15,\ SOC_{per} = 50\% \tag{3.2}$$

This probability function, together with the one describing the infrastructure availability, are fundamental to understand the impact on V2G technologies and grid flexibility. For this reason, an additional output is derived from the charging process to describe the vehicle connection time-series. Both user and battery capacity connection level are computed, and the impact of the charging probabilities is assessed through their variation. The analysis of the number of vehicles connected to the grid instant-by-instant is crucial to estimate the potential of V2G technology, which is a powerful solution to reduce peak power and offer flexibility services to the grid. This is important seen new challenges in managing grid power dispatch created by the increasing number of Electric Vehicles, which also open to new possibilities of storage.

The simulations performed to assess the impact of charging parameters on the time-series of connected vehicles and of the aggregated battery capacity are now described. Two infrastructure probability functions have been tested: a constant default value, and a piecewise with different key parameters for weekdays and weekends. Four cases have been set up to assess the possible combining effects of infrastructure availability and user behaviour:

- *Baseline*: include the default infrastructure probability set at 80% for all time-steps;
- *Case 1*: evaluates the impact of the *user behaviour* function keeping the default infrastructure probability;
- *Case 2*: includes the piecewise infrastructure function with the parameters assessed in *Chapter 6*;
- *Case 3*: combines the effects of both piecewise and *user behaviour* functions.

The *Uncontrolled* charging strategy has been adopted to avoid the influence of smart charging management on the results. The simulations adopts the last developed version of RAMP-mobility for Italy, including the integration of VCAM. Charging profiles, percentages of charging users, and percentages of connected ones will be compared for the highlighted cases.

4 | Case studies

In this chapter the improvements of RAMP-mobility methodologically described in *Chapter 3* are applied to two specific case studies: Italy and The Netherlands. Italian input values are updated after a detailed analysis of specific regional databases to better characterize the country and determine single trip features. For The Netherlands instead a limited variation of input data is applied since no specific database has been considered. The step-by-step application of RAMP-mobility structural mobility improvements is adopted for both countries, and the data used for each step are highlighted in the following paragraphs.

4.1. Italy

4.1.1. Data analysis

In this section a description of the analysis performed to obtain accurate description of Italy and to assess realistic trip features is provided. Regional databases from various sources have been scanned, cleaned, and filtered to obtain the data required as input to RAMP-mobility by aggregating regional data and weighting them according to the population distribution. Three main investigations have been completed: (i) a study of commuting trips records to address the peculiarities of typical travels; (ii) the car fleet composition updated to 2019 [26] to classify the vehicle types and their shares; (iii) exploration of different datasets to investigate aggregated mobility data in terms of functioning windows and population share.

Commuting trip analysis

A large set of commuting trips records of around 29 million people, regionally specific and released in 2011 is available from Istat [18]. Each collected trip is defined by origin, destination, purpose (study or work), estimated number of individuals and class of duration. The scope of this analysis is to examine the relation between duration and average speed of journeys and determine typical values of trip characteristics.

Records are filtered to consider only car movements and are coupled with a database of distances and driving times [18] between municipalities to estimate trip lengths and duration. Some assumptions have been introduced to compute non-available distances: missing municipalities have been substituted with the closest available, and trips with abroad destinations have been discarded. Features of trips driven inside the same town have been estimated considering a fictitious city radius, computed from the square root of the urban surface using a specific Istat database [19]. The driving time is determined with a linear regression on a selection of other short trips for which the time and length data were available. *Figure 4.1* illustrates the first step of the data processing: trip time and distance are added and the inserted duration is compared to the duration class of the original database. A mark based on the difference between the two classes is assigned and used as metric to evaluate the accuracy of the matching.

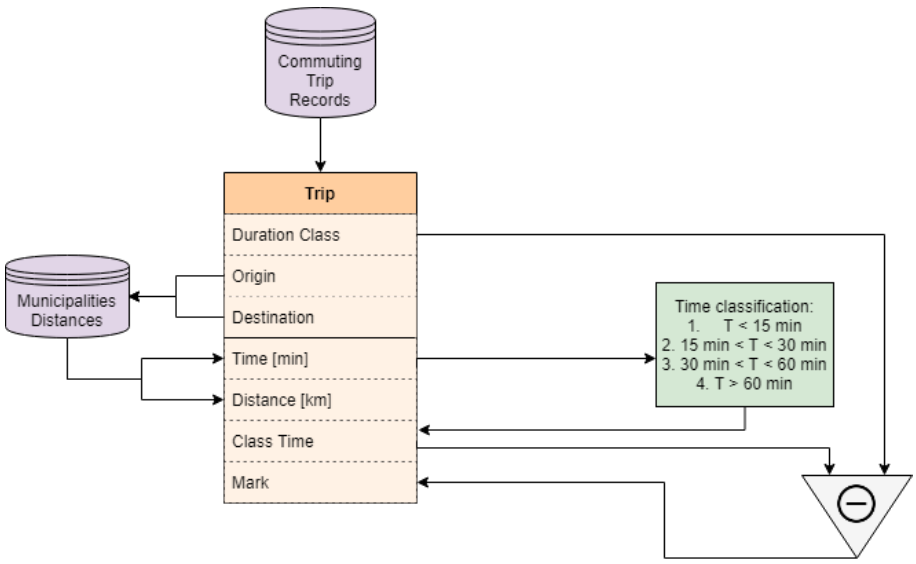

Figure 4.1: First step of the data processing.

The Istat database [18] from which distances have been obtained is accurate in estimating the lengths since it is based on a Geographic Information System (GIS) software. However, as stated in the metadata report [17], the estimation of driving time is made in ideal conditions without considering traffic. For this reason having a rough estimation of trip time divided in four-time classes of duration, a delay coefficient has been tuned to increase the duration of trips and to improve the match between the estimated time and the time class associated in the original Istat database [18]. The delay coefficient has been evaluated for each region excluding some time classes if they already have good matching, as in the case of the first class (time $< 15min$) or if they would create too long unrealistic trips, as in the fourth class (time > $60min$). Once the coefficient is chosen, the delayed duration is computed and the mark is updated; these steps are repeated until a satisfactory matching is achieved. The iterative process to assess the effect of the delay coefficient is showed in *Figure 4.2*. Having the delayed time which accounts for traffic conditions, for each trip a value of average speed is computed as ratio of the distance and delayed time.

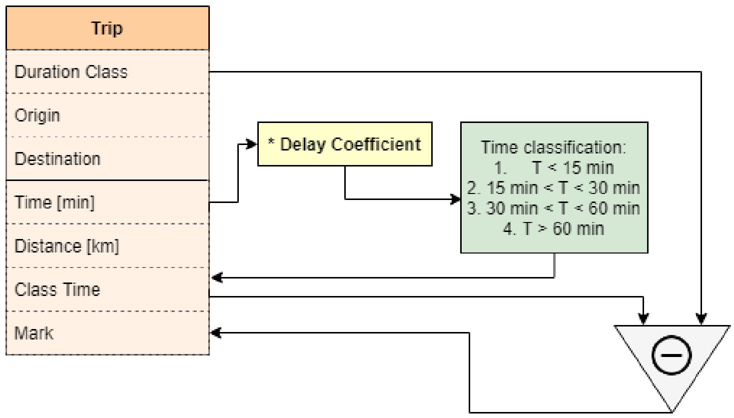

Figure 4.2: Second step of the data processing highlighting the delay coefficient.

The processed database is used to obtain three main outputs: values of average trip duration, a distribution of typical speed values, and probability tables that links duration classes and average speed classes. In *Table 4.1* the average trip duration is showed for each region together with the corresponding the aggregated value for Italy. In *Table 4.2* the velocity distribution is described with its mean value and the values of percentage variation. These are computed using the first and third quantile which are used to model the stochastic variation of the average speed.

Average Trip Time

Abruzzo	Basilicata	Calabria	Campania	Emilia	Friuli	Lazio
14.4	16.3	15.6	14.8	18.2	14.6	23.0
Liguria	Lombardia	Marche	Molise	Piemonte	Puglia	Sardegna
16.5	17.1	14.3	14.5	16.1	19.1	14.9
Sicilia	Toscana	Trentino	Umbria	Valle d'Aosta	Veneto	**Italia**
16.2	18.2	14.5	18.8	14.1	16.4	17.8

Table 4.1: Average trip duration in *minutes*.

Average Trip Speed

	Abruzzo	Basilicata	Calabria	Campania	Emilia	Friuli	Lazio
$\mathbf{v_{avg}}$ **[km/h]**	47.6	48.5	44.4	38.6	43.3	47.2	48.6
$\mathbf{var_{[\%]}}$	14.4	13.3	22.9	25.3	15.4	12.6	15.5
$\mathbf{var_{[\%]}}$	-11.2	-8.8	-21.2	-21.4	-15.3	-8.1	-17.0
	Liguria	Lombardia	Marche	Molise	Piemonte	Puglia	Sardegna
$\mathbf{v_{avg}}$ **[km/h]**	42.3	40.2	44.9	41.1	44.4	40.4	53.3
$\mathbf{var_{[\%]}}$	24.1	23.6	12.0	12.7	19.9	24.1	8.1
$\mathbf{var_{[\%]}}$	-20.5	-19.7	-8.5	-14.8	-17.6	-21.7	-7.8
	Sicilia	Toscana	Trentino	Umbria	V. d'Aosta	Veneto	**Italia**
$\mathbf{v_{avg}}$ **[km/h]**	43.6	40.9	48.3	50.0	42.4	42.2	43.2
$\mathbf{var_{[\%]}}$	30.3	20.6	18.0	25.1	20.6	19.1	18.0
$\mathbf{var_{[\%]}}$	-25.2	-14.9	-15.3	-21.4	-20.8	-16.3	-21.0

Table 4.2: Trip average speed distribution in km/h.

As described in *Section 3.2.1*, to improve the consumption estimation an average speed value is associated to each trip, to characterize both the duration and the average speed. Since RAMP-mobility defines trips on a time-basis, the linkage between duration and speed of *real-world* trips is investigated to find probability distributions to randomly select an average speed. For this purpose, Time-Velocity tables (TV-tab) is built analyzing the commuting trips database. Duration and speed are clustered and the probability to obtain a certain average speed class is computed for each time class, considering the absolute frequencies of trips with the same characteristics. The probability table used for Italy to model the link between trip duration and average speed is reported in *Figure 4.3*. These tables aims to introduce a realistic dependence between how much a trip last and its average speed, and to improve the consumption estimation, since average speed is a key parameter for its assessment.

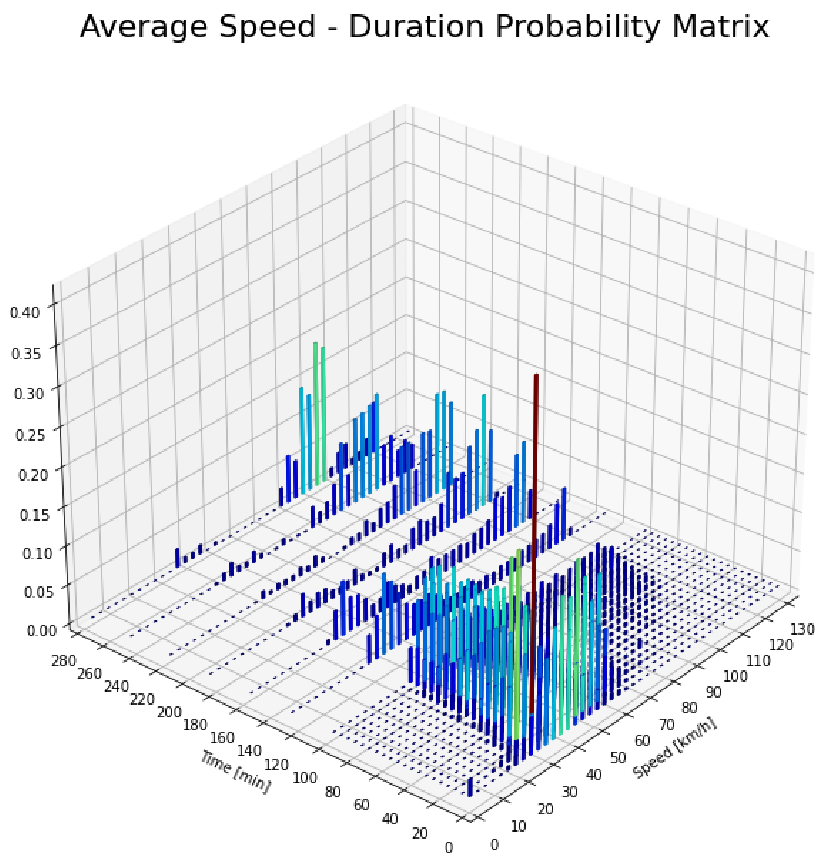

Figure 4.3: Graphical picture of the matrix linking trip duration and speed.

Vehicle fleet composition analysis

A further step is the analysis of the vehicle fleet for each Italian region to obtain an accurate picture of the vehicle fleet. The dataset from Ministero delle Infrastrutture e dei Trasporti (MIT) [26], containing region-specific information about road vehicles, including both cars and motorcycles, is analyzed. Data are obtained from the national vehicle registry and the last version of 2019 is considered. The raw dataset classifies all vehicles according to different characteristics as vehicle type (car or motorcycle), intended usage, brand, displacement, type of fuel, power, date of registration, Euro class and total vehicle mass. The information used to classify the vehicles into six reference segments are displacement, power, and total vehicle mass. Only internal combustion engine cars with transport of people as intended usage are considered, all other details are not taken into account.

As first step of the analysis the dataset is cleaned from vehicles with missing information or too high values of mass and displacement, to delete those which are not properly passenger cars. The reference vehicles are selected according to the same three parameters previously highlighted, and divided into six segments to represent all the types of cars available on the market. These categories have been named: *Utility, Small, Medium, Station Wagon, Sport-Utility-Vehicle (SUV)* and *Executive.* For each of them a reference vehicle model is chosen among the ones available on the market. Additionally, reference EVs models have been selected aiming to have the corresponding electric vehicle classification, necessary to implement in RAMP-mobility the vehicle share composition and characteristics. The selected couple of vehicles for each segment is showed in *Table 4.3*, highlighting the key parameters used for the classification of the ICEV database.

	ICEV MODEL	[cc]	**Power** [kW]	**Mass** [kg]	**ELECTRIC MODEL**	**Battery** [kWh]	**Mass** [kg]
Utility	Fiat 500	1000	51	1300	Fiat 500e	24	1365
Small	VW Polo	1000	85	1500	Peugeot 208e	50	1530
Medium	VW Golf	1500	110	1700	VW ID3	58	1805
SW	Audi A4	2000	140	2100	Tesla Model 3	79.5	1931
SUV	Toyota RAV4	2500	160	2500	Audi E-Tron	95	3170
Executive	Mercedes E class	3000	245	1830	Tesla Model S	100	2175

Table 4.3: Reference vehicle models for each segment.

For each vehicle a match with one of the reference models is searched considering all the three single parameters. The reference class is assigned when at least two out-of-three parameters match with the same segment. If this does not happen an average of the matching classes is computed and attributed to the vehicle. To be noticed that the order of the six classes depicts increasing values for the whole set of parameters, except weight. The results obtained for each Italian region are showed in *Figure 4.4*, and through the population share the national average is estimated. National vehicle fleet is mostly composed by smaller segments, while *Suv* and *Executive* vehicles have only few percentage points. Northern regions are characterized by lower values for *Utility* and *Small* cars, whereas larger ones have shares higher than the Italian average.

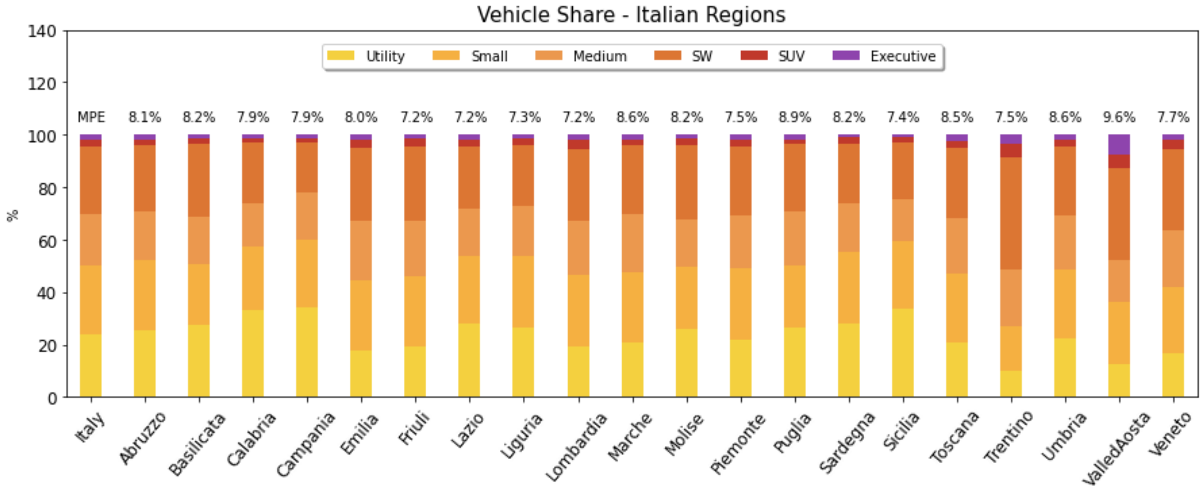

Figure 4.4: Vehicle breakdown into segments as assessed from MIT [26]. The deviation between the real vehicle fleet mix and the represented one is evaluated through the computation of the Mean Perecentage Error (MPE) displayed on the top of each bar.

To evaluate the validity of this classification, a mean percentage error is also returned as average of the relative errors for mass, power and displacement. This to estimate the inaccuracy of assignment of the vehicle to the selected segment. Looking at the values reported in *Figure 4.4*, for all the regions the error is on average lower than 10% which is considered acceptable seen the high number of vehicles. The analyzed vehicle fleet is almost only composed by ICEV; however, it is assumed that in a nearly future there will be BEV models in all car segments, and that the distribution will be very similar to the one of conventionally-powered cars.

The higher level of detail in modelling the vehicle fleet is adopted to understand if the level of accuracy of the framework could be improved. This is going to be tested in *Chapter 7* for Italy since the processed database contains information only for the Italian country.

Kilometer analysis

The last step of this analysis is the kilometer characterization. The input of RAMP-mobility that determines the total transport demand is the daily distance travelled by each user type, which is subsequently split on the different functioning windows. The region-specific annual kilometer from *UnipolSai* [38] is fixed as reference, and is used as average of total annual kilometer for the given region. The dataset comes from the analysis of black boxes installed on cars, and the values are showed in *Figure 4.5*. The first column is associated to the country value obtained considering the population share.

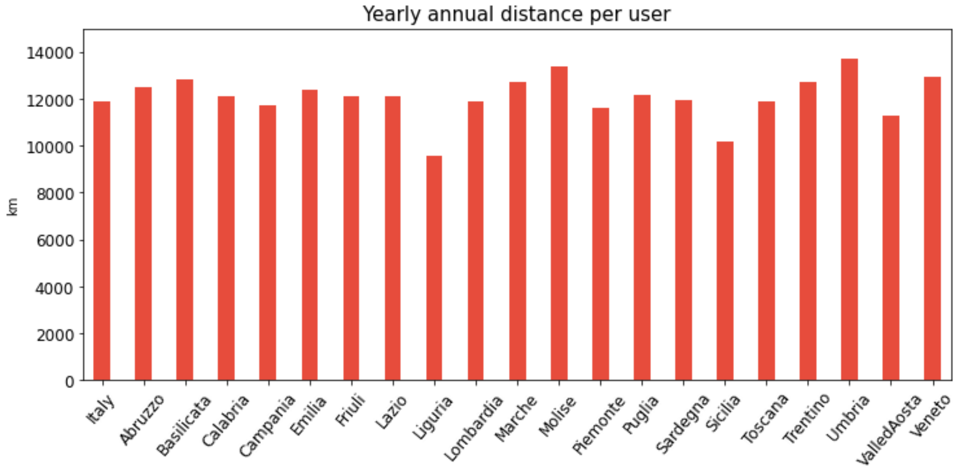

Figure 4.5: Vehicle yearly driving distance from *UnipolSai.* [38]

The daily driving distance specific for type of user (*Worker, Student* and *Inactive*) and for day-type (*Weekday* or *Weekend*) is computed. The breakdown is obtained respecting (i) the ratio between average distance of workers and students given by the analysis of data from commuting trips records [18]; (ii) the regional population distribution in the three user classes according to Istat [16]; (iii) and the ratio between weekday and weekend kilometer fixed at 1.1 from the JRC survey [1]. This ratio is respected only for *Inactive* users which are modelled considering the *UnipolSai* average annual value. Total distance for the weekend is assumed constant and independent on the user. Considering the number of weekdays and weekends the total annual values are divided accordingly, and the daily driving distance for each user type and day of the week is computed. Results of the division for a sample region (*Valle d'Aosta*) are reported for clarity in *Table 4.4*, and the same process is followed for each of the other regions. The breakdown of population into type of user required by RAMP-mobility is showed in *Figure 4.6* and it is estimated from Istat database [16] which splits the population into employed or non employed and estimate percentages of students inside these two main groups.

Valle d'Aosta

	Weekday	**Weekend**	**Total**
Worker	8470	3647	12117
Student	4875	3647	8522
Inactive	7985	3647	11632

Table 4.4: Valle d'Aosta - Yearly per user driving distance in *km*.

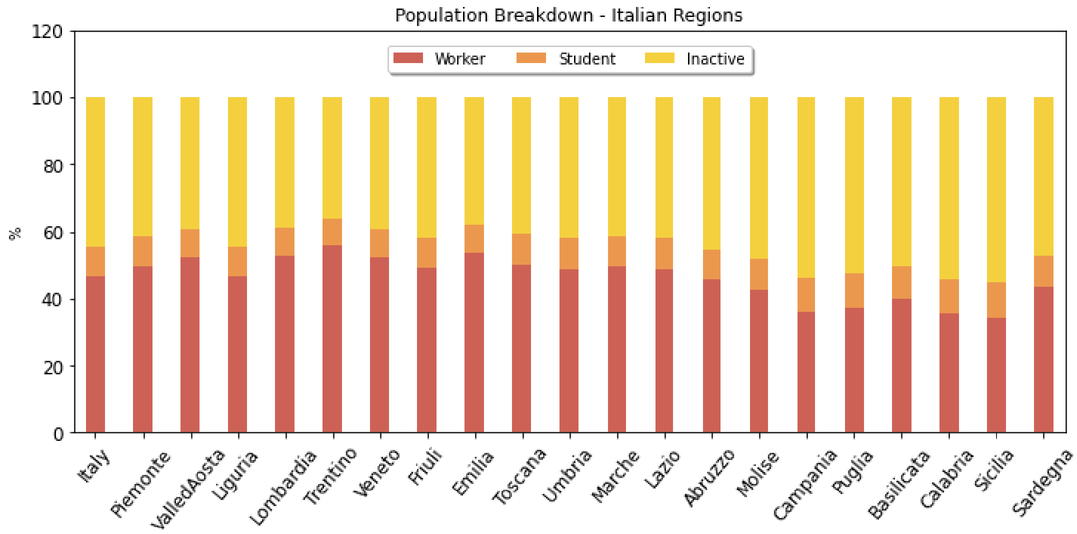

Figure 4.6: Population breakdown into user classes.

The following step consist in the identification of the functioning windows necessary to split the average daily distance during a day. Istat database has been used for this purpose describing the share of people doing certain daily activities with a 10 *min* resolution [15]. From the database two different datasets with different level of aggregation have been analyzed. The activity *Finalized Trips* is the one selected in both datasets, but some differences are found in the aggregation level. The first one is region-specific and is used for distributing the driving distance along the day; while the second one characterizes different types of users as occupied or non-occupied, and is used to identify the functioning windows. In common they both specify different distributions for *Weekday, Saturday,* and *Sunday.* In this analysis workers are associated with occupied people in working days, students with non-occupied people in working days, inactive as the total of weekends and inactive during weekdays as those on Saturdays.

The first dataset with the percentage of people doing *Finalized Trips* every 10 *min* is multiplied by the average kilometers for each user and day type to distribute the total daily travelled distance. The fundamental assumption behind this characterization is that kilometers' division follows the same distributions of the percentage of travelling people. From the second dataset functioning windows are obtained differentiating peak hours from off-peak ones. Weekdays and Sundays are characterized by two peak functioning windows (*Main*), one in early morning and the other one in evening hours; and three off-peak (*Free Time*); Saturdays have instead one *Main* and two *Free Time.* With the arrangement of users and day of the week four different combinations are identified: *Worker* and *Student* in weekdays, *Inactive* for weekdays and Saturday, and lastly *Inactive* on Sundays. The assumption behind this reasoning is that all users behave as *Inactive* during the weekend, and the *Inactive* users have the same behavior on weekdays and Saturdays, while specific windows are chosen to model Sundays. A graphical representation of the four types of windows is displayed in *Figure 4.7*, and a variability of 10% on *Free Time* duration is considered as input random parameter in RAMP-mobility to introduce stochasticity on functioning windows duration.

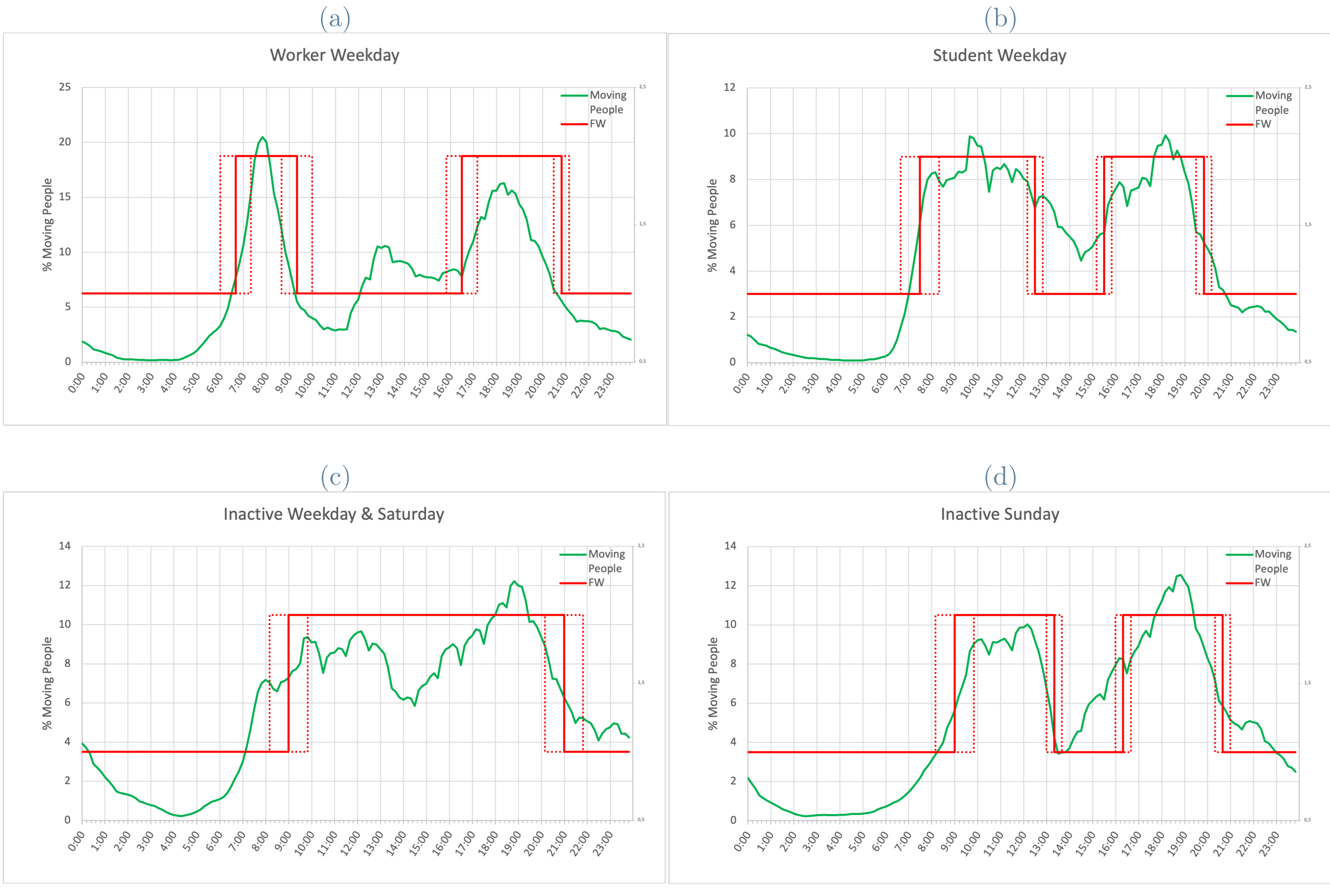

Figure 4.7: Functioning Windows compared with moving people profiles from Istat. [15]

Functioning windows are used to filter the daily kilometers and compute the average distance in *Main* and *Free Time* for each user type and day of the week. This process is followed considering data for each single region, and then aggregated using the regional population as weights to obtain the Italian average. The results for the sample region *Valle d'Aosta* and for the Italian average are summarized respectively in *Table 4.5* and in *Table 4.6*.

Valle d'Aosta

	Worker	Student	Inactive	Saturday	Sunday
Main	16.7	12.1	21.6	24.6	20.8
Free Time	15.3	6.3	8.5	8.6	12.3
Total	32.0	18.4	30.1	33.1	33.1

Table 4.5: Daily driving distance for each functioning window in km.

Italy

	Worker	Student	Inactive	Saturday	Sunday
Main	16.7	11.9	22.2	25.0	22.2
Free Time	16.3	6.7	8.3	8.6	11.4
Total	33.0	18.6	30.6	33.7	33.6

Table 4.6: Daily driving distance for each functioning window in km.

After this detailed analysis a comparison with the national values currently used as inputs in RAMP-mobility and coming from the JRC report [1] is presented in *Table 4.7*.

Italy - JRC

	Worker	Student	Inactive	Saturday	Sunday
Main	16.9	16.9	36.1	46.4	46.4
Free Time	33.1	33.1	13.9	8.6	8.6
Total	50.0	50.0	50.0	55.0	55.0

Table 4.7: Daily driving distance for each functioning window in km according to original RAMP-mobility dataset, based on JRC survey. [1]

Looking at the input data computed with the original RAMP-mobility source [1], it is evident the lower overall driving distances produced with this analysis, and a greater fraction of kilometers driven in *Free Time* functioning windows for weekdays and even higher for weekends. Considering as comparison the data from Istituto Superiore di Formazione e Ricerca per i Trasporti (ISFORT) [20] they are closer, as overall driving distance, to the results obtained with the data processing explained in this chapter. Indeed, ISFORT surveys reported an average driving distance of about 28 km for weekdays and 34 km for weekends, which are in line with the results reported in *Table 4.6*.

4.1.2. Mobility

The methodology illustrated in *Section 3.2.1* concerning the introduction of structural improvements to RAMP-mobility is here applied to Italy. The changes implemented are those related to the mobility module, hence dealing with the functioning windows definition, the daily distance coherence, and the vehicle consumption estimation. Using the updated data for Italy derived in *Section 4.1.1*, the structural mobility improvements are introduced step-by-step to underline the effect of each single change on both mobility profiles and energy consumption. An overview of these implementation is summarized in *Table 4.8*.

Name	Description
Reference	Updated input data: Population and vehicle composition Driving habits
Mobility behaviour	Complementary functioning windows Distance recovery
Trip specific consumption	Trip link to Driving Cycle Trip specific consumption
Vehicle consumption model	VCAM introduction

Table 4.8: Overview of the changes implemented in RAMP-mobility applied to Italy.

Reference

Starting from RAMP-mobility in its original version for Italy, the *Reference* model is obtained updating data about population breakdown, vehicle fleet composition, and driving habits; derived from the aforementioned analysis of national data sources.

Population breakdown and vehicle fleet

The breakdown of population into *Worker, Student,* and *Inactive* classes is updated using the aggregation of regional data. Similarly for the vehicle fleet composition, which number of segments is increased up to six *(Utility, Small, Medium, Station Wagon, SUV and Executive)* since this breakdown is considered more detailed, and able to depict the whole variety of vehicle types powered with electric motors. The new fleet breakdown is implemented adding new *Appliances* to the model and inserting new battery capacity values, as in *Table 4.3*. Seen the new vehicles introduced, to use the JRC consumption function the closest set of coefficients is assigned to each class since these are defined only for the three original vehicle classes *(Small, Medium, Large)*. Additionally, the *Free Time* occasional use, which aims to model the possibility of not using at all the car in a *Free Time* functioning window, is updated considering taking the car once a weekday hence set to 20% instead of 15%, whereas the weekend value is fixed at 35%, keeping the original difference between the two values.

Driving habits

New functioning windows derived from moving people profiles are implemented, and some trip characteristics are changed according to the values found in the previous analysis. The original model takes as input average trip duration and distance, using them to compute an average randomized speed that is assumed to be the mean velocity of the car for the whole day. This is then used to estimate the daily driving time and the average consumption for each trip. A more direct approach is adopted for the new model version, using data from the Italian analysis of commuting records described in *Section 4.1.1*. A value of mean velocity empirically estimated is inserted with its variability as reported in *Table 4.2*. Also the average trip time is updated according to the analyzed Italian trip records. Variability on the average trip time of 20% is also inserted, since this is the only input data without this characteristic in the original framework. As final input data change, the average daily driving distance is updated with values derived from the regional analysis of *Section 4.1.1*. These values are set for each user, day of the week and are already divided into type of functioning window, hence pre-processing the daily kilometers. Since the original RAMP-mobility instead splits inside the model the input total distance in the different types of functioning windows, the *percentage usage* variable is removed. In *Figure 4.8* the original stochastic process and the updated one are showed, highlighting the differences concerning variable name changes and new variability introduced.

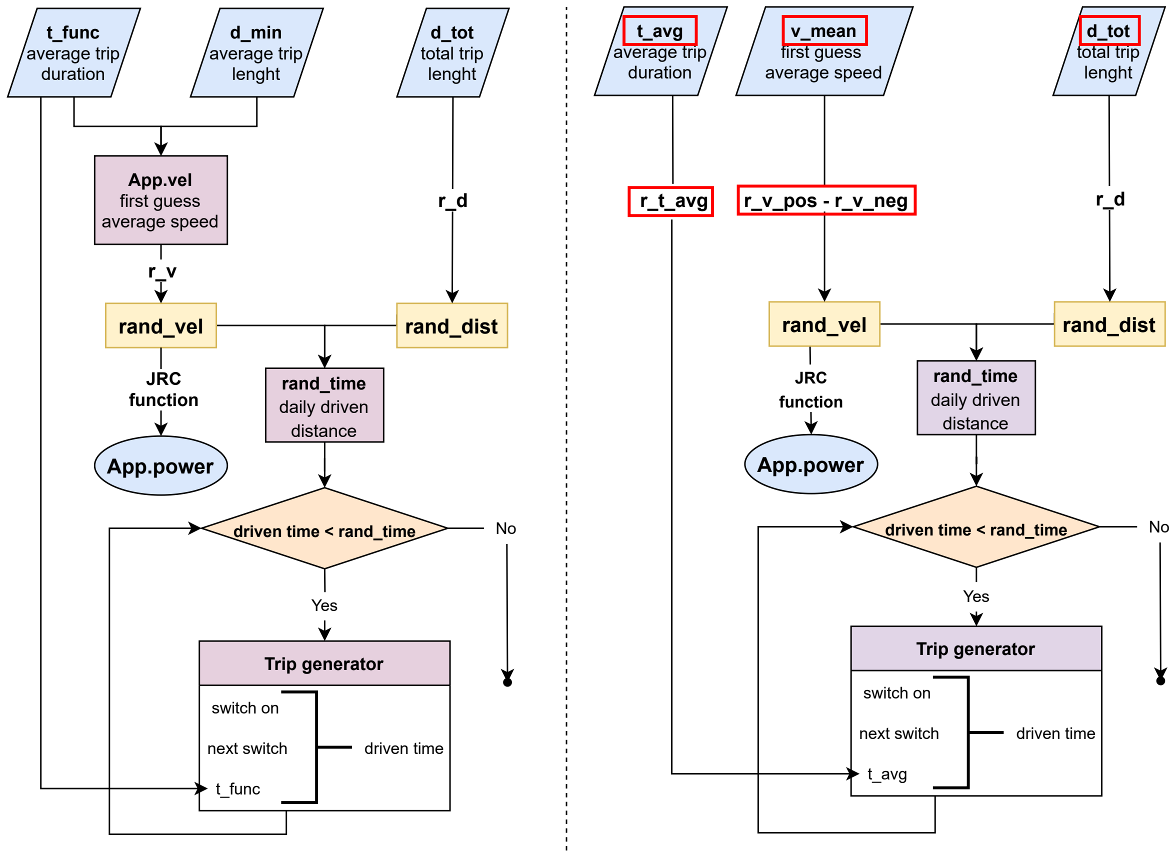

Figure 4.8: Synthesis of the modifications applied to the model variables in the first steps related to input data variation.

Mobility behaviour

In this section methodological changes already described in *Chapter 3* are introduced aiming at improving the inconsistencies found in the study of the original model structure. These variations affect the core of the mobility profile generation process.

Complementary functioning windows

The first change implemented is related to the definition of functioning windows extremes. As already described in *Section 3.2.1*, a complementary approach for the definition of *Main* windows is applied. Concerning the *Free Time* windows another change is implemented to represent the lower probability of using the car in a night time-frame instead of the mid-day hours. This is set for *Appliances* characterized by three *Free Time* functioning windows as those on weekdays for *Worker* and *Student*, and on Sundays. The chosen probabilities are 20% for early morning and late-night trips, whereas 60% is selected for mid-day ones. This solution comes from considerations about the shapes of the profiles used to define the functioning windows, which show a clear difference among trips frequency between day peaks and time-frames before or after them.

Distance recovery

The variation here implemented is introduced to solve the incoherence between the input daily distance and the one which is effectively simulated by RAMP-mobility. The implementation of this correction requires the inversion of the order in which the *Appliances* are run. The application of this improvement to *Italy* do not require any additional input and restore the coherence between input driving distance and simulated one.

Trip specific consumption

This step deals with the vehicle consumption estimation in particular with its specificity which is moved to the trip level, avoiding the adoption of a daily average value. Firstly, an empirically generated probability distribution, derived from the aforementioned Italian analysis, is used to link the trip duration to a travel velocity. In this way each trip is described by the couple *duration* and *speed*, and can be linked to one of the driving cycles previously created using the Driving Cycle Generator, described in *Section 3.1*. As explained in *Section 3.2.1*, the implementation of this trip-specific consumption, using the original consumption model based on the JRC correlation [31], occurs through pre-computed consumption tables. These additional inputs are not specific to the case study, and a matching between the six-segment Italian vehicle fleet and the three types of vehicle modelled by JRC equation is implemented. *Utility* and *Small* are modelled with *Small* parameters, *Medium* and *Station Wagon* with *Medium*, while *SUV* and *Executive* with *Large*.

Vehicle consumption model

A new consumption model is implemented using VCAM dynamic simulator to compute the average power consumption associated to each driving cycle. This approach increases the technological detail of the power estimations through a more accurate physical description of the vehicle dynamics. The same probability distribution used in the previous paragraph, and obtain from data as explained in *Section 4.1.1*, is adopted to determine the average trip speed and to link single generated trips to realistic driving cycles. The difference is in the adopted consumption tables which are computed using the VCAM model. Six tables, one for each vehicle class, are created applying VCAM to each DC, and given as input to RAMP-mobility. The model links average consumption values to trips according to the key features duration and average speed. The vehicle types used to model each segment are the same adopted for the Italian vehicle fleet analysis in *Section 4.1.1*, then no update of the tables is required. If a new vehicle fleet characterization would be implemented using different reference cars, consumption tables need to be recomputed.

4.2. The Netherlands

4.2.1. Data analysis

For The Netherlands case study no specific update of the input dataset is planned, since the focus of this work is on the effect of structural improvements. The application of the upgraded RAMP-mobility structure to the original dataset, mainly based on JRC source [1], provides insights on the output variations independently from an input data refinement. However, the adaptation of the daily driving distance is required when coupled with the distance recovery, thus a scale down of the original dataset is applied to each European country. Indeed the distance estimated by JRC [1] seems to overestimate the transport demand and given the similarity between the value obtained for Italy from data processing, and the distance reported by Isfort [20], a rescaling coefficient is computed. Average distances of JRC survey are reduced of about 40% dividing them by the ratio between JRC value for Italy and Isfort one, which is around 1.7. The new distances obtained are presented and compared with original ones in *Table 4.9*. Thereafter these are used as inputs in RAMP-mobility to model the European countries, and in particular applied to The Netherlands case study.

	Original		Rescaled	
Country	**Weekday**	**Weekend**	**Weekday**	**Weekend**
FR	50	60	27	32
DE	55	55	32	32
IT	50	55	29	32
PL	80	80	47	47
ES	70	80	41	46
UK	40	40	23	23

Table 4.9: Daily driving distance for each country in *km*.

The correction of average distance is tested in *Chapter 6* by computing the vehicle annual kilometers and comparing them with an external source. The accurate estimation provided by the model proves that the rescaling is necessary. Additionally, the trip duration-velocity table is needed as new input, and since no trip database is analyzed for this country the one obtained for Italy is extended.

4.2.2. Mobility

The step-by-step implementation described for Italy is applied to The Netherlands since this country will be object of charging profile assessment in *Chapter 6*. Few data are varied since no significant studies have been made specific for this country, hence the difference between the two applications lies in the input data which have different sources: European databases for The Netherlands, as in the default RAMP-mobility version, and national databases for Italy.

Reference

The Italian analysis described at the beginning of this chapter allowed to determine specific characteristics for Italian trips. Given the similarity of computed average speed for Italy to the one determined through JRC data, the value for all the other European countries is determined using the same values of distance and time of the original model, with the difference of being pre-computed and given as inputs to the model. This method is adopted since the differences in velocity limits in European countries and in driving behaviour are significant, thus the daily average velocity computed for Italy cannot be extended to other countries. The variability on this input velocity is instead updated following the one introduced for Italy, which is set to 18% for the positive direction and 21% for the negative one. Concerning the average trip time it is kept as the initial value of RAMP-mobility for the same reasoning above, but 20% variability is introduced on it, since this is the only parameter without this feature in the original model. Seen the incoherence revealed in the Italian analysis between computed daily distance and the JRC data, given as input to RAMP-mobility, the distances for the other European countries have been rescaled. Input data have been updated as illustrated in *Section 4.1.1*. Differently from Italy, the input distance is the daily average not divided in functioning windows, thus the *percentage usage* variable is kept. Additionally, as for Italy *Free Time* occasional use is updated to 20% for weekdays instead of 15%, while weekend value is fixed to 35%.

Mobility behaviour

The same approach used for Italy is introduced for The Netherlands to solve modelling limits found in the analysis of the model. Complementary functioning windows and driving distance coherence are then implemented.

Trip specific consumption

The necessary element to allow the coupling of trips generated with RAMP-mobility to a driving cycle is the relation between trip duration and average speed. Time-velocity probability distribution produced for Italy is assumed to be valid for all the other European countries since no specific national databases have been investigated. Consequently, Italian distribution is extended to all the European countries and is used as input to RAMP-mobility.

Vehicle consumption model

Also in this step the probability distribution derived for Italy is extended to The Netherlands to obtain average trip velocities corresponding to trip duration. VCAM is used to estimate the vehicle consumption associated to each driving cycle. The only difference with respect to Italy is in the tables used to find the consumption value associated to the couple of trip parameters. Three out of six tables produced for Italy are chosen to model the vehicle fleet, which is divided in only three segments *(Small, Medium, Large)* in the original model version.

In *Table 4.10* all the changes introduced are synthesized dividing them per type of action implemented, whereas in *Appendix B* a more detailed description is presented.

<table>
<tr><th></th><th>Driving time/distance</th><th>Functioning windows</th><th>Input distance coherence</th><th>Consumption</th></tr>
<tr><td>Reference</td><td rowspan="4">App mean velocity from data analysis
New average time (t_avg) + variability
New daily distance (d_tot)</td><td>Original definition</td><td>Missing</td><td rowspan="2">Daily average,
JRC equation</td></tr>
<tr><td>Mobility behaviour</td><td rowspan="3">Complementary definition
Inverting App sequence</td><td rowspan="3">Solved
(Free Time distance
is recovered)</td></tr>
<tr><td>Trip specific consumption</td><td>Trip specific,
JRC equation</td></tr>
<tr><td>Vehicle consumption model</td><td>Trip specific,
VCAM</td></tr>
</table>

Table 4.10: Synthesis of the main improvements introduced in RAMP-mobility.

5 | Results

In this chapter the results of the Driving Cycle Generator tool, together with the improvements introduced in the original RAMP-mobility for Italy and The Netherlands, described in *Chapter 4*, are presented. Lastly, the results of user connection time-series are displayed to assess the impact of charging probabilities.

5.1. Driving Cycles generator

For what concern the output of the Driving Cycles Generator, the results of the different types of generated DCs are illustrated. Several values of average velocities are considered to analyze how this parameter influence the shape of the driving cycle, and the input time is chosen in relation to the driving cycle needed. Afterwards, the comparison with *Emobpy* generator is carried on to assess the differences between the two tools.

5.1.1. Construction

Urban driving cycles

Starting with the *Urban* driving cycle, two cases are reported at 12 km/h and 22 km/h both with 20 min as duration. The *Urban* WLTC section is repeated until the total trip time is reached; in *Figure 5.1* the two DCs are compared. In the fastest DC the maximum velocity is higher than in the other one due to a higher scale factor needed to rescale the reference section, and reach the input average speed. In the slowest one the final transition can be noticed, which is added to bring the final value of velocity down to zero and have a condition of stop at the end of the driving cycle.

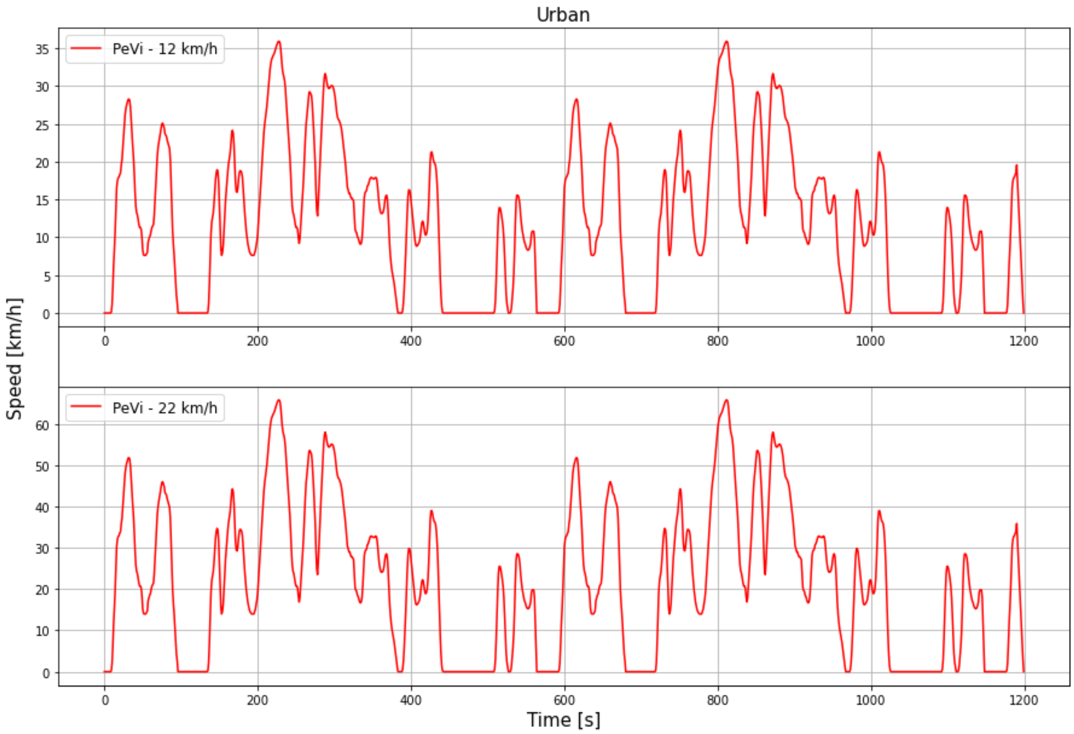

Figure 5.1: *Urban* driving cycles with different average velocities.

Urban-ExtraUrban driving cycles

The selected *Urban-ExtraUrban* driving cycles are characterized by average speeds of 30 km/h and 45 km/h with 40 min as duration. The longer time is selected to have more than one section of reference *ExtraUrban* replicated, and to graphically notice the impact of higher average speed on the Urban Share. A higher average speed, as in the case at 45 km/h, produces a reduction in the urban sections and more space is reserved for the *ExtraUrban* WLTC section. Two sections with maximum speed at 100 km/h are replicated in the upper plot of *Figure 5.2*, and less urban seconds are placed at the beginning and at the end of the driving cycle.

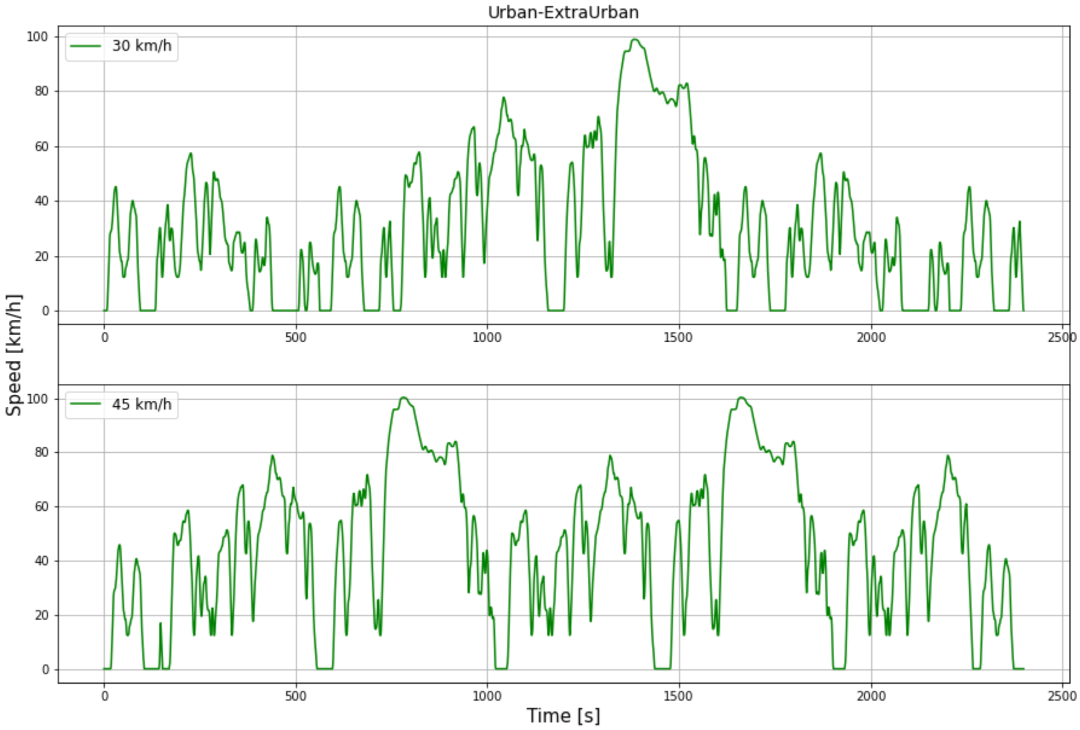

Figure 5.2: *Urban-ExtraUrban* driving cycles with different average velocities.

Urban-Highway driving cycles

In *Figure 5.3* the simplest custom *Urban-Highway* driving cycle is presented with input parameters of 50 km/h and 10 min. The short duration is chosen to represent the case with less than one reference *Highway* section, hence avoiding the *Probabilistic Highway* approach. At the border between central highway section and final urban an important transition can be noticed, since the last value of velocity is around 120 km/h and the following section starts from 0 km/h. The time reserved for this connection is computed assuming a conservative constant deceleration of about $0.1g$.

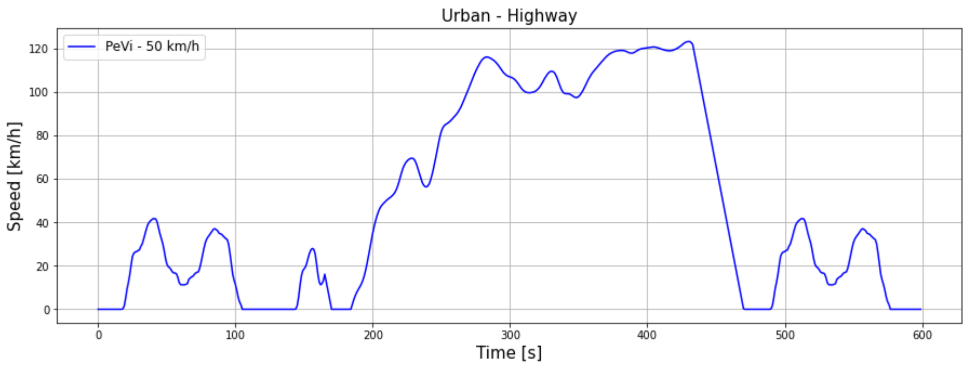

Figure 5.3: *Urban-Highway* driving cycles in its simplest configuration.

Urban-Highway Probabilistic driving cycles

Before illustrating the *Probabilistic Highway*, the Transition Probability Matrix (TPM) representing the velocities states is presented. As already mentioned in *Section 4.1.1*, the TPM is used to create the driving pattern for central *Highway* DC, when more than one WLTC highway sections should be repeated. Given an initial velocity, the following one is defined with a random choice according to the probability distribution obtained from the analysis of the reference WLTC *Extra-High* section. The TPM, defined by actual and next velocity, is obtained clustering data with a 2 km/h gap. A graphical representation of the matrix is reported in *Figure 5.4*.

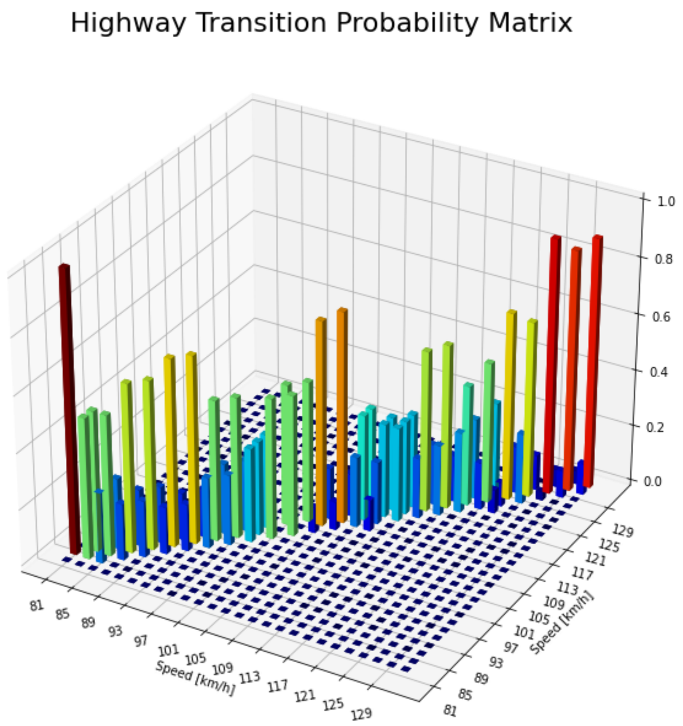

Figure 5.4: Transition Probability Matrix (TPM) from which the *Probabilistic Highway* is generated.

Probabilistic Highway approach is followed to avoid periodic start-and-stops in the central highway part, which is considered an unrealistic driving pattern. Some sample cases of *Urban-Probabilistic Highway* are reported with chosen input velocities of 50 km/h and 110 km/h. The custom DCs obtained are characterized by a central highway section, depending on the path followed with the TPM, and by initial and final urban, which length is computed from the Urban Share considering *Highway* reference average velocity.

In the two selected cases the US varies significantly due to the different average speed, and this is reflected in less time steps in urban driving environment (*Figure 5.5*).

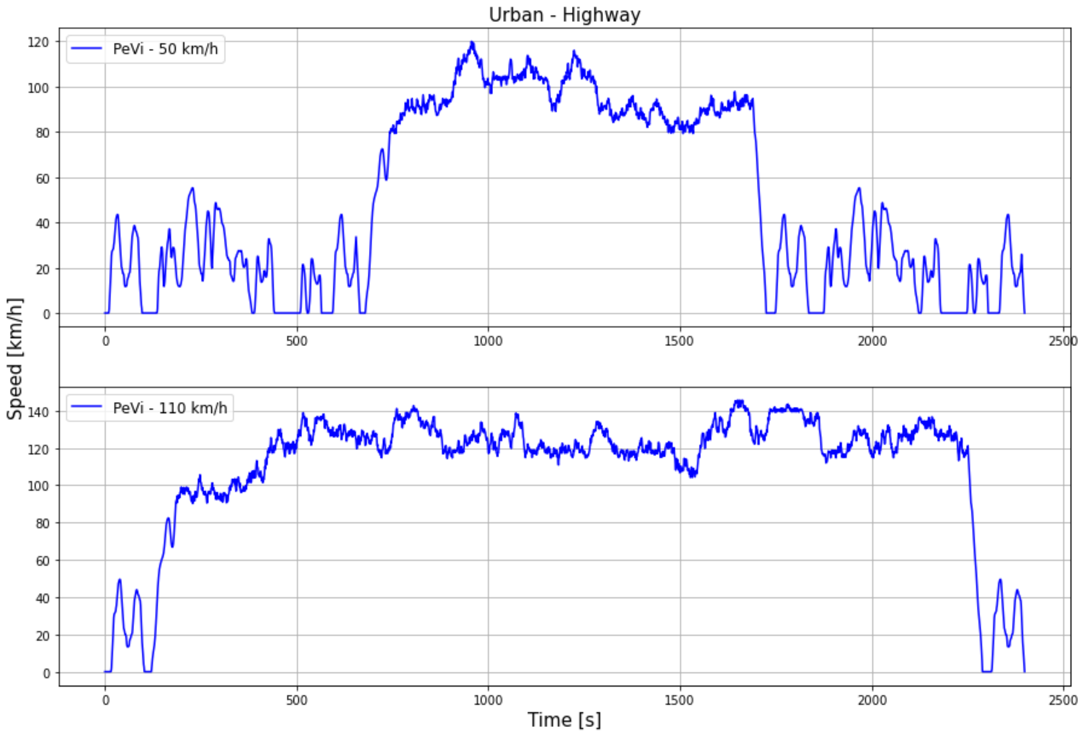

Figure 5.5: *Urban-Highway Probabilistic* driving cycles.

Highway Probabilistic driving cycles

This case is a particular situation in which the input average speed is high, while the duration is relatively short, hence large scaling factors are required to keep the desired input velocity. Consequences of this rescaling are over-stressed acceleration and deceleration, which cannot be followed by all types of cars. Two cases have been selected to clarify this situation. Having 10 min as selected time with 70 km/h as velocity, the scale factor does not represent a limit, hence initial and final urban sections are kept. Instead, with average speed up to 90 km/h the scale factor reaches values higher than the threshold causing accelerations above 2 m/s^2, which is considered the acceptable limit. A new driving cycle is consequently generated avoiding the urban sections, as in the lower chart in *Figure 5.6*. This control feature allows to generate realistic driving cycles even for uncommon couple of input values.

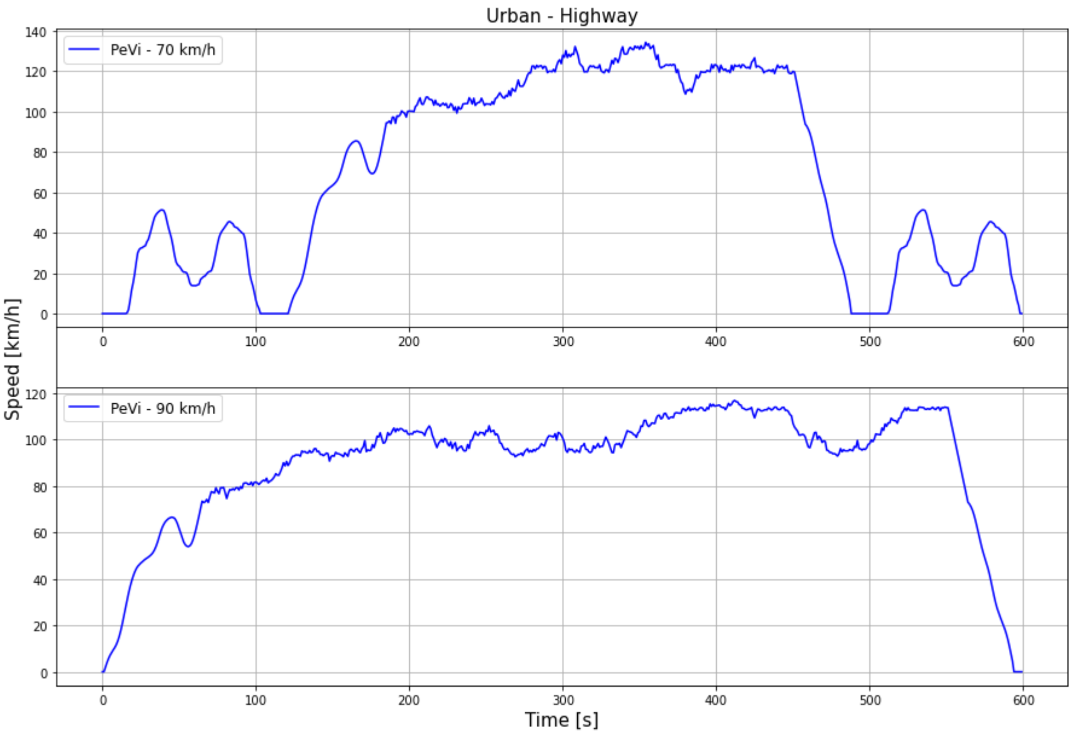

Figure 5.6: *Highway Probabilistic* driving cycles in which urban sections are avoided to limit the scale factor.

5.1.2. Comparison with *Emobpy* Driving Cycles generator

A comparison with *Emobpy* methodology is performed to evaluate the differences of these two similar approaches. The selected driving cycles are the critical ones, meaning those with average speed closer to the limit of each class for both the generator developed with this thesis, named *PeVi*, and the one used in *Emobpy*. The input time is set at 15 *min*, while the average velocity values for the five selected cases are illustrated in *Table 5.1*.

		Speed [km/h]
Emobpy limits	**Case 1**	30.7
	Case 2	49.1
	Case 3	71.9
PeVi limits	**Case 4**	22.0
	Case 5	48.6

Table 5.1: Cases analyzed to compare *Emobpy* and *PeVi* generator tools.

For both approaches the five driving cycles are represented in *Figure 5.7* and differences can be identified. The first important aspect is the last time step velocity in *Emobpy* DC which is often not at 0 km/h. This happens since the reference WLTC sections are replicated until the total input time is reached, and this could be at any value of velocity, hence representing an unrealistic driving pattern. In the *PeVi* generator this problem is tackled and solved thanks to transitions reducing the last velocity value to reach always a final stop condition.

Analyzing more in detail the different cases, *Case 1* which is a Low-Speed driving cycle for *Emobpy*, is instead an *Urban-ExtraUrban* in the *PeVi* generator. The same urban pattern can be seen for the first 250 seconds in which the two DCs differ only for the scale factor. *Case 2* is in a Medium-Speed environment for *Emobpy* generator, while in the *PeVi* approach the custom DC is obtained through the *Probabilistic Highway*. This is also adopted in the following *Case 3* but with a lower urban share and higher maximum velocities. For what concern the other two limit cases, *Case 4* is in urban conditions and is very similar for both since this is the simplest option and the reference Low-Speed is just replicated; the only difference is the handling of the last time-steps velocities. In *Case 5* differences can be found in initial and final urban sections for the *PeVi* methodology, which are instead not inserted in the Medium-Speed *Emobpy* driving cycle.

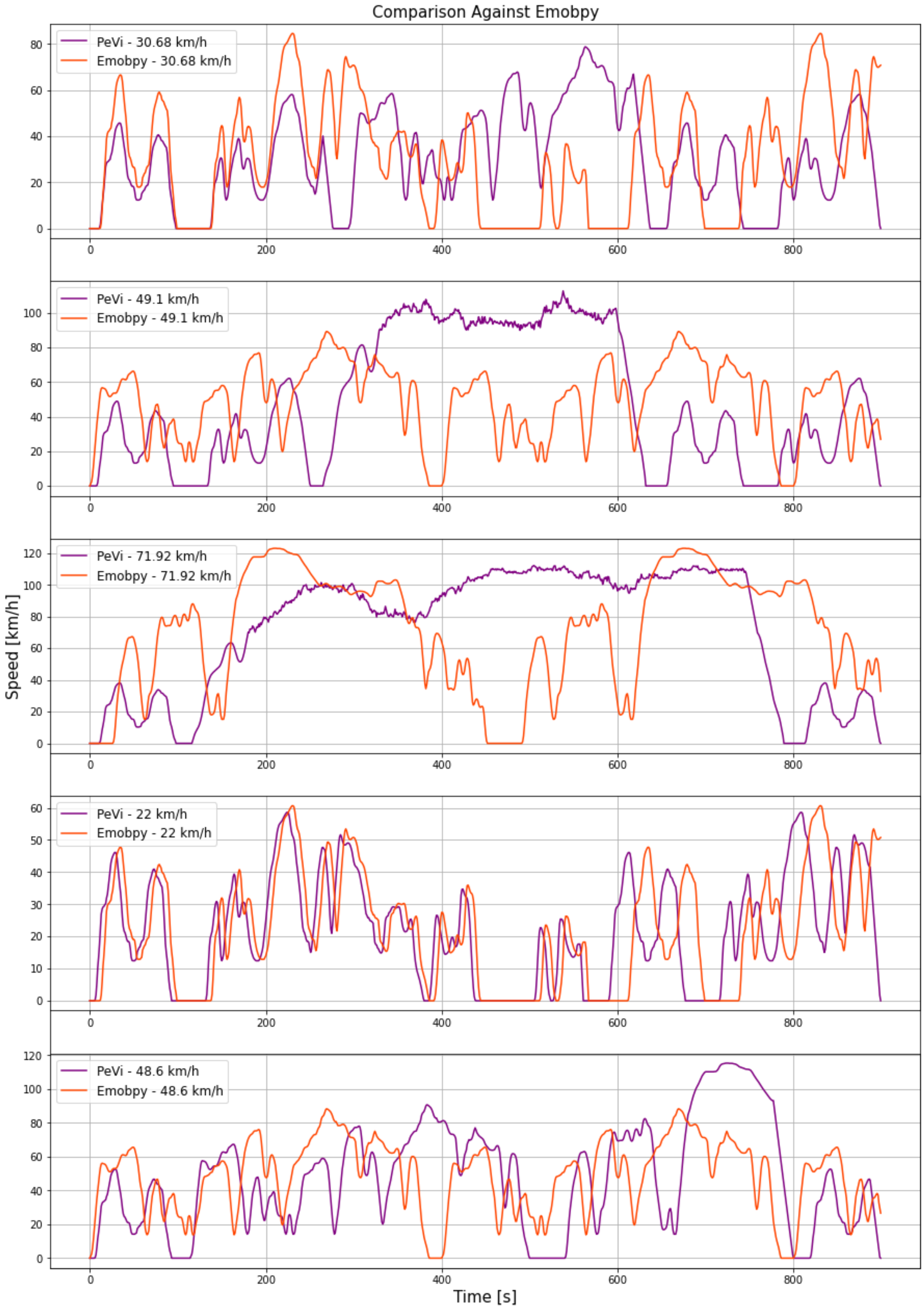

Figure 5.7: Comparison between *PeVi* and *Emobpy* driving cycles generators.

A numerical comparison between the generators is made according to significant indicators which are: maximum speed, maximum acceleration/deceleration and driving share in accelerating, decelerating and idling mode. The values for the WLTC are also reported in *Table 5.2*.

	v_{max} [km/h]	acc_{max} [m/s²]	dec_{max} [m/s²]	$idle_{\%}$	$acc_{\%}$	$dec_{\%}$
WLTC	131.3	1.8	-1.5	17.1	42.4	40.6
Case 1 PeVi	78.8	1.6	-1.5	16.6	46.7	36.7
Case 1 Emobpy	84.6	2.4	-2.3	25.7	37.8	36.5
Case 2 PeVi	125.7	1.5	-1.4	14.5	45.6	39.9
Case 2 Emobpy	89.3	1.9	-1.8	6.7	52.3	41.1
Case 3 PeVi	120.5	1.3	-1.5	6.9	47.4	45.7
Case 3 Emobpy	123.0	2.2	-1.9	16.6	40.9	42.5
Case 4 PeVi	58.6	1.7	-1.6	23.4	37.8	36.5
Case 4 Emobpy	60.6	1.7	-1.6	25.7	37.8	36.5
Case 5 PeVi	115.4	2.1	-1.8	14.2	46.2	39.6
Case 5 Emobpy	88.4	1.9	-1.7	6.7	52.3	41.1

Table 5.2: Numerical comparison between *PeVi* and *Emobpy* driving cycles generators according to selected indicators.

Considering the limit cases for *Emobpy* (*Case 1, Case 2, Case 3*), the maximum acceleration and deceleration values are always higher than those of the WLTC due to a strong rescaling effect, while *PeVi* corresponding driving cycles are closer to reference values. The maximum velocities are slightly higher for *Emobpy Case 1* and *Case 3*, whereas *Case 2* with *PeVi* approach pushes the velocity to 125 km/h. This is due to the *Probabilistic Highway*, which is compared with a Medium-Speed driving cycle having consequently lower speed. Looking at *PeVi* limit cases, the values of acceleration and deceleration are much closer to reference WLTC and lower than *Emobpy*. In *Case 5* the maximum acceleration is above 2.0 m/s^2, previously identified as threshold acceleration, but this is a limit case with the highest rescaling factor not obtainable for other input parameters. For what concern the percentages in idling, accelerating and decelerating modes, *PeVi* driving cycles are always closer to the WLTC values, the only exception is in *Case 3* in which idle mode has a lower share. This is due to the large share of *Probabilistic Highway* with respect to *Urban* which reduces the idling states, however this is realistic considering trips mainly driven in highway conditions.

5.2. RAMP-mobility improvements: mobility

The results of the improvements of RAMP-mobility applied to the two cases presented in *Chapter 4* are showed in these paragraphs. Firstly, the step-by-step implementation of the improvements is presented for Italy and the intermediate steps are compared with the *Reference* model in terms of mobility profile and energy demand. Secondly, the step-by-step application is applied to The Netherlands, to show the effects of structural improvements to a *Reference* case with limited data changes.

5.2.1. Italy

Before proceeding with the presentation of the results, the general data used to produce the mobility profiles are explained. Italy is simulated considering 2500 users and reproducing a series of the three day-types which are weekday, Saturday, and Sunday for 60 days, which means a total of 180 days simulated for each step. 2500 users have been estimated by Mangipinto [24] as a good trad-off between required computational time and the detail of the output. For the comparisons, the average of each day type is computed and represented in all the figures reported in the following sections. This approach is chosen to reduce the impact of stochastic parameters on the mobility profiles and highlight only the differences of the introduced changes. Concerning the number of days, 180 days are selected to catch the average yearly temperature oscillation by simulating almost half a year. Default input data for the stochastic parameters are summarized in *Table 5.3*.

Stochastic Values

	%		%
Windows $_{Variability}$	20	**Occasional use** $_{MainWeekday}$	100
AvgTime $_{Variability}$	20	**Occasional use** $_{MainSaturday}$	60
Distance $_{Variability}$	30	**Occasional use** $_{MainSunday}$	50
Speed $_{PositiveVariability}$	18	**Occasional use** $_{FreeTimeWeekday}$	20
Speed $_{NegativeVariability}$	20	**Occasional use** $_{FreeTimeWeekend}$	35

Table 5.3: Default values for input stochastic parameters adopted for the simulations.

Reference

A general description of the input data updates considered in the *Reference* case is here provided, comparing the new values, assessed in the Italian data analysis, with the original ones of RAMP-mobility. The qualitative comparison aims to show the differences between the two datasets, and for the impact assessment of this data changes on mobility profiles and total energy demand, a dedicated section is added in *Chapter 7*.

Population breakdown and vehicle fleet

The *Reference* case considers an update of the population breakdown as reported in *Table 5.4* where only a minor shift between the percentages of *Inactive* and *Student* can be observed. The vehicle fleet composition is also updated, including a more detailed description of the breakdown with six segments instead of three. The comparison with the original case, reported in *Table 5.5*, highlights a fleet composed of smaller cars. Indeed almost a half is composed by the first two segments and larger cars, classified as *Suv* and *Executive* segments, covers only 4% of the fleet.

	Original	**Reference**
Worker	46.10 %	46.48 %
Student	3.69 %	9.10 %
Inactive	50.20 %	44.42 %

Table 5.4: Population breakdown into user classes.

Original	**Share**	**Battery Capacity [kWh]**	**Reference**	**Share**	**Battery Capacity [kWh]**
-	-	-	**Utility**	24.16 %	24
Small	24.41 %	37	**Small**	25.95 %	50
Medium	68.62 %	60	**Medium**	19.70 %	58
-	-	-	**Sw**	25.74 %	79.5
Large	6.97 %	100	**Suv**	2.59 %	95
-	-	-	**Executive**	1.86 %	100

Table 5.5: Vehicle breakdown implemented after data analysis described in *Section 4.1.1*

Driving habits

Reference case includes also some changes of mobility variables, which are related to the update of input data, and to the introduction of formal changes which modifies only variability aspects, not structural ones. New functioning windows, assessed from the analysis of moving people profiles described in Section 4.1.1, are implemented. An additional variability is applied to the average trip length, which is the only variable not subjected to stochastic oscillation in the default version. The percentage variability on the daily average velocity, v_{mean}, is split in positive and negative values (*see Table 5.3*), obtained from the velocity distribution assessed in *Section 4.1.1*. The average trip features, speed and duration, are updated considering the values assessed from the trip records analysis performed. Lastly, the total daily distance travelled for each user is updated, and a sensible reduction of about 40% is clearly displayed in *Table 5.6*. The reduction of driving distance has great impact on the model since this variable is linearly related with the total transport demand. The large difference is however grounded on the data processing, and is linked to the structural improvement introduced afterwards in the *Distance recovery* step. Without that structural change the real simulated distances are consistently lower, as reported in *Table 5.7*, which shows the results of a post process analysis of the simulated trips. Even if the input-output consistency is not respected, the output average distance of the *Original* simulation is similar in magnitude to the one used as input for *Reference* case. Consequently, a balancing between distance reduction and distance recovery is applied.

Day	User	Window Type	Original	Reference
weekday	**worker**	**main**	16.88	16.73
		free time	33.12	16.27
	student	**main**	16.88	11.91
		free time	33.12	6.65
	inactive	**main**	36.07	22.27
		free time	13.93	8.34
saturday	**inactive**	**main**	46.42	25.03
		free time	8.58	8.64
sunday	**inactive**	**main**	46.42	22.23
		free time	8.58	11.45

Table 5.6: Comparison of daily driving distance per user, data in km.

Original	**Input** [daily km/user]	**Output** [daily km/user]
Weekday	50	30
Weekend	55	39
Reference	**Input** [daily km/user]	**Output** [daily km/user]
Weekday	31	21
Weekend	34	23

Table 5.7: Difference between input driving distance and output simulated one.

Mobility behaviour

The first structural improvements, described in *Section 3.2.1*, require important changes to the stochastic process and solve inconsistencies of the framework. A different procedure to compute the functioning windows is applied and the coherence between input and output distance is solved. The distance skipped during *Free Time* windows due to the stochastic occasional use is recovered and the average daily driving distance is almost equal to the input one, as reported in *Table 5.8*.

As it is possible to assess from *Figure 5.9*, the increase in the total simulated distance causes a higher transport demand, concentrated in the *Main* windows, and significant spikes in the profile during Weekdays about 300 kW higher than the *Reference* case. Less important changes can be observed in Weekends since the *Free Time* occasional use parameter is higher and is present also for *Main* windows. Changing functioning windows extremes has minor consequences both on profiles and total demand, because effects are hidden when different user profiles are summed together. In *Figure 5.8* also the *Original* profile is highlighted to show that the coupling of new input distance and distance recovery produces similar profiles in shapes, but concentrates the demand in peak hours for Weekdays. Saturday and Sunday profiles are less increased by this modification since are characterized by a higher probability of using the car in *Free Time* windows. Moreover, the effect of having a probability of not taking the car even in *Main* windows do not allow the full distance recovery. Looking at values in *Figure 5.9* the overall energy demand is close to the one obtain for *Original*, whereas the increase in demand with respect to *Reference* is about 35% for each day type, and is completely related to the distance recovering mechanism.

Mobility behaviour	Input [daily km/user]	Output [daily km/user]
Weekday	31	31
Weekend	34	33

Table 5.8: Similarity between input driving distance and output simulated one.

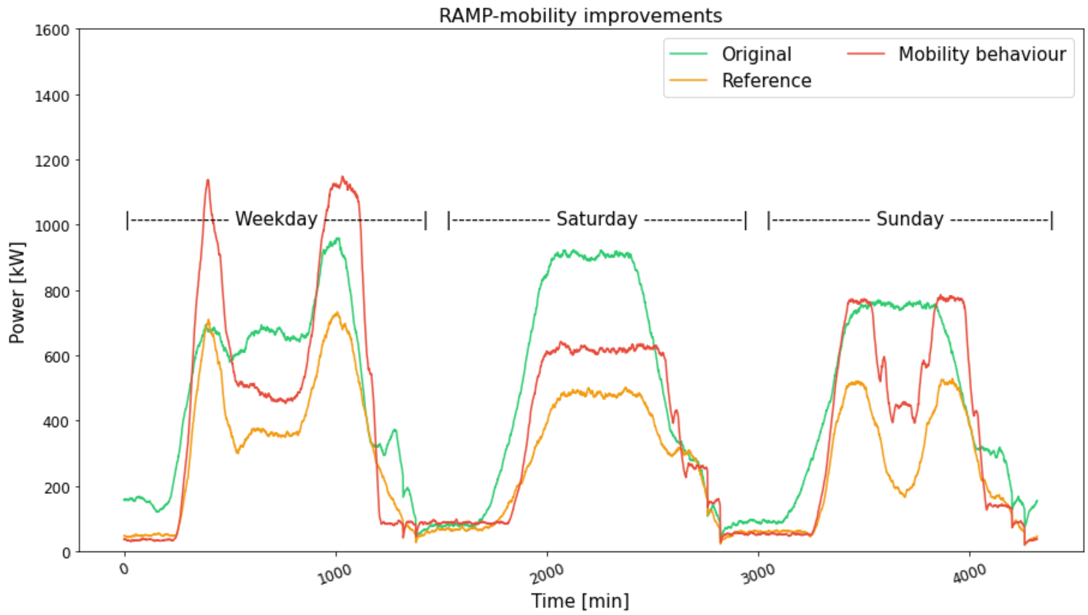

Figure 5.8: Profile comparison between *Original*, *Reference* and *Mobility behaviour* cases.

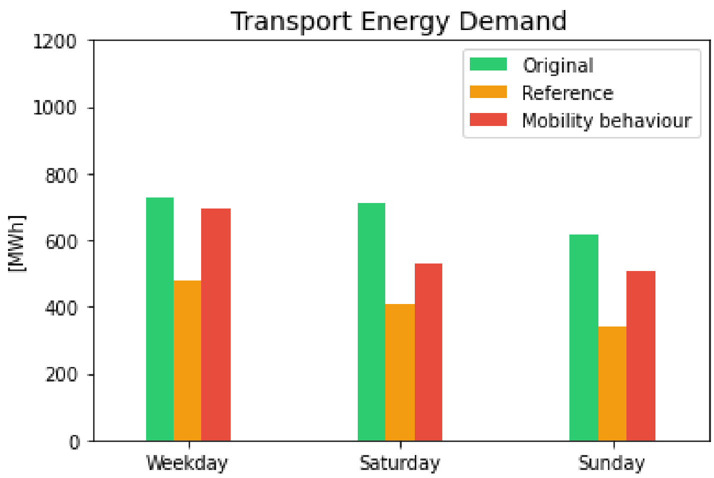

Figure 5.9: Comparing total transport demand of *Original*, *Reference* and *Mobility behaviour* cases.

Trip specific consumption

Trip specific consumption is the key step to improve the technological detail of the consumption modelling. It consists in associating each generated trip to a *real-world* driving cycle, for which a specific value of consumption is computed. This methodological step changes the parameter used to estimate the vehicle consumption, which in the original model was the daily first guess average velocity. The new approach assigns a driving cycle to each trip according to the couple of key parameters, average *speed* and *duration*, and computes the average consumption through the JRC equation [31], applied to each point of the DC.

Having a trip specific consumption causes an important increase in the consumption of about 400 kW for the peaks, 200 kW for the valleys, and 300 kW for the Saturday profile. This increase is reflected also in the total energy demand, as showed in *Figure 5.11*, with an increase of around 35-40%. Looking at *Figure 5.10* the trip specific consumption affects more the shorter *Main* windows of Weekdays, which is caused by a higher average power demand of shorter trips. This important change is a key intermediate step for the implementation of the coupling with VCAM model; these results are displayed in the next paragraph. The approach here presented overestimates the vehicles consumption, and the adoption of this model as final solution should be carefully considered since it assumes that the JRC equation can be applied on each instant of the driving cycle velocity profile. In the next paragraph a more accurate solution is proposed since the trip-detailing of consumption is computed with a vehicle dynamic simulator.

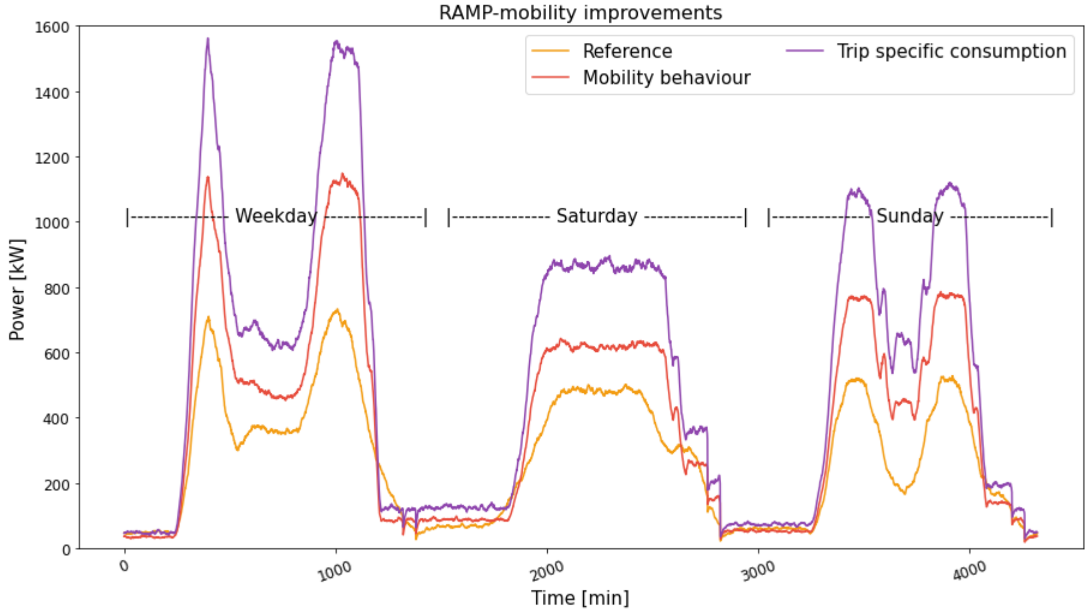

Figure 5.10: Profile comparison between *Reference*, *Mobility behaviour* and *Trip specific consumption* cases.

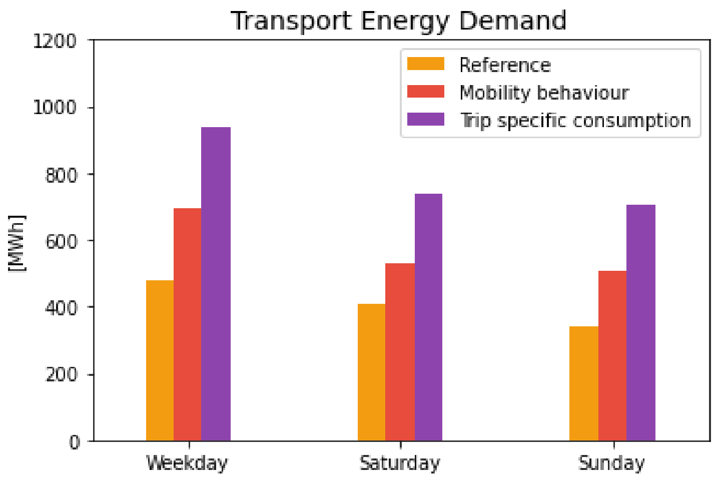

Figure 5.11: Comparing total transport demand of *Reference*, *Mobility behaviour* and *Trip specific consumption* cases.

Vehicle consumption model

The results of the final version of the model, which includes the coupling with VCAM, are showed in this paragraph. This last step refines the trip-specific consumption by applying VCAM to the driving cycle associated to each couple speed-time. Looking at the curves in

Figure 5.12, the new consumption model causes a scale down of the profile, which drops the Weekday peaks of about 500 kW compared to previous step, without affecting the curve shape. The implementation of a trip-specific vehicle dynamic consumption evaluation creates demand curves similar to the ones of *Mobility behaviour* case, with a slight decrease of about 50 kW corresponding to 5% of the peak power. This is also observed in the total transport demand which decreases of 10%. This reduction is linked to the totally different approach adopted to compute the average consumption, no more based on a literature equation [31], but obtained applying the VCAM dynamic simulator to the driving cycle associated to the trip. Looking at energy tables in *Figure 5.13*, a uniform drop of about 32% in all day-types is observed compared to *Trip specific consumption* values.

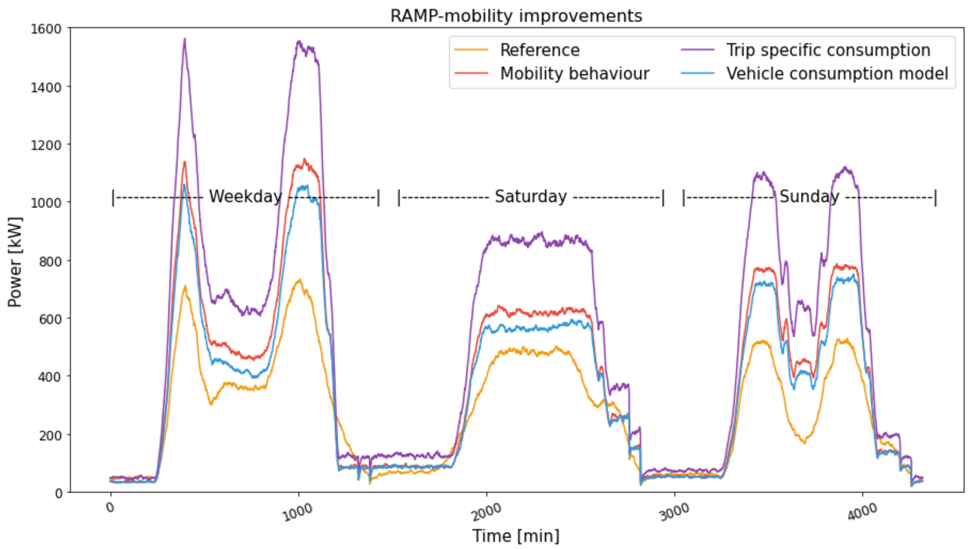

Figure 5.12: Profile comparison between *Reference*, *Mobility behaviour*, *Trip specific consumption* and *Vehicle consumption model* cases.

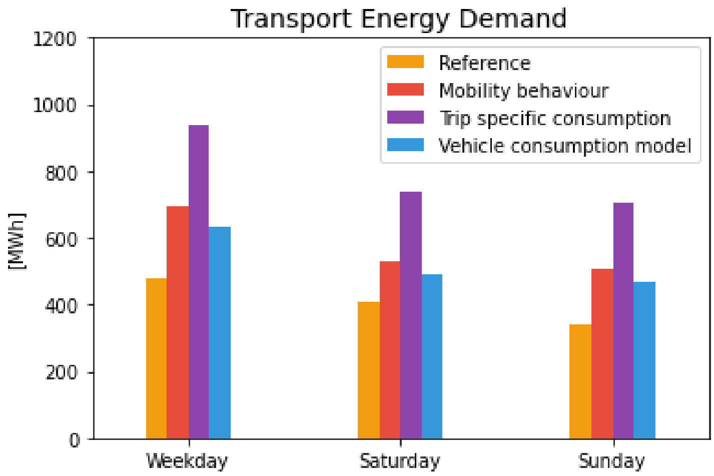

Figure 5.13: Comparing total transport demand of *Reference*, *Mobility behaviour*, *Trip specific consumption* and *Vehicle consumption model* cases.

Comparing the *Reference* case with the last implementation of *Vehicle consumption model*, the result is an uneven increase in the demand profile, of about 300 kW in weekday peaks while of less than 100 kW during the larger *Main* window of Saturday. Looking at *Figure 5.13*, the overall effect of the introduced improvements is an increase in the total transport demand of around 30%. This rise is caused by the distance recovery mechanism and is mitigated by the new consumption evaluation method, which is proved to reduce the power demand. The less evident effect on weekends is a consequence of a lower distance recovery, which is not complete due to lower *occasional use* in *Main* windows. The introduction of a per second trip description not coupled with an appropriate consumption model would produce a further 60% increment, proving that transport energy demand is highly sensible to the refinement of the consumption evaluation method.

As described in the methodology in *Section 3.2.1*, the last two steps related to the vehicle consumption are introduced through consumption tables. These are specific for each car segment and represent the non-thermal power consumed in each driving cycle, meaning for the couple *speed* and *time*. Thermal demand, which depends on external temperature, is added separately. Initially these tables were computed from 5 to 300 min with 5 minutes as time-step, and from 5 to 120 km/h for all velocity values. However, analyzing the power values in relation to the two parameters characterizing the driving cycle, power consumption highly depends on average speed, while a limited dependence from trip duration has been noticed. Variations with this parameter are significant only for short trips, for this reason the tables have been reduced in dimension limiting the time variable to 100 min. This analysis is valid for all the vehicle types and for both the steps, hence all the tables have been modified. A graphical result of these considerations is reported for different values of velocity in *Figure 5.14*, showing the limited variability after 100 min of trip duration.

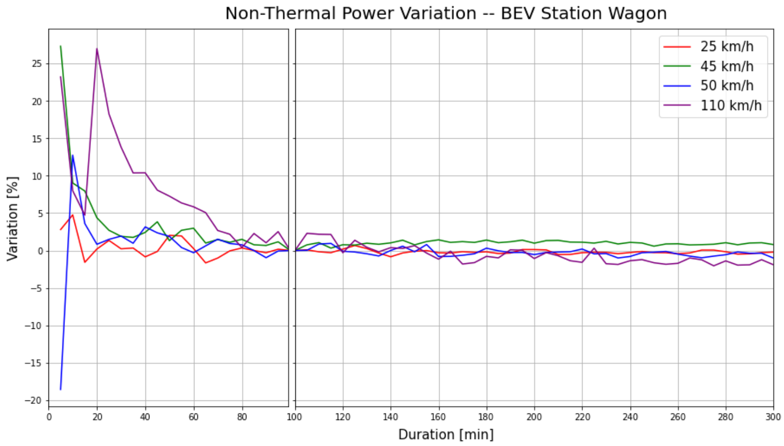

Figure 5.14: Percentage variation of vehicle consumption with respect to 100 min cycle, for four speed classes and all values of trip duration.

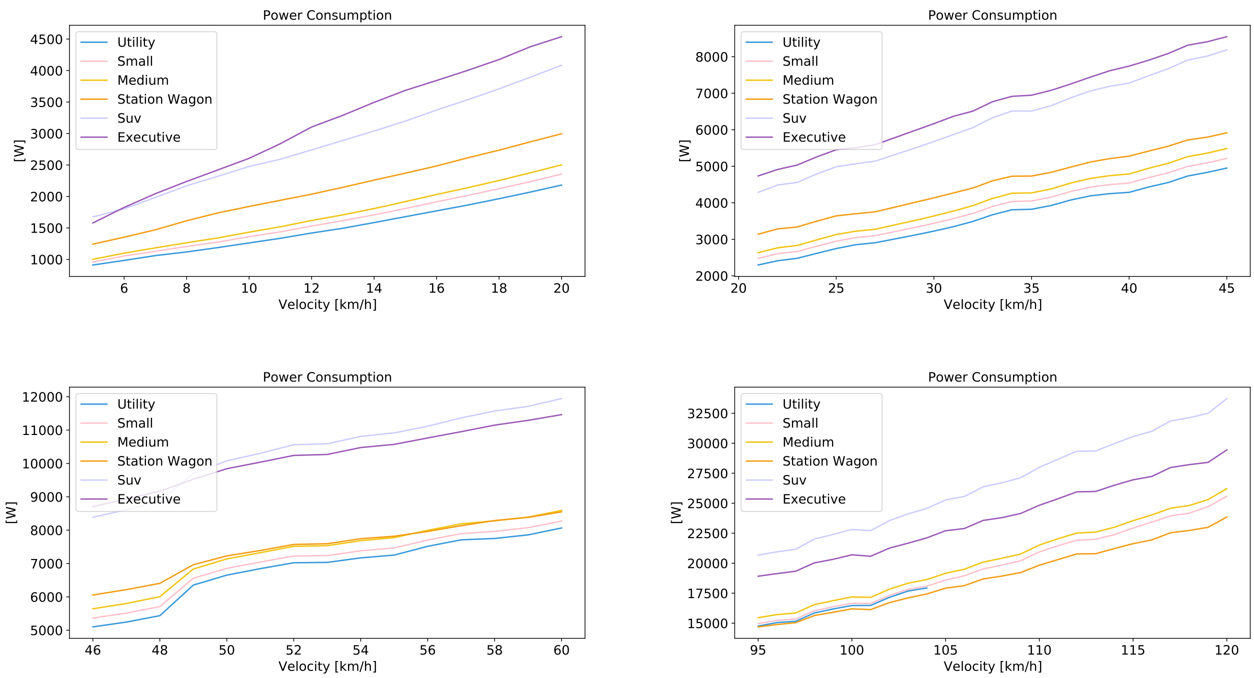

Figure 5.15: Power consumption variation with trip velocity for all the vehicle segments and for a selected trip duration set to 50 min.

In *Figure 5.15* the values of power consumption for all the vehicle segments and for a selected trip duration are reported, highlighting their variation with velocity. Values increase with velocity, and vehicles with larger battery capacities are characterized by higher consumption for the selected driving cycle. At higher speed two different trends are evident, reducing the differences between vehicles.

As final analysis, to assess the impact of the introduced changes on the annual mobility profiles, *Reference*, *Mobility behaviour* and *Vehicle consumption model* cases have been compared in terms of energy demand as illustrated in *Figure 5.16*. An increase of 44% is highlighted seen the introduction of distance recovery mechanism; this increase is mitigated with the vehicle consumption model, which limits the increase to 27%. Therefore, the consumption estimation has to be carefully modelled seen the influence on the aggregated mobility profiles. Additionally, the mobility curves for three selected weeks of the year are represented in *Figure 5.17*, and the effects of temperatures and stochastic variables can be understood.

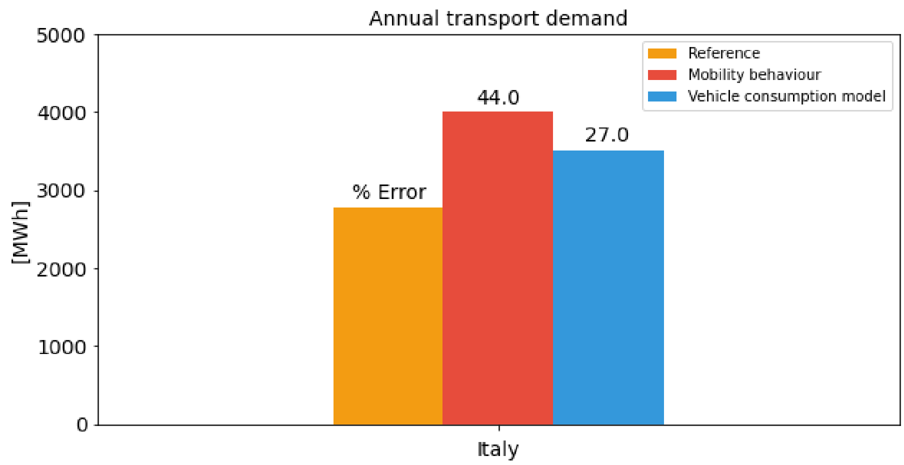

Figure 5.16: Annual transport demand for cases: *Reference*, *Mobility behaviour* and *Vehicle consumption model*.

(a) January

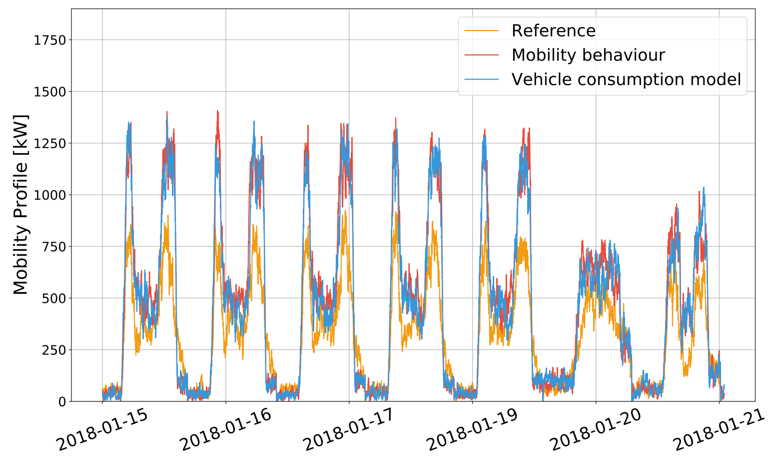

(b) July

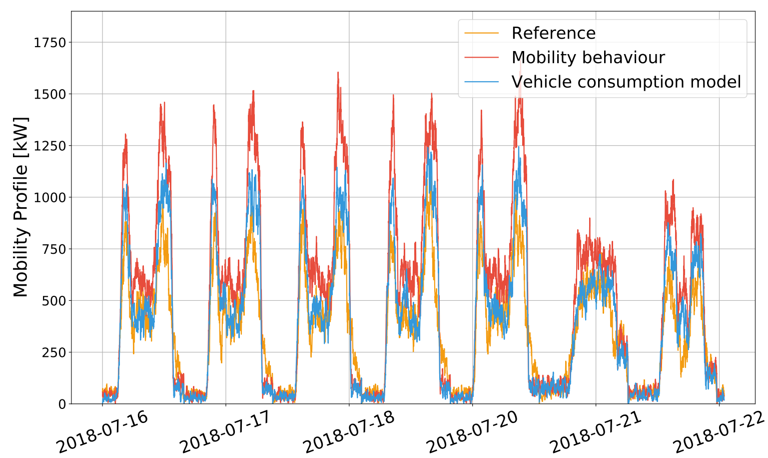

(c) November

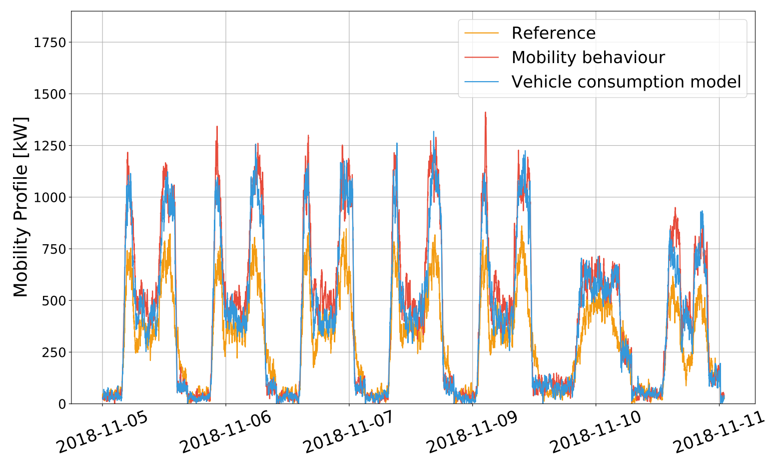

Figure 5.17: Three sample weeks to compare the mobility profiles of cases: *Reference*, *Mobility behaviour* and *Vehicle consumption model*.

5.2.2. The Netherlands

The step-by-step analysis of the application to The Netherlands is here described. As for Italy, four cases are presented highlighting the starting model and the improvements introduced in the stochastic process.

Reference

The input data changes are very limited for The Netherlands since no specific databases have been analyzed to better characterize the country. The major change is related to the reduction of the input daily distance, considering the incoherence noticed for Italian values between computed data and original ones. Minor updates are related to the *occasional use* variables, and to the variability introduced on velocity and average trip time derived from Italy case.

Mobility behaviour

Focusing on structural improvements, complementary functioning windows and distance recovery are implemented. The resulting profiles in *Figure 5.19* highlight higher transport demand concentrated in *Main* windows. Weekday peaks, which correspond to *Main* windows, increase of around 400 kW, whereas less important changes can be observed in Weekends with an increase of 100 kW. The *Free Time* occasional use parameter is indeed higher, and it is also introduced for *Main* windows, hence reducing the distance recovered. A similar conclusion is derived for the transport demand in *Figure 5.18* which increases as expected with higher differences on Weekdays.

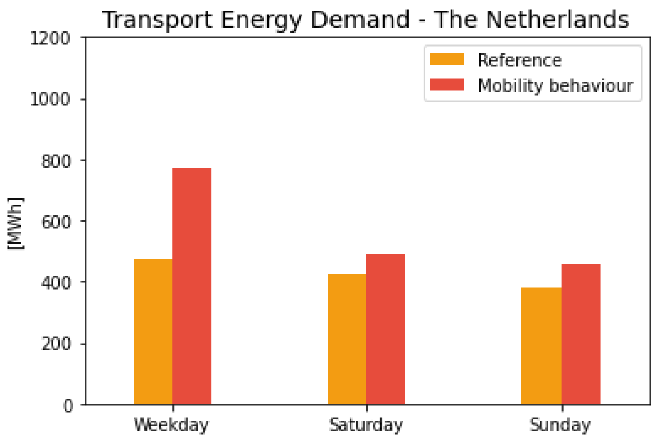

Figure 5.18: Comparing total transport demand of *Reference* and *Mobility behaviour* cases for the Netherlands.

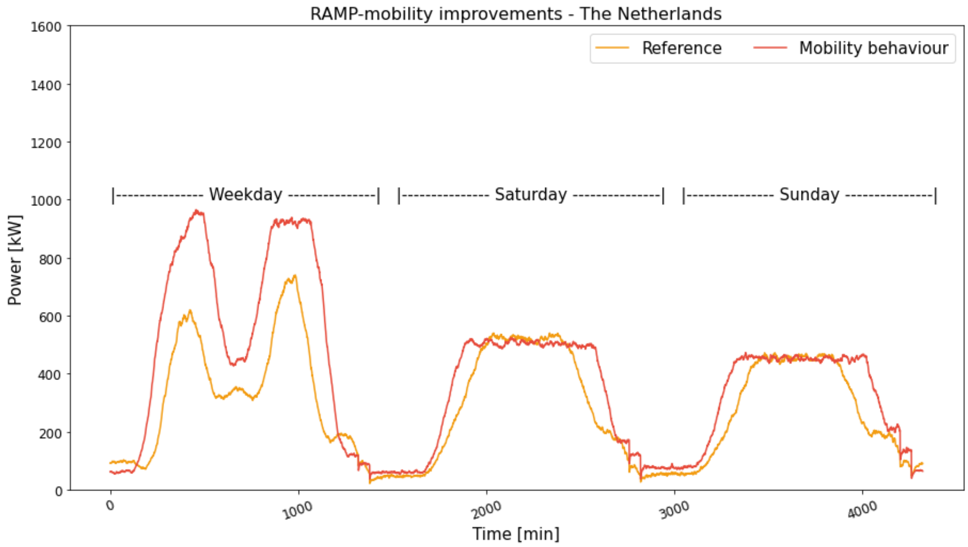

Figure 5.19: Profile comparison between *Reference* and *Mobility behaviour* cases for the Netherlands.

Trip specific consumption & Vehicle consumption model

The impact of the last two steps on the mobility profile is similar to the ones showed for Italy. In *Figure 5.20* the change in the specificity of the vehicle consumption causes higher profiles. This increment is around 200 kW for Weekday peaks, and about 100 kW for Saturday; a strange behavior is noticed for Sunday profile, for which no significant change is highlighted. The same relative increase can be observed in the total transport demand showed in *Figure 5.21*. With the introduction of VCAM, the power values are reduced of 400 kW for Weekday peaks, and of about 200 kW for Weekends. Similarly the transport demand is affected with Weekday increase of around 40%, which instead does not vary significantly during Saturday and Sunday, due to the lower distance recovery.

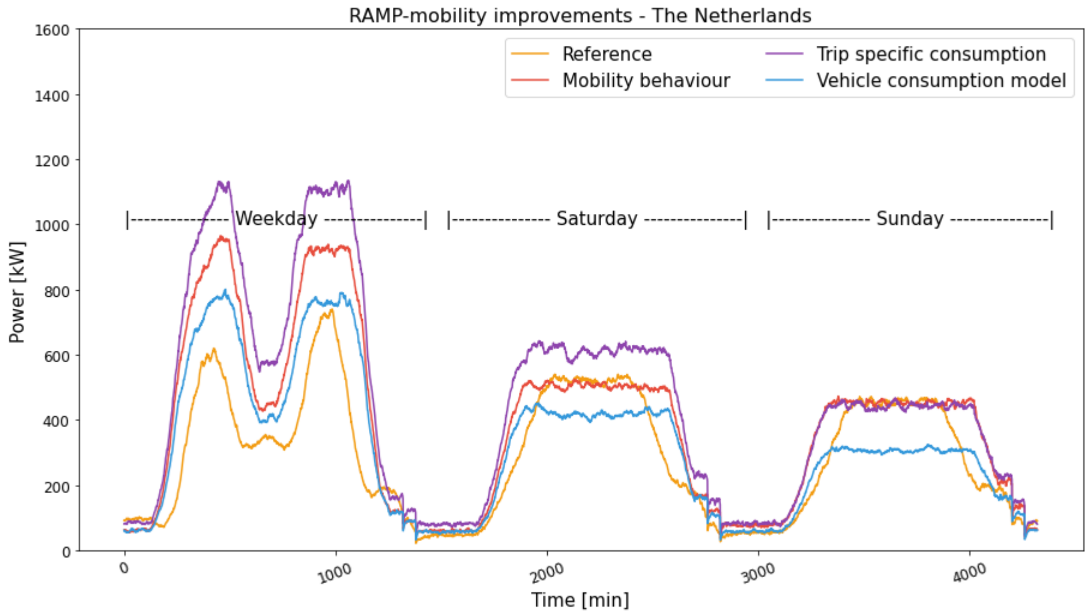

Figure 5.20: Profile comparison between *Reference*, *Mobility behaviour*, *Trip specific consumption* and *Vehicle consumption model* cases for The Netherlands.

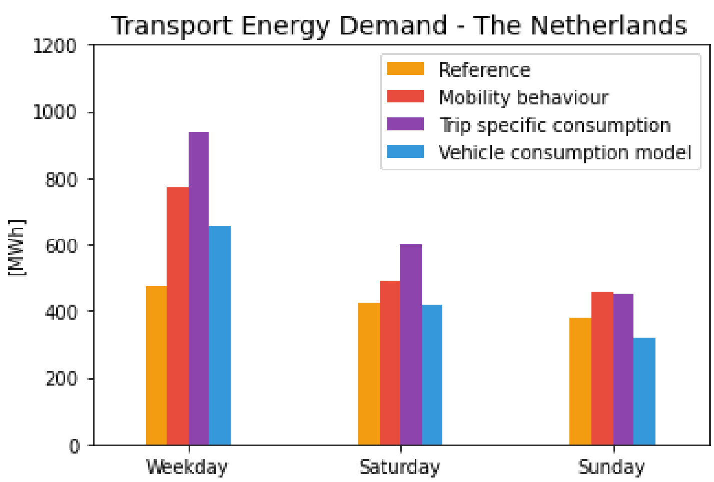

Figure 5.21: Comparing total transport demand of *Reference*, *Mobility behaviour*, *Trip specific consumption* and *Vehicle consumption model* cases for the Netherlands.

Computational time

To conclude the analysis of the step-by-step improvements for the applications to Italy and The Netherlands, the impact in terms of computational time is here pointed out. The values are reported in *Table 5.9* and refer to simulations without the charging module, for 2500 users and 180 days. The device used to test the proposed solutions has M1 CPU with 8 core and 8 GB of memory. The *Mobility behaviour* case, which introduces changes in the stochastic process, has a low influence on computational time which remains stable around 5 min. More significant impacts can be noticed for the last two cases: the time for simulations increases of 63% for Italy and 52% for The Netherlands. This difference is related to the lower average trip time used for Italy which generates a higher number of trips. The general increase of computational time is clearly related to the new approach introduced to estimate the vehicle consumption, which is associated to each generated trip instead of computing an average consumption value for each $Appliance$. Even though the computational time is higher, it is still acceptable seen the greater level of realism introduced.

	Reference	**Mobility behaviour**	**Trip specific consumption**	**Vehicle consumption model**
Italy	4min 57s	5min 15s	8min 30s	8min 15s
Netherlands	4min 56s	5min 2s	7min 40s	7min 30s

Table 5.9: Comparison of computational times for the two applications: Italy and the Netherlands.

5.3. RAMP-mobility improvements: charging

The results of the user connections are here reported analyzing the effects of different charging probabilities. The simulated fleet is composed of 2498 vehicles, which corresponds to about 143 MWh of nominal battery capacity. The number of connected user and the available battery capacity for each time-step have been determined, differentiating between charging and non-charging ones. The profiles generated for a sample week in January are displayed adopting the updated RAMP-mobility version for all cases, using the same mobility output and differing only for charging parameters. A first result evident looking at *Figure 5.22*, is the similar trend between the number of connected users and the amount of battery capacity available, both in percentage. The results of the two perspectives have no significant differences, because weighting each vehicle with its battery capacity have limited effects on percentage results. Indeed the outcomes of the following analysis showing the connected battery capacity, can be extended to the number of user connections.

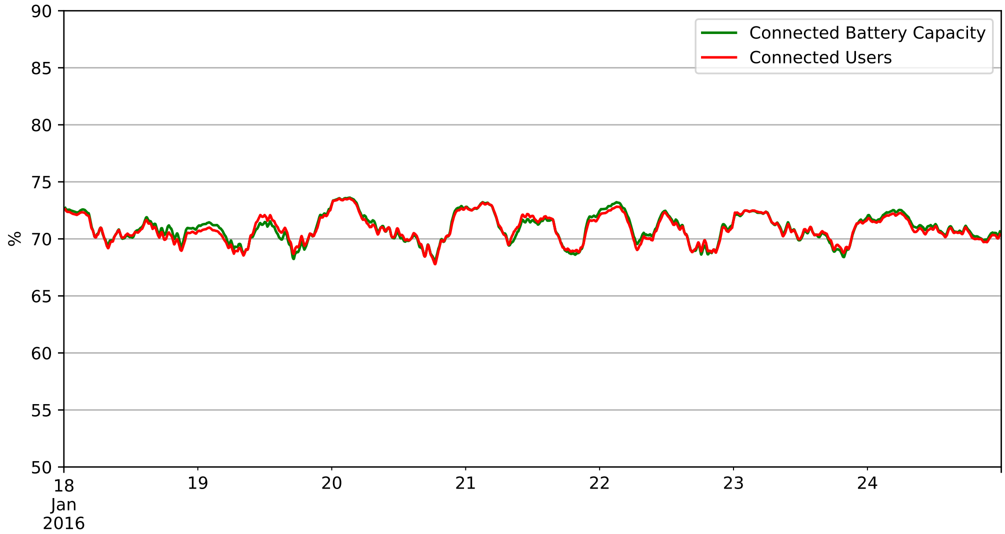

Figure 5.22: Comparison between connected users and connected battery capacity in percentages.

Two steps influence the plug-in events: (i) the infrastructure availability, meaning the probability for the user to find an available charging point when parking; and (ii) the user decision of recharging his vehicle, which highly depends on his behavior and is consequently affected by uncertainty. The results of the four cases highlighted in *Chapter 3* are showed in *Figure 5.23* where different charging probabilities are implemented.

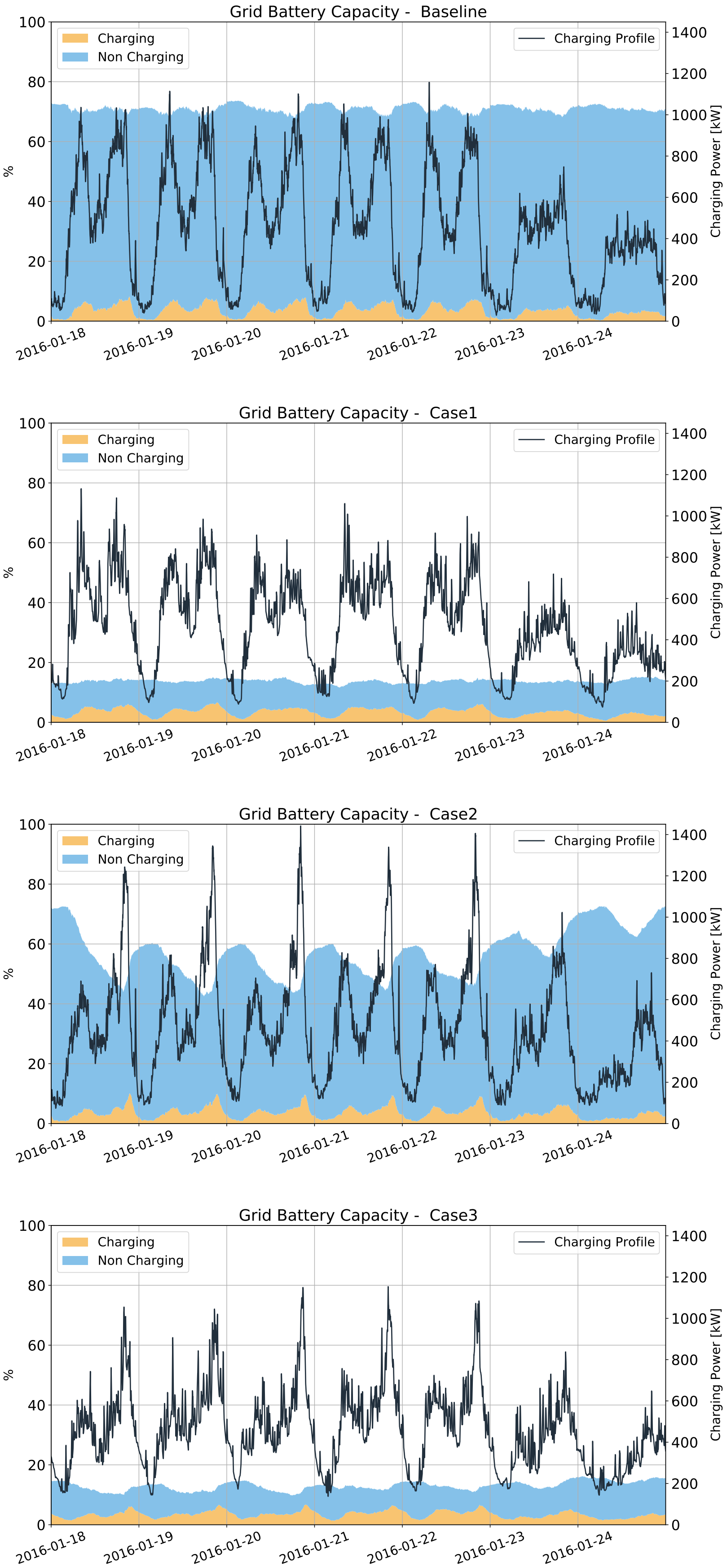

Figure 5.23: Impact of different charging probability functions on the battery capacity connected to the grid.

The impact of the charging probability functions influence significantly the battery capacity connected to the grid. In the *Baseline* case the total number of connected people do not vary with time and its value is close to the constant default infrastructure probability of 80%. The slight difference is present since the available battery capacity is defined including even vehicles not moving in the day, while the 80% would be reached excluding them. Considering the number of connected people which are charging in the *Baseline* case, but also in all the others, this percentage is below 5% and the shape follows the one of the charging profile. The adoption of the *user behavior* function in *Case 1* lowers the total amount of connected people, which drops to about 15%, without changing the shape of the profile during the selected week. The introduction of the piecewise function in *Case 2* to model the infrastructure availability, reduces the percentage of available battery capacity of about 20%, giving a characteristic shape to the profile which is complementary to the charging demand. The lower probability of finding available charging points during mid-day hours produces high peaks as soon as the probability value increases, since the charging events are accumulated during the day due to the higher level of occupancy. The combination of the two functions in *Case 3* creates profiles of available battery capacity that are quite similar to *Case 1*, underlining the higher influence of the *user behavior* function, with only few time oscillations caused by the piecewise. Finally, looking at the charging profiles the reduction of infrastructure availability (*Case 2*) creates higher spikes in the profiles, while the behavioral choice is beneficial for lowering the peak power.

In conclusion, two findings can be derived: (i) the user behavior can be an important limit for the V2G implementation reducing the available storage, while the impact of a variable infrastructure probability during the day, meaning the reduced number of charging points due to higher occupancy, is less evident; (ii) infrastructure availability must be carefully model since it causes charging coincidence, and rises the profile spikes; while the introduction of the behavioral model lowers peak heights, hence representing a conservative way to estimate maximum charging demand. As final disclaimer this analysis has been carried out without analyzing in detail the parameters for the Italian infrastructure availability and for the behavioural function. This limits the accuracy of these conclusions that, however, could be a starting point for further investigations.

6 | Model quality assessment and sensitivity analysis

In this chapter the model quality of the final RAMP-mobility version is assessed. Two different approaches have been followed in relation to the *real-world* data availability. Firstly, the accuracy of the mobility demand is evaluated considering national statistics and aggregated mobility information, and additionally through data about petrol consumption. This approach is followed seen the absence of measured mobility time-series. Secondly, a validation is carried on comparing the results of the charging demand with measured profile available for the Netherlands. Both the methodology and the results for mobility and charging assessment are presented in the following sections.

6.1. Mobility time-series

The comparison between the overall transport demand simulated by RAMP-mobility and *real-world* mobility data is crucial to assess the modelling quality of the framework. The restricted availability of data related to the energy demand of electric vehicles is a limit, hence two methods are here presented to overcome the lack of specific databases.

Aggregated mobility data

Aggregated mobility statistics, as annual vehicle kilometers, are useful to validate the simulated transport demand and its fragmentation into single trips. These data are generally available for different countries, since do not require to be specific for electric mobility. The assumption relying behind this reasoning is the similarity of mobility behaviour independently on the type of car, hence user of conventional vehicles behave in the same way of electric car drivers. It is important to highlight that this comparison do not assess the accuracy of the consumption estimation, since it is independent from the total energy computed.

Eight European countries have been selected for this purpose. Vehicle kilometers is the chosen variable, representing the average annual kilometers per car. This average value is obtained from RAMP-mobility through the analysis of the collected trip information. Mean distances for each user type and day of the week are produced as output from the model, and, through the population share, the annual average distance per car is computed. Billion passenger-kilometers, abbreviated as *pkm*, is instead the available data from *European Commission* report [6] with a country specificity. A passenger-kilometer is the unit of measurement representing the transport of one passenger by a defined mode of transport over one kilometer. Data for passenger cars from 2018 are selected, since this is the focus of RAMP-mobility. Together with this parameter, number of cars and average passenger car occupancy rate for urban mobility [9] are considered to compute the vehicle passenger kilometers and allow the comparison with RAMP-mobility results. The car occupancy rate is the average number of people transported by each vehicle, and two extreme values are used to determine minimum and maximum annual distances, hence the model results should be in this range. This comparing approach is preferred instead of choosing a single value of occupancy rate due to the high uncertainty of this parameter. Occupancy rate for urban mobility is available for ten European countries and for some nations is also divided in values considering people of all ages or only those in the range 15-84 years old; the *Eurostat* values [9] are reported in *Figure 6.1*.

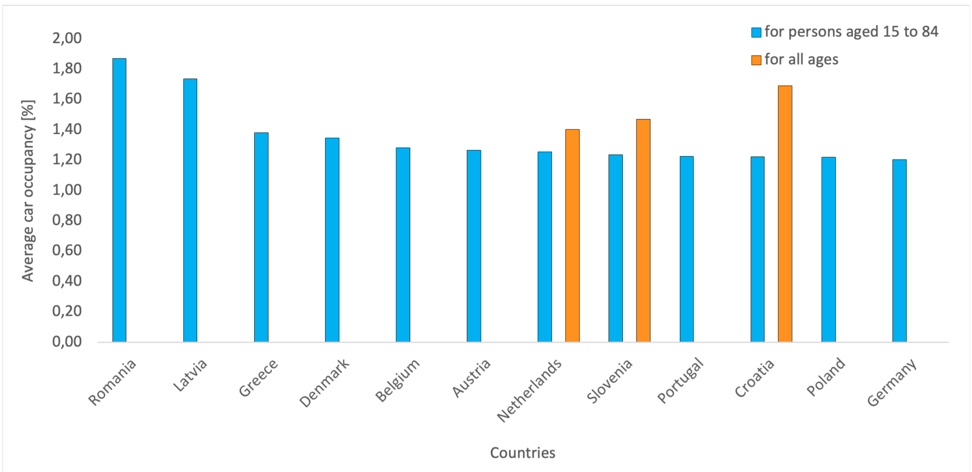

Figure 6.1: Car occupancy rate from *Eurostat* database. [9]

The selected limit values for occupancy rate are 1.2 and 1.87 which are used to determine the range of annual vehicle kilometers. The country total vehicles from *Eurostat* are used afterwards to determine the average annual distance specific for vehicle, and characterized in minimum and maximum annual value. The results for the selected eight countries are summarized in *Figure 6.2*, proving a good estimation of the mobility demand with

RAMP-mobility. The computed average annual distances are indeed in the range set through *Eurostat* database for most of the analyzed countries.

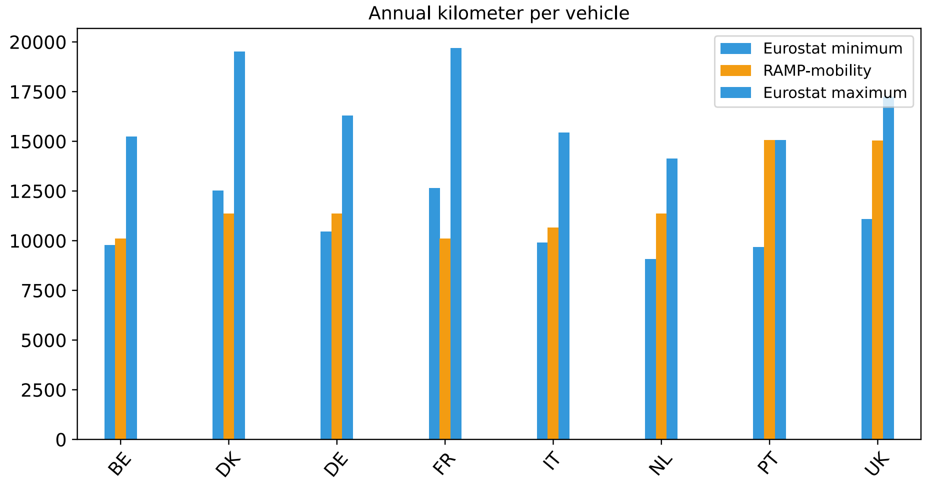

Figure 6.2: RAMP-mobility annual vehicle kilometers for eight selected countries and the corresponding *Eurostat* minimum and maximum values.

Petrol consumption estimation

An alternative approach to evaluate the quality of the simulated transport demand is the measure of conventional mobility consumption in terms of petrol demand. This approach requires the application to RAMP-mobility of consumption models able to simulate even ICEV, as in the case of VCAM which can model different types of vehicles. This comparison is adopted to assess the model quality of Italy since specific databases have been analyzed. Petrol consumption is a good source of information to estimate aggregated mobility demand since petrol is mainly used for passenger car fueling, thus it is reasonable to assume that the overall consumption is imputable only to this sector. However, this method of quality assessment is limited in accuracy, since values depend on many uncontrollable variables, and cannot grasp the precision of the EV power estimation.

Data of petrol consumption and number of petrol-powered vehicles are taken respectively from the oil bulletins published by *Ministero dello Sviluppo Economico (MISE)* [27], and from a car market analysis carried on by *Unione Nazionale Rappresentanti Autoveicoli Esteri (UNRAE)* [30]. The same version of RAMP-mobility used for electric vehicles is adopted, but consumption tables have been updated with values specific for ICEV obtained through the corresponding VCAM tool. A change in the thermal demand function is needed to model the effect on ICEVs: a quadratic function is implemented for cooling, while only a constant value of consumption is considered for fans in heating mode, since the heat demand of conventional power-trains is fully satisfied by engine recovery. In this way the mobility profile is estimated in liter of fuel per minute, instead of kW, and the yearly total consumption for each user, corresponding to a single petrol car, is computed. The vehicle-specific yearly consumption is compared with the one derived from the amount of petrol sold in the distribution network and with the number of petrol vehicles. Diesel vehicles are not considered since these do not account only for cars but include also trucks, which are not modelled by RAMP-mobility. The result for the vehicle-specific yearly petrol consumption is showed in *Table 6.1* and the comparison is made according to absolute error. Nationally a 12% error is estimated, highlighting the good accuracy of the generated mobility demand for Italy.

	Measured [l/vehicle/y]	**RAMP-mobility** [l/vehicle/y]	**Relative error** [%]
Italy	541.14	604.77	11.76

Table 6.1: Comparison of petrol specific consumption between measured data and RAMP-mobility generated trips.

6.2. Charging time-series

6.2.1. Methodology

Differently from mobility time-series, charging ones can be directly measured, since are the curves of power absorption from the grid. Nevertheless, few *real-world* data collected are made accessible by charging infrastructure operators, hence this accurate model quality assessment is limited by data accessibility. The measured data used for this comparison comes from the dutch company *ElaadNL*. The comparison between *real-world* charging profile and simulated one is assessed through normalized profiles, obtained dividing by the total yearly energy demand. This is made since the empirical dataset and the simulated profile do not consider the same number of users, and the collected records do not account for all the charging events made by each user. For these reason, a dimensional comparison is not possible, and the profiles are transformed into non-dimensional ones.

Dataset

The validation dataset is composed by charging transactions metered in The Netherlands between January 2012 and May 2016, and the year selected is 2015 since this is the most recent and complete one. The database consists in user-specific charging transactions covering around 1750 charging points and representing 16% of the whole public infrastructure available at the time of metering. The raw data are recorded based on an ID code of the card used by the customers to start and end the charging transactions.

The database has been processed by Beltramo *et al.* [3] to obtain the charging time-series. The initial dataset is filtered selecting only full electric vehicles, thus deleting PHEV which are also recorded. Only frequent electric vehicles users with more than ten recorded transactions are selected to include only habitual customers, which describe better the typical charging pattern. In addition, transactions with values of maximum charging power lower than 4 kW and maximum energy charged lower than 12 kWh, representing the PHEV behavior, are disregarded. The resulting dataset is composed by 2215 users which are split in 40% with large vehicles and 60% with small ones. From the data analysis the charging infrastructure results being composed by around 80% charging points working at 3.7 kW, 15% charging in the range 8-12 kW and the remaining 5% distributed on the other values.

Modelling in RAMP-mobility: alignment to *ElaadNL* dataset

To compare with this dataset and simulate conditions as similar as possible to the empirical ones, RAMP-mobility default values for The Netherlands are updated to the specific characteristics of *ElaadNL* population. A new vehicle share composed by 60% *Small* cars and 40% *Large* ones is introduced together with updated values for the charging points power distribution, with 80% of slower chargers, 15% for intermediate types and 5% for faster ones.

Lastly, the probability to find a charging point (CP) is modelled to reflect the higher availability of charging columns in night hours rather than central day ones. This occurs through the piecewise function, described in *Section 3.2.2*, characterized by two probability values in different day windows. Since the values for this function are highly uncertain, a sensitivity analysis is performed. The charging strategy adopted for the simulations is the *uncontrolled* one, meaning that users charge their vehicles at CP nominal power until the maximum defined SOC is reached.

Quantitative parameters

Concerning the quantitative parameters used to estimate the accuracy of the model, two different statistical values are considered which are the *Normalized Root Mean Square Error (NRMSE)* and the average *Load Factor (LF)*, defined in *Equations 6.1* and *6.2*.

$$NRMSE = \frac{\sqrt{\frac{\sum_x^{N_t}(P_{model}(x) - P_{measured}(x))^2}{N_t}}}{P_{measured,max} - P_{measured,min}} \tag{6.1}$$

$$\overline{LF} = \sum_{d=1}^{365} \frac{P_{average}(d)}{P_{peak}(d)} . \frac{1}{365} \tag{6.2}$$

The NRMSE is used to evaluate the difference point-by-point between simulated and measured data, and is applied to both the charging time-series and the load duration curve. In *Equation 6.1*, $P_{model}(t)$ and $P_{measured}(t)$ are respectively the charging power estimated by the model and the one measured at time t; N_t is the number of time-steps in a year. The denominator is the difference between $P_{measured,max}$ and $P_{measured,min}$, which are the maximum and minimum values of the measured dataset. The load duration curves are built from the time-series by ordering the power data and re-indexing them to delete the effect of time shift on the curves, focusing only on the frequency of power values. The NRMSE is computed between the load duration curves point-by-point in the same way explained for the time-series.

Another way of evaluating the two profiles is represented by the average LF which represent the variability inside the charging demand between daily peak power consumption, $P_{peak}(d)$, and daily average power consumption, $P_{average}(d)$. This is an indicator of the profile shape and is highly influenced by the peak power. The average LF is computed for both the simulated and measured profile, considering an hourly-resampled time-series to smooth possible short steep peaks, and the comparison between the two values is made in terms of relative error.

Piecewise sensitivity analysis

The piecewise function, describing the infrastructure availability, is a crucial aspect characterized by high uncertainty. Consequently, its parameters are varied to understand which values suits better to simulate conditions similar to the ones of the measured *real-world* profile. The parameters subject to investigation are probability values, maximum and minimum, and the hours of the day for their switch. Ten cases are obtained by varying singularly the parameters, and other five cases are identified combining the best changes of the previous analysis. In *Table 6.2* an overview of the methodology followed to vary the default values is reported and in *Figure 6.3* the directions followed in the sensitivity are represented. As described in *Section 3.2.2*, a different piecewise is introduced for weekends with *Case 1* since the charging profiles differ importantly from the empirical curve during Saturdays and Sundays due to time shifting. Therefore six parameters are object of sensitivity for all the new cases assuming that maximum and minimum probabilities are the same for weekend and weekdays. Until *Case 9* one parameter at the time is changed (time-related parameters meaning start and end of both weekday and weekend windows are changed together). From *Case A* the variations are combined to reach better values for the validation metrics.

	Case Original	**Case 1**	**Case 2**	**Case 3**	**Case 4**	**Case 5**	**Case 6**	**Case 7**	**Case 8**	**Case 9**
Max$_{prob}$	90%	90%						↓		↑
Min$_{prob}$	40%	40%					↑		↓	
Start$_{WD}$	06:00	06:00		↑		↓				
End$_{WD}$	19:00	19:00	↑		↓					
Start$_{WE}$	-	09:00		↑		↓				
End$_{WE}$	-	15:00	↑		↓					

	Case Original	**Case 1**	**Case A**	**Case B**	**Case C**	**Case D**	**Case E**
Max$_{prob}$	90%	90%					↓
Min$_{prob}$	40%	40%				↑	
Start$_{WD}$	06:00	06:00	↓	↑	↓	↓	↓
End$_{WD}$	19:00	19:00	↑	↑	↑	↑	↑
Start$_{WE}$	-	09:00	↓	↑	↓	↓	↓
End$_{WE}$	-	15:00	↑	↑	↑	↑	↑

Table 6.2: Scheme of the cases tested in the piecewise sensitivity analysis.

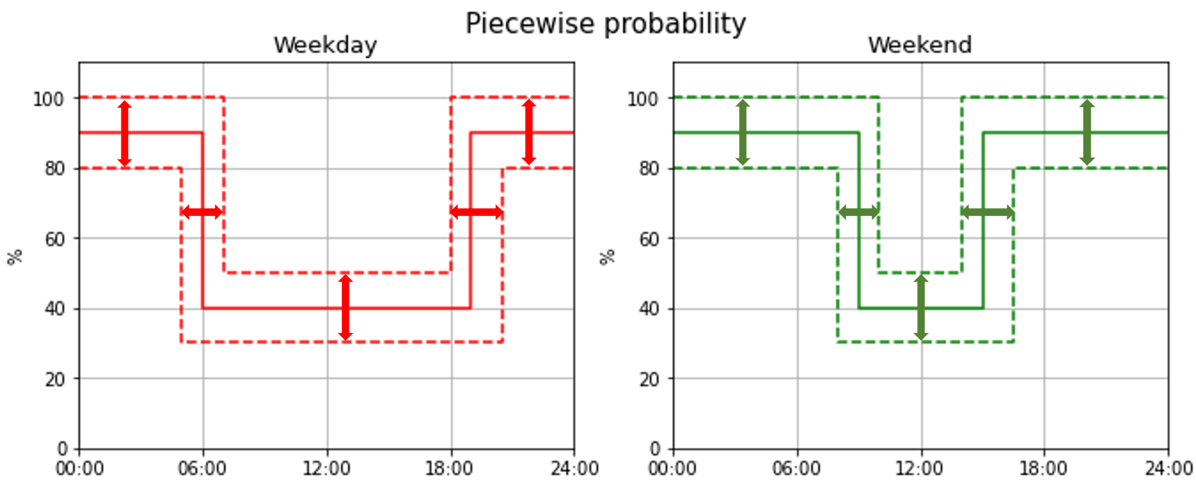

Figure 6.3: Graphical representation of the investigated parameters for the infrastructure probability function.

Parametric uncertainty analysis

Given the high uncertainty of input variability analyzing the impact of these parameters is of fundamental importance. All the input stochastic parameters need to be studied and varied independently to assess their effects on the selected metric. Five types of occasional use are defined in RAMP-mobility: three parameters are used for *Main* windows of each day type and the last two are for *Free Time*, one during weekdays and one for weekends. All the parameters are varied bidirectionally and the effect on NRMSE and LF error is evaluated; additionally the load duration curves are analyzed and compared with reference ones.

The variables under studies are the variability on functioning windows duration (r_{windows}), on the average trip time ($r_{\text{average time}}$), on the daily average distance (r_{distance}) and on the daily average velocity ($r_{\text{velocity positive}}$ and $r_{\text{velocity negative}}$). Random on power is not object of study since this value is obtained from the analysis of power consumption tables, hence set to 5% and not varied. All the default randomicities have been studied independently, except for those on the average velocity, since they refer to the same variable, varying them bilaterally of 10%. An overview of the default values and of the applied variation is reported in *Table 6.3*.

	Default values [%]	**Variation [%]**
$\mathbf{r}_{\textbf{windows}}$	20	±10
$\mathbf{r}_{\textbf{average time}}$	20	±10
$\mathbf{r}_{\textbf{distance}}$	30	±10
$\mathbf{r}_{\textbf{velocity positive}}$	18	±10
$\mathbf{r}_{\textbf{velocity negative}}$	20	±10

Table 6.3: Default stochastic variables and applied variation for the sensitivity analysis.

Lastly the *occasional use* probability, which describes the probability of taking the car at least once a day, is investigated. Five types of occasional use are defined in RAMP-mobility: three parameters are used for *Main* windows of each day type, and the last two are for *Free Time*, one during weekdays and one for weekends; the default values are reported in *Table 6.4*. Since during weekdays the users are modelled considering to always take the car during *Main* windows, only four values are object of variations. Firstly, the two *Main* occasional use are changed together of 10%, and secondly the *Free Time* ones, both couples in the same direction.

	Weekday Main	**Saturday Main**	**Sunday Main**	**Weekday Free Time**	**Weekend Free Time**
Occasional use [%]	100	60	50	20	35

Table 6.4: *Occasional use* default input values.

6.2.2. Results

In this section the quantitative results of the model evaluation are displayed, showing the comparison with the *ElaadNL* charging profile. Firstly, the input data used to implement in RAMP-mobility the same peculiar conditions of the real-life charging demand are reported. The simulation cases, which differ for the parameters applied to the piecewise charging probability function, are presented highlighting the two steps followed during the analysis: varying independently each parameter, and combining different modifications. The outcomes of the validation metrics on the different cases are reported and commented, showing the reasoning behind the combination procedure and the choice of the best-case.

Lastly, the other stochastic parameters are varied and the impact on the validation metric is assessed.

Dataset

Two input data changes are required to adapt The Netherlands model to the measured data coming from *ElaadNL* charging infrastructure. Firstly, the vehicle share is adapted to the characteristics of the metered vehicle fleet which is assumed to be composed of only *Small* and *Large* cars. Secondly, the charging infrastructure probability is updated with values estimated from the analysis of the recorded charging transactions. These data are summarized in *Table 6.5*.

Charging point type	Nominal power [kW]	Relative share [%]
Slow	3.7	60
Intermediate	11	30
Fast	120	10
Vehicle type	Battery capacity [kWh]	Relative share [%]
Small	37	60
Medium	60	0
Large	100	40

Table 6.5: *ElaadNL* dataset.

Piecewise sensitivity analysis

The default values for the piecewise charging probability function are considered as starting point with the same time intervals for both weekdays and weekends. *Case 1* is considered as the baseline including a first guess modelling of the different time intervals for weekends. This distinction between weekdays and weekends, already presented in *Section 3.2.2*, is applied since the charging profiles differ importantly from the empirical curve during Saturdays and Sundays, resulting in important *Load Factor* errors and *NRMSE*. Consequently, an attempt to modify how the charging demand is computed during weekends is introduced. The first set of cases, *Case 1* to *Case 9*, is chosen to assess the impact of every single parameter and to highlight the best directions of improvement. Starting and ending time-steps of weekday and weekend are changed together since they affect independently the time-series. The values adopted for each case are summarized in

Table 6.6, while the quantitative results are presented in *Table 6.7*.

	p_{max}	p_{min}	$start_{weekday}$	$end_{weekday}$	$start_{weekend}$	$end_{weekend}$
Case Default	90%	40%	06:00	19:00	-	-
Case 1	90%	40%	06:00	19:00	09:00	15:00
Case 2	90%	40%	06:00	20:00	09:00	16:00
Case 3	90%	40%	07:00	19:00	10:00	15:00
Case 4	90%	40%	06:00	18:00	09:00	14:00
Case 5	90%	40%	05:00	19:00	08:00	15:00
Case 6	90%	50%	06:00	19:00	09:00	15:00
Case 7	80%	40%	06:00	19:00	09:00	15:00
Case 8	90%	30%	06:00	19:00	09:00	15:00
Case 9	100%	40%	06:00	19:00	09:00	15:00

Table 6.6: First piecewise sensitivity analysis.

	$NRMSE_{timeseries\ [\%]}$	$NRMSE_{LDC\ [\%]}$	$LF_{error\ [\%]}$
Case Default	14.9	4.0	-20.6
Case 1	14.8	3.6	-16.5
Case 2	14.7	2.8	-1.5
Case 3	16.7	2.8	-13.5
Case 4	15.3	5.8	-18.3
Case 5	14.0	3.9	-18.3
Case 6	15.3	1.9	-11.0
Case 7	14.3	2.5	-10.3
Case 8	15.5	5.7	-21.7
Case 9	15.6	4.9	-21.4

Table 6.7: Impact of the first piecewise sensitivity analysis on the reference validation metric.

Considering globally the values of the reference metric, the relative error between simulated and measured data in terms of load factor, ranges from -22% and -10% for most of the sensitivity cases. This highlights that RAMP-mobility is generally characterized by higher peaks compared to average power values. An exception is found in *Case 2* in which the LF error is set to -1.5%, meaning that delaying the end of the time windows is beneficial. This change influence positively also the other parameters, therefore this improvement is chosen as starting point for the combinations. NRMSE values for the time-series range between 13.9% and 15.5%; while those on the load duration curve are significantly lower, between 2.8% and 5.7%. This difference is related to the load duration curve nature, since it does not compare power values for single time-steps which could differ importantly for many subsequent steps. Indeed thanks to its distributional approach the variations of the two profiles can be reduced. A change of the beginning of the time windows improves the time-series match if anticipated (*Case 5*), while it improves both the load duration curve and the load factor error if delayed (*Case 3*). Maximum and minimum probabilities produce better results if respectively reduced (*Case 7*) and increased (*Case 6*). They both affects the load duration curve improving the error, while reducing the higher probability is also slightly beneficial for the time-series modelling. Seen these considerations an attempt to reach even better values for the reference metric is made through the combinations of the highlighted best directions of variations.

In *Figure 6.4* a graphical comparison of the sensitivity cases is presented comparing the load duration curves of all the ten simulations with the reference *ElaadNL* profile. A good match is found in the central part of the curves for a large portion, while for highest and lower values a higher difference is noticed. This is related to the higher peaks reached with RAMP-mobility profiles which also explain the difference in the load factors previously presented. The cases which align for larger portions to the reference curve are *Case 2* and *Case 6*, which are indeed characterized by lower NRMSE on the load duration curve.

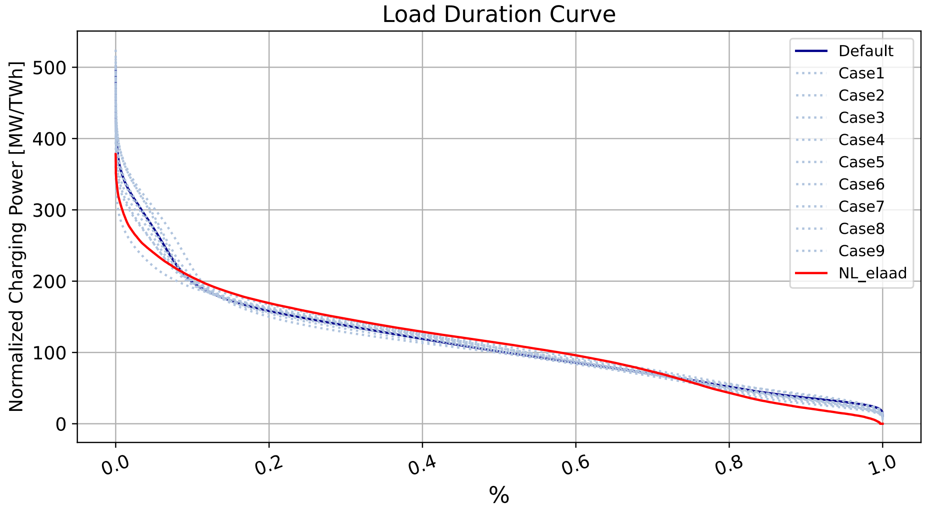

Figure 6.4: Load duration curve for *Case 1*-*Case 9*.

The combination of the highlighted variations lead to the definition of other five cases reported in table *Table 6.8*. Globally the selected validation metric reaches better results in all the values with respect to the initial default case, with the highest improvements in the load factor error (*Table 6.9*). The best combination is found in *Case D* where the increase of the lower probability (*Case 6*), the anticipation of starting windows (*Case 5*) and the delay of ending values (*Case 2*) are implemented. Even considering the load factor error without the hourly resampling, the error is limited to 16%. In *Figure 6.5* the load duration curves from *Case A* to *Case E* are reported, with highlighted in blue the best case. Making a comparison with *Figure 6.4*, a better match can be found: the highest values are reduced thanks to the new piecewise values and the curves are consequently closer to the *ElaadNL* profile also in the lower values.

	p_{max}	p_{min}	$start_{weekday}$	$end_{weekday}$	$start_{weekend}$	$end_{weekend}$
Case A	90%	40%	05:00	20:00	08:00	16:00
Case B	90%	40%	07:00	20:00	10:00	16:00
Case C	90%	40%	05:30	20:30	08:30	16:30
Case D	90%	50%	05:00	20:00	08:00	16:00
Case E	80%	40%	05:00	20:00	08:00	16:00

Table 6.8: Second piecewise sensitivity analysis: combinations of selected variations.

	$\text{NRMSE}_{\text{timeseries [\%]}}$	$\text{NRMSE}_{\text{LDC [\%]}}$	$\text{LF}_{\text{error [\%]}}$
Case A	13.6	2.6	-3.4
Case B	16.9	2.6	1.9
Case C	14.2	3.7	6.2
Case D	14.7	2.2	0.3
Case E	13.6	2.8	1.5

Table 6.9: Impact of the second piecewise sensitivity analysis on the reference validation metric.

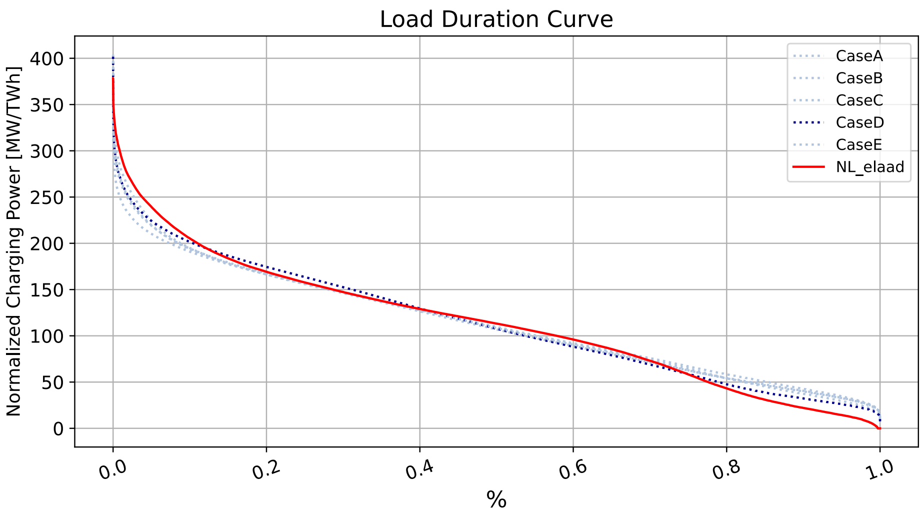

Figure 6.5: Load duration curve for *Case A*-*Case E*.

To assess the improvements with respect to the original RAMP-mobility, a comparison with its validation is made. For both validations the selected *real-world* reference profile is *ElaadNL*, and the input parameters introduced for the simulations are compared to ensure the same representation of vehicle fleet composition and charging infrastructure. Improvements can be noticed in the load factor error which was set to -9.9% [25] for the best sensitivity case, and also in the NRMSE time-series which decreases of 1.1%. In addition, the updated RAMP-mobility developed with this thesis work solves some inconsistencies of the original framework as the definition of functioning windows and the incoherence between input and output average daily distance. Thorough these advancements a more accurate and realistic model is created and the coupling with the consumption model VCAM allows to increase its technological level of detail.

Figure 6.5 shows the time-series cloud-plots for both groups of simulations in six typical weeks of the year. The shape of the time-series is well replicated by the cloud even if the variations from day-to-day are important. The choice of adding different piecewise parameters for weekends is justified by looking at the *ElaadNL* profile that shows different behavior during weekend days. Looking at the same week month by month for the two set of cases, the high spikes at the end of the evening peak, which worsen the match with *ElaadNL* curve during weekdays, are reduced with the combination of variations. The measured curve has peaks ranging between 150 and 300 MW/TWh, with highest values during weekdays caused by coincidence of movements imposed by working hours. For the first group of cases the cloud plot has peaks up to 500 MW/TWh and up to 300 MW/TWh for the combinations. This last reduction is linked to a better distribution of plug-in moments, which are constrained by the infrastructure availability.

During May and August there is a lowering of *ElaadNL* curve, while the cloud plots are characterized by few seasonal variations mainly caused by temperature differences. The drop of *real-world* charging demand during summer months is due to vacations, which are instead not modelled with RAMP-mobility where only public holidays are considered. The graphs show that the piecewise function can significantly influence the shape of the charging profile, having a crucial role in decoupling mobility and charging profiles if no specific charging strategies are adopted. This tuning process of the piecewise function parameters is necessary since the *real-world* infrastructure is unknown a priori. However, it requires that no charging strategy is implemented, otherwise it would not be possible to distinguish between a load shift forced by the availability of plug-in points, and a smart decoupling between mobility and charging demand.

January

(a) Case 1 - Case 9

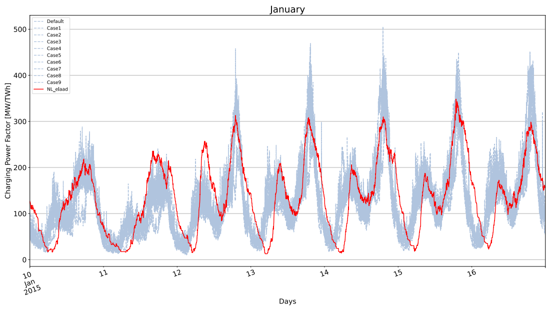

(b) Case A - Case E

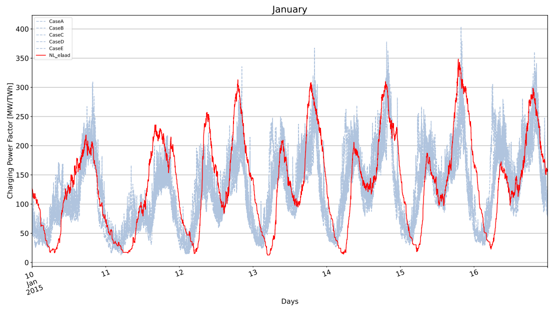

March

(c) Case 1 - Case 9

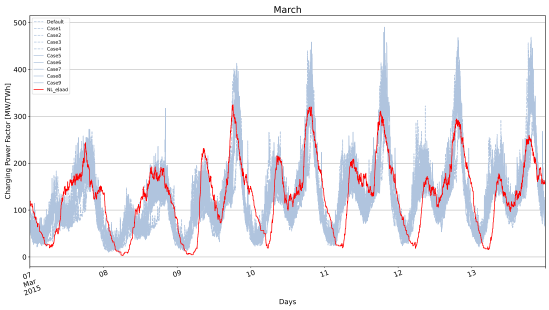

(d) Case A - Case E

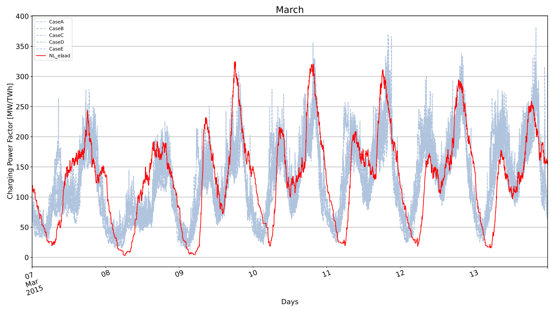

May

(e) Case 1 - Case 9

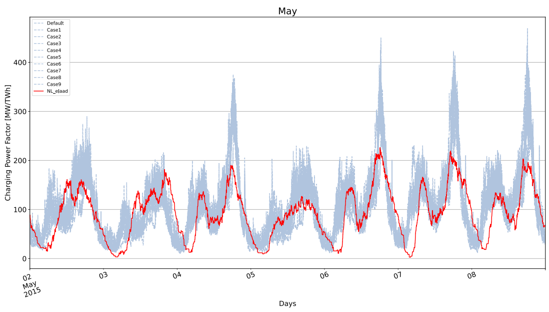

(f) Case A - Case E

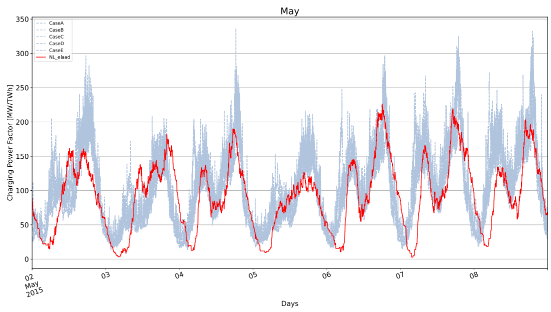

August

(g) Case 1 - Case 9

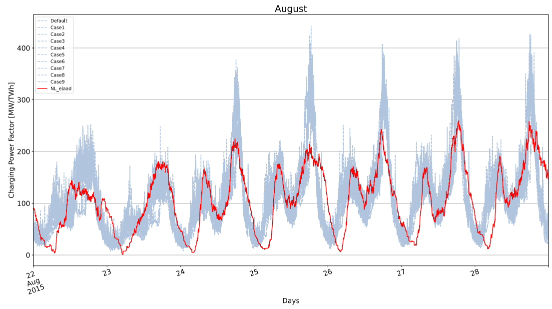

(h) Case A - Case E

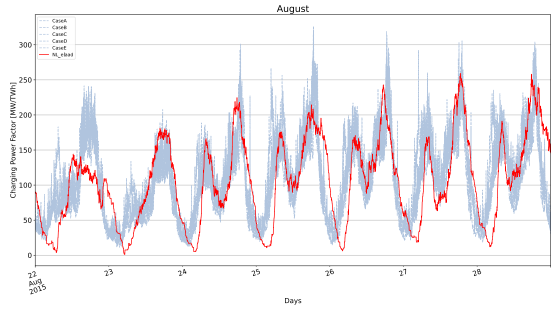

October

(i) Case 1 - Case 9

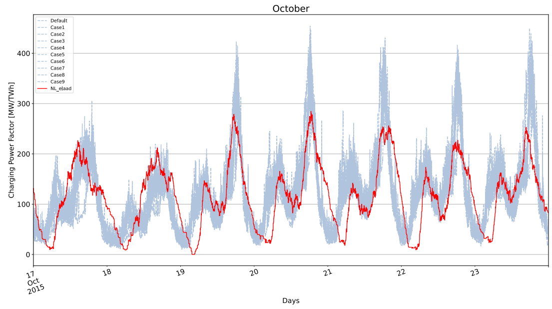

(j) Case A - Case E

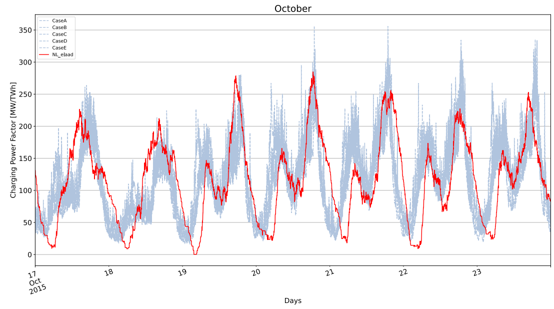

December

(k) Case 1 - Case 9

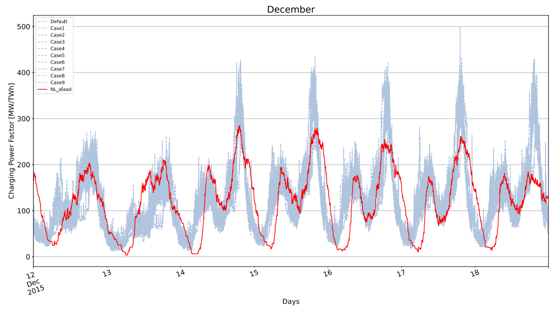

(l) Case A - Case E

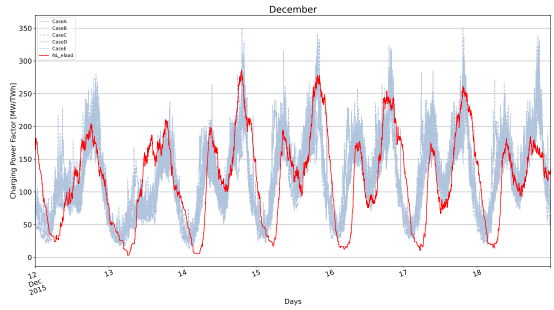

Figure 6.5: Cloudplot of the profiles obtained with different values of piecewise parameters for a selection of weeks.

Parametric uncertainty analysis

Travel-related variables

A second analysis is carried on to assess the impact of input stochastic parameters on the validation metrics. The first group of parameters analyzed are the ones related to travel characteristics, which means the variability on the daily average travelled distance, $r_{distance}$, on the average trip time, $r_{average\ time}$, and on the daily average trip velocity, $r_{velocity\ positive}$ and $r_{velocity\ negative}$. The parameters used in the seven cases are presented in *Table 6.10*.

	$\mathbf{r_{distance}}$ **[%]**	$\mathbf{r_{average\ time}}$ **[%]**	$\mathbf{r_{velocity\ positive}}$ **[%]**	$\mathbf{r_{velocity\ negative}}$ **[%]**
Case Ref.	30	20	18	21
Case 1	20	20	18	21
Case 2	40	20	18	21
Case 3	30	10	18	21
Case 4	30	40	18	21
Case 5	30	20	8	11
Case 6	30	20	28	31

Table 6.10: Travel-related sensitivity cases.

To compare the results, the quantitative values of the validation metric for all the cases are computed and summarized in *Table 6.11*. The impact of the implemented changes cannot be appreciated, since the variation on both time-series error and on load duration curve error have a difference of less than 0.5%. Only the load factor error varies more significantly with a worsening in the order of 2%. A graphical representation of the load duration curve is also shown in *Figure 6.6* giving an overall overview of the yearly mobility demand. All the cases are almost coincident showing the robustness of the model to these stochastic parameters.

	$\text{NRMSE}_{\text{timeseries [\%]}}$	$\text{NRMSE}_{\text{LDC [\%]}}$	$\text{LF}_{\text{error [\%]}}$
Case Ref.	14.7	2.2	0.3
Case 1	14.8	2.0	-1.6
Case 2	14.7	2.0	-1.5
Case 3	14.8	2.0	-1.8
Case 4	14.8	1.9	-2.0
Case 5	15.0	2.0	-1.7
Case 6	14.5	2.2	0.4

Table 6.11: Impact of the travel-related sensitivity cases on the reference validation metric.

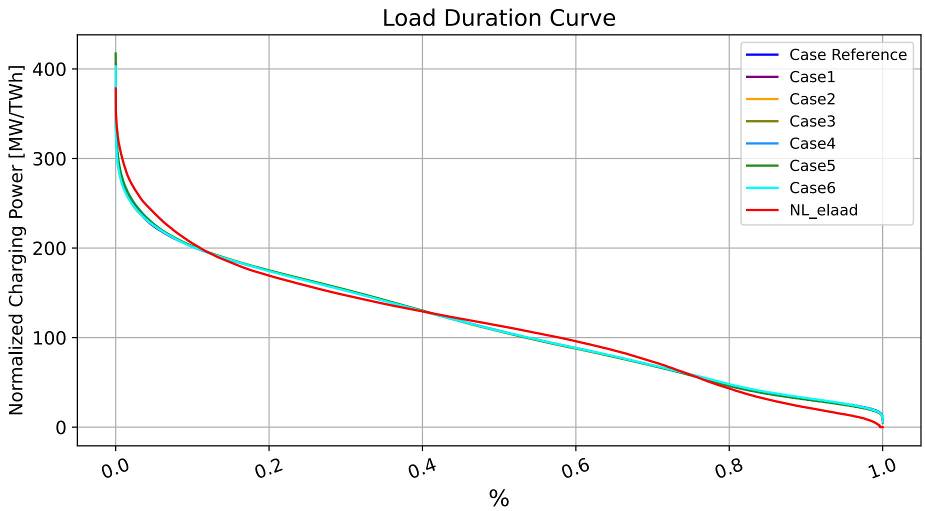

Figure 6.6: Load duration curve for travel-related sensitivity cases.

Functioning windows

The second group of stochastic values is related to the functioning windows variability, which is used to vary the starting and ending times. Seen the improvement introduced to RAMP-mobility in which *Main* windows are defined complementary to *Free Time* ones, this variability is applied only to the last-mentioned type. The simulated cases and the obtained results are reported in *Table 6.12*. In these cases a more important variation is highlighted for what concern the load factor error, which worsen of 6% with the decrease of the stochastic parameter. Looking globally at the results both the directions of variation do not reach a local maximum for the time-series and the load duration curve, hence the optimal random value can be further improved. For completeness, also the load duration curve is showed in *Figure 6.7* with a slightly more evident difference between the curves. *Case 1*, which is characterized by a better load duration curve error, is closer to *ElaadNL* especially for the highest values of the curve.

	$\mathbf{r_{windows}}$ **[%]**	$\mathbf{NRMSE_{timeseries}}$ **[%]**	$\mathbf{NRMSE_{LDC}}$ **[%]**	$\mathbf{LF_{error}}$ **[%]**
Case Ref.	20	14.7	2.2	0.3
Case 1	10	15.1	1.7	-5.6
Case 2	30	14.5	2.3	2.1

Table 6.12: Impact of the functioning windows sensitivity cases on the reference validation metric.

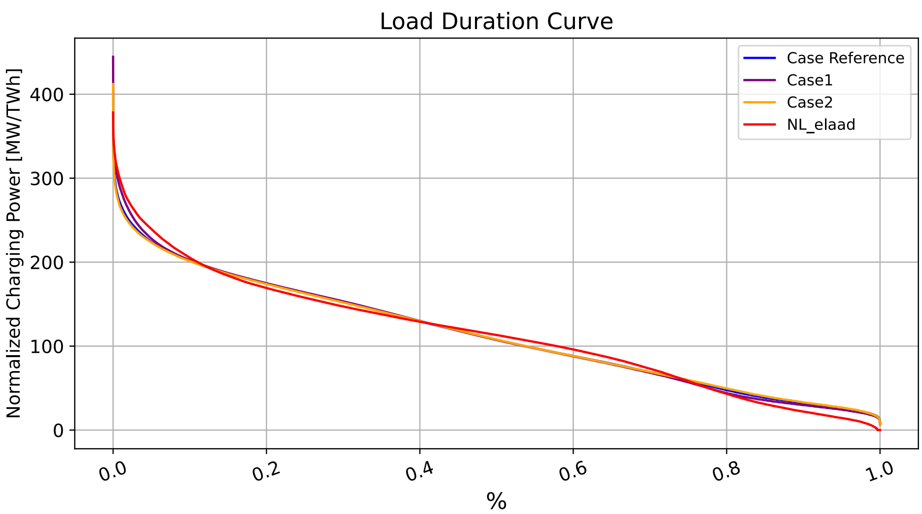

Figure 6.7: Load duration curve for functioning windows sensitivity cases.

Occasional use

The last group of parameters is represented by the occasional use for which the sensitivity analysis is applied to four values and an overview of the simulated cases is showed in *Table 6.13*.

	Weekday Main [%]	Saturday Main [%]	Sunday Main [%]	Weekday Free Time [%]	Weekend Free Time [%]
Case Ref.	100	60	50	20	35
Case 1	100	60	50	10	25
Case 2	100	60	50	30	45
Case 3	100	50	40	20	35
Case 4	100	70	60	20	35

Table 6.13: Occasional use sensitivity cases.

Looking at the results summarized in *Table 6.14* and at the load duration curve in *Figure 6.8*, where all the cases are plotted, this parameter is the one mostly affecting the results. *Case 1* and *Case 2*, characterized by the variation of the occasional use in *Free Time*, are those with the largest effects on the validation metrics, in particular on the load factor error. This worsens in both cases, while the variation of the *Main* probability has a more limited impact. Thus, attention should be used in varying the default occasional use values, especially *Free Time* ones, seen the good degree of accuracy reached with the inserted parameters and already validated.

	$\mathbf{NRMSE_{timeseries\ [\%]}}$	$\mathbf{NRMSE_{LDC\ [\%]}}$	$\mathbf{LF_{error\ [\%]}}$
Case Ref.	14.7	2.2	0.3
Case 1	16.2	2.5	-7.6
Case 2	14.1	3.2	4.9
Case 3	15.2	2.1	-0.3
Case 4	15.3	2.1	-0.6

Table 6.14: Impact of the occasional use sensitivity cases on the reference validation metric.

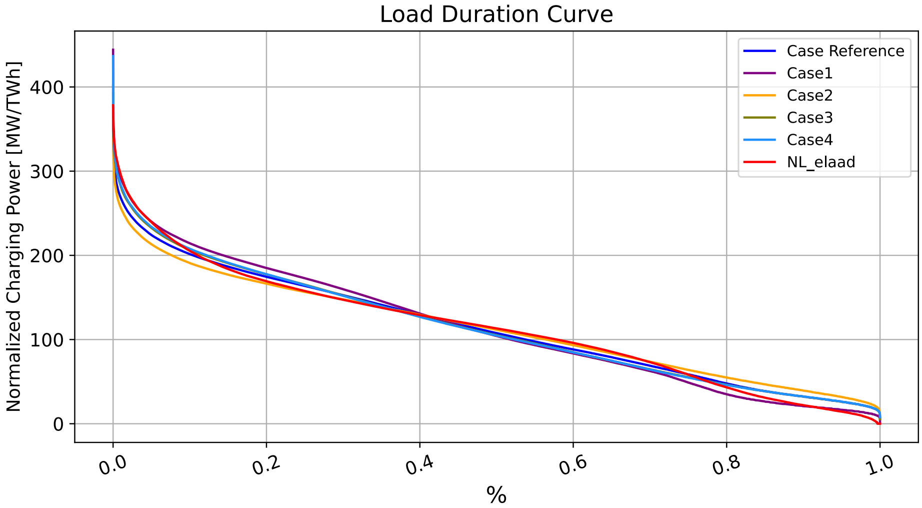

Figure 6.8: Load duration curve for occasional use sensitivity cases.

7 | Model Testing

In this chapter RAMP-mobility is tested analyzing the impact of data changes, increased vehicle fleet resolution, and enhanced geographical characterization on the mobility profiles. The first one is assessed to highlight the differences of the *Reference* case of Italy with the *Original* model version, and determine how updating data affects the output. The vehicle fleet definition is tested to determine the impact of a more detail characterization, and lastly the differences between national and regional profiles for Italy are analyzed.

7.1. Impact of new input data

This analysis is focused on analyzing the impact of data changes described in *Section 5.2.1* which allowed to determine the *Reference* version of RAMP-mobility, used as baseline for the introduced improvements.

General data

The first updated datasets are related to population breakdown, vehicle fleet and functioning windows. The impact of these new input data is illustrated in *Figure 7.1*, where different shapes of the profiles can be noticed since the functioning windows are changed. This is particularly evident in the Sunday profile, which has peaks about 100 kW higher than the *Original* profile, while on Saturday only a minor time-shift is observed. The weekday profile of *General data* is characterized by a more evident two-peaks shape, instead the morning peak cannot be seen in the *Original* model. The total transport demand in each day, reported in *Figure 7.1*, decreases of about 7%, as a consequence of a different vehicle distribution. Indeed the number of cars modelled as *Small* in the original model, which includes both *Small* and *Utility* cars, doubles.

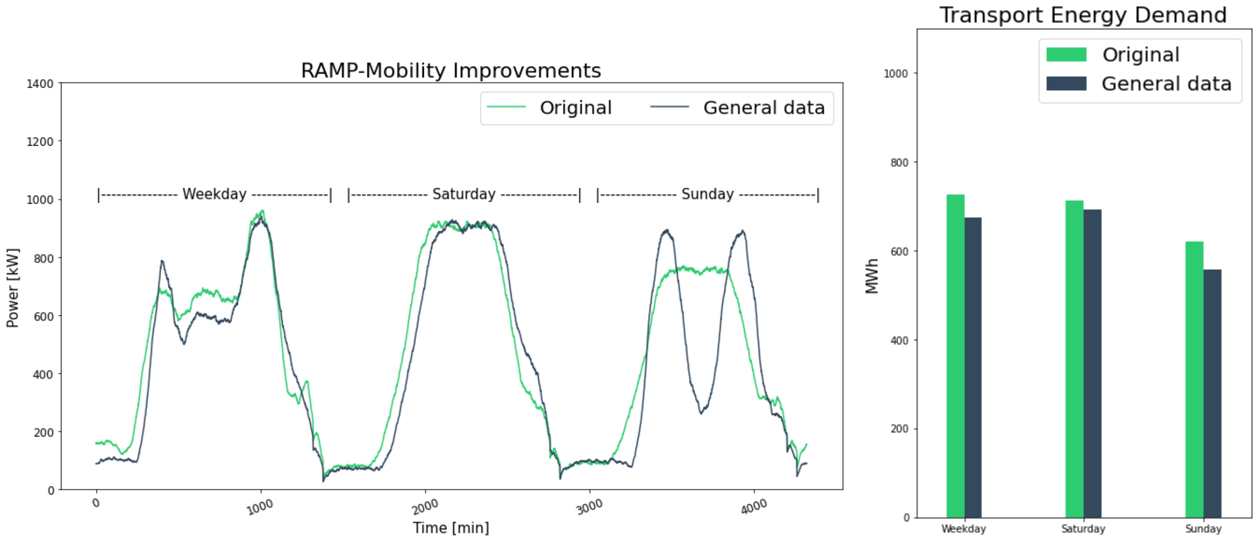

Figure 7.1: Comparison between *Original* and *General data* cases.

Trip features

The changes of trip features are related to the variability of parameters, indeed a new randomicity is applied to the average trip length. The percentage variability on the daily average velocity, v_{mean}, is split in positive and negative values (*see Table 5.3*), obtained from the velocity distribution assessed for the Italian regions in *Section 4.1.1*. These improvements cannot modify the shape of profiles, since affecting variability their effect is cancelled when performing the average of the profile. Looking at *Figure 7.2*, the total energy demand does not change, with variation of the daily energy around 1% caused by the model stochasticity. *Figure 7.2* shows overlapping profiles proving the goodness of this comparison approach in deleting variability effects.

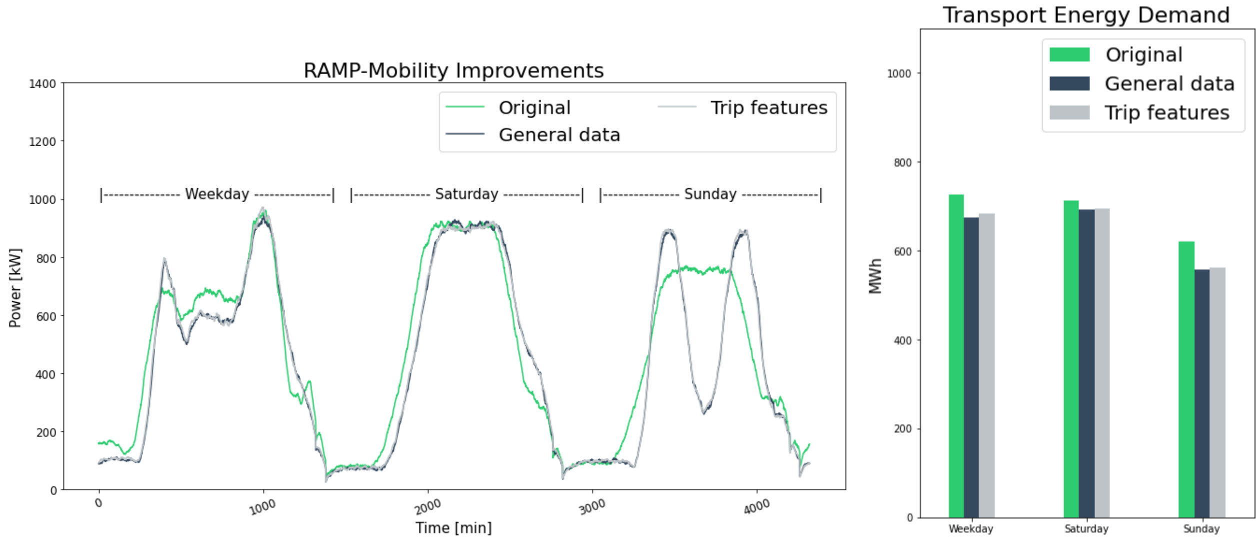

Figure 7.2: Comparison between *Original*, *General data* and *Trip features* cases.

Daily driving distance

The last updates are related to the daily driving distance, creating the *Reference* case. This new data source significantly affects the overall mobility demand, since the daily distance driven by each user is lowered considerably, as displayed in *Section 4.1.1*. A drop of about 35% in the mobility profile can be observed in *Figure 7.3*, showing an almost linear dependence between the distance driven and the power required by the mobility demand. The reduction of the profile affects unevenly the time-series depending on the time window, with the Weekday profile having a different shape due to the unequal reduction of driving distance in *Main* and in *Free Time* windows. As further consequence, Weekday peaks of the *Reference* profile are lowered of only 20% and the morning peak becomes almost as high as the evening one. Distance assigned to *Main* and *Free Time* windows is treated differently not only for the time-frame in which is driven, but even for the probability of being driven or not due to the occasional use effect. The total daily transport demand is lowered of around 35% according to *Figure 7.3*.

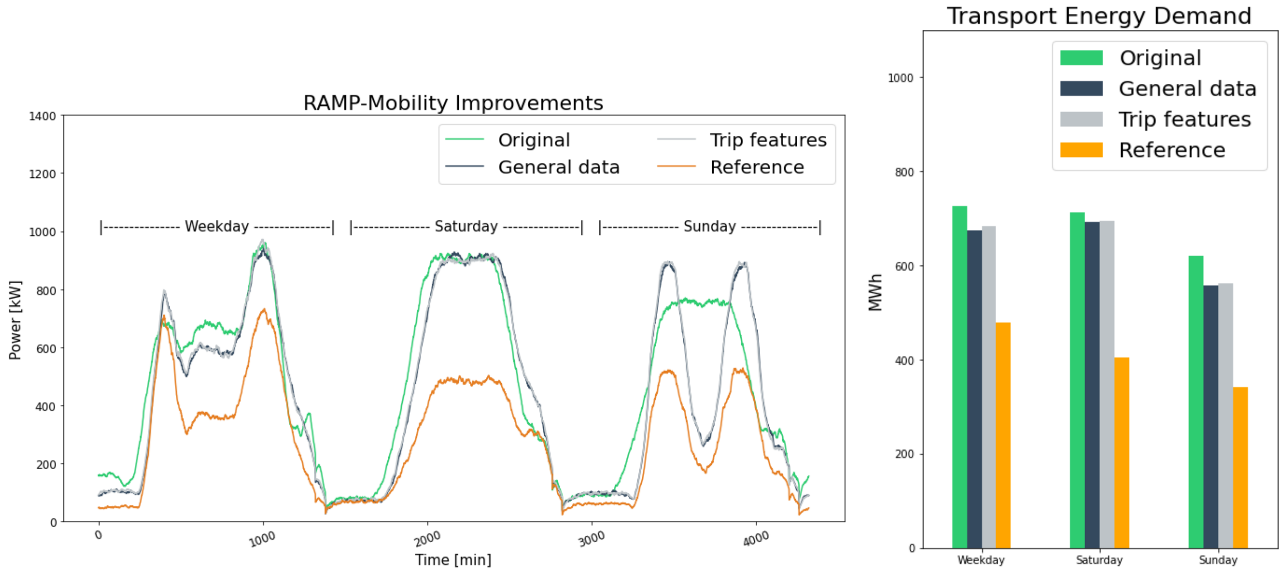

Figure 7.3: Comparison between *Original*, *Reference* and intermediate data change cases.

7.2. Vehicle fleet resolution

The first analysis of the model resolution is related to the vehicle fleet composition, given as input to the model, to assess the impact of a more detailed vehicle characterization on the output mobility profile, and to understand possible future scenarios in terms of energy demand. A higher number of vehicle segments could improve the accuracy of the estimated energy demand if a dynamic simulator, specific for different types of cars, is used. The analysis of this approach and the detailed representation of the vehicle fleet composition is here described.

In *Chapter 4*, a higher level of detail in modelling the Italian vehicle fleet is adopted, hence this approach is here tested to understand the effect of this change on the output. The vehicle fleet is composed of 24% *Utility*, 26% *Small*, 20% *Medium*, 26% *Station Wagon*, and of only 2% for both *Suv* and *Executive* vehicles. Six extreme scenarios with 100% of vehicles in the same vehicle segment are simulated to highlight the variations of the output mobility. In *Figure 7.4* the annual energy for the six cases, and the energy computed with the Italian vehicle share are compared.

The increased characterization of cars with smaller sizes does not produce visible differences in the energy demand, hence this higher level of detail can be avoided. Instead larger vehicles, as *Suv* and *Executive*, differ more significantly from the previous group. Thereafter, detailing vehicles with battery capacities higher than 90 kWh is needed seen the differences in the output. This characterization will be important if the vehicle fleet composition will evolve towards larger cars, thus requiring a more specific distinction of models. However, a level of detail as the one here presented is not needed and only two reference cars, *Small* and *Large*, are sufficient as evident from the bar plot. In the today situation where the vehicle mix is mainly composed by the first four classes with 96% of the fleet, even a two-segments level of detail is not required. Indeed the relative error is close to zero if a *Medium* vehicle is considered for modelling the whole fleet.

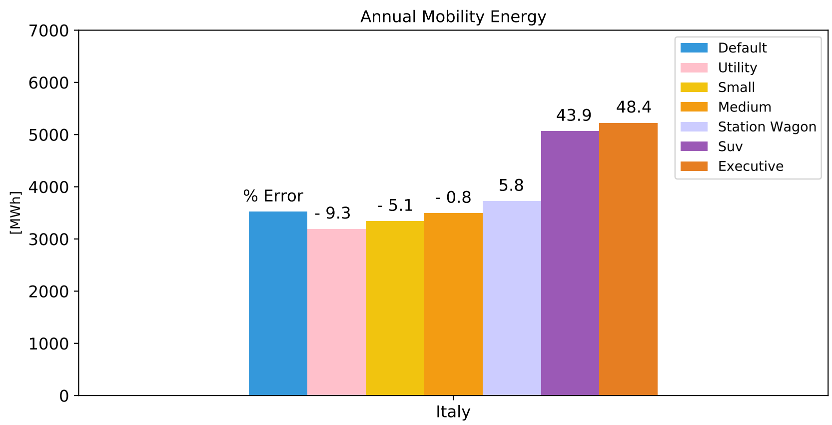

Figure 7.4: Annual mobility energy for the simulated cases for Italy with higher detail of the vehicle fleet composition.

The same analysis has been performed on four European countries, modelled with the default dataset of RAMP-mobility which include a three-segment vehicle fleet representation. The European countries are characterized by *Small, Medium* and *Large* cars, thus three extreme scenarios have been selected varying only these data entry: (i) 100% *Small* cars, (ii) 100% *Medium* cars, and (iii) 100% *Large* ones. For this purpose four countries, differing in the vehicle share distribution and in the geographic area, have been selected. The values representing the vehicle fleet are reported in *Table 7.1* highlighting the differences. Italy is characterized by the highest share of vehicles in the *Medium* class compared to the other countries, whereas Norway by the highest *Large* share; Portugal *Small* and *Medium* values are close, while Germany is similar to Italy, but with a more even distribution among the three classes.

Vehicle Share

	Small	Medium	Large
DE	34.9	50.0	15.0
IT	24.4	68.6	7.0
NO	17.9	61.4	20.6
PT	44.6	45.3	10.1

Table 7.1: Vehicle share of the selected European countries.

The simulations of the three cases, with vehicles all in one class, have been compared in terms of total annual energy derived from the mobility profiles. In *Figure 7.5* the results are reported representing for each country the default vehicle share and the three extreme cases. In addition, in *Table 7.2* the relative errors in the annual energy demand, with respect to the one computed for the default vehicle share, are reported. Limited differences are visible between the only *Small* and *Medium* scenarios, instead for *Large* vehicles the annual energy increases considerably. These differences on annual energy are similar to those on power consumption reported in *Figure 5.15*.

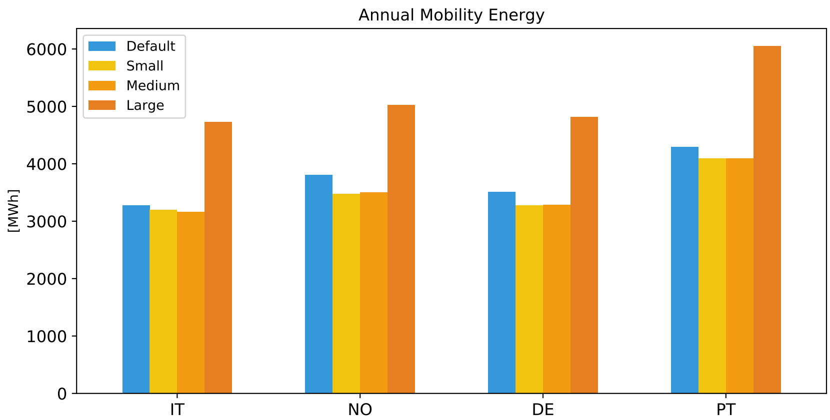

Figure 7.5: Annual mobility energy for the simulated cases in four selected European countries.

Relative Error

	Small	Medium	Large
DE	-6.6	-6.4	37.3
IT	-2.4	-3.6	44.1
NO	-8.7	-8.1	31.9
PT	-4.6	-4.6	41.0

Table 7.2: Relative error in the annual mobility energy for the three extreme cases with respect to the default values.

Two conclusions can be understood from *Figure 7.5* and *Table 7.2*:

- A change of the vehicle share in the direction of *Small* or *Medium* vehicles does not impact significantly on the annual energy demand since these are already the today prevailing classes; whereas the *Large* class produces an increase of around 40% of the mobility demand, slightly lower for Norway which is already characterized by 21% of *Large* vehicles.
- The detailed vehicle share divided into three groups produces a value of annual energy which is less than 10% higher than the one of the only *Small* or *Medium* scenario. This highlights the limited utility of characterizing in detail the vehicle fleet of all the countries, as in the previous analysis for Italy with six reference vehicles. One single medium reference vehicle could be considered as representative of the most diffused class, accepting a low error. This is valid also for Norway even though it is characterized by a higher *Large* share, thus only more important percentages in this class have an impact on the annual energy.

7.3. Geographical resolution

The data used to update the modelling of Italy comes from regional databases, except for functioning windows. This deeper geographical characterization has been previously set aside, aggregating input data according to population share to model the whole country. In this section this further detailing is tested, mobility demand for each Italian region is computed verifying the quality of the modelling with aggregated mobility data. The petrol consumption of single region simulations is additionally compared with the disaggregation, on population basis, of the country output. Finally, a coherence check is added comparing the aggregation of inputs, used with Italy model, and the aggregation of outputs, simulated with single region representation.

	RAMP night share [%]	UnipolSai night share [%]
Abruzzo	4.15	4.17
Basilicata	4.10	4.11
Calabria	4.01	3.66
Campania	4.06	4.56
Emilia	4.23	4.05
Friuli	4.18	3.14
Lazio	3.99	4.69
Liguria	4.17	4.10
Lombardia	4.25	4.19
Marche	4.04	4.42
Molise	4.15	3.83
Piemonte	4.21	4.55
Puglia	4.06	4.60
Sardegna	3.95	3.47
Sicilia	3.81	4.69
Toscana	4.03	4.12
Trentino	4.24	3.17
Umbria	3.99	4.35
Valle d'Aosta	4.23	3.75
Veneto	4.23	3.63

Table 7.3: Night share of driven kilometers: *UnipolSai* and RAMP-mobility percentages.

The generated mobility demand is firstly compared with data of *UnipolSai* [38] collected through car black boxes and the percentage of night-driven distance, specific for each region, is considered. RAMP-mobility simulated trips are collected in a trip report and post-processed to estimate the travels starting in the time window *23pm - 6am*; their distance is compared with the simulated annual kilometers to determine the share of night kilometers.

In *Table 7.3* measured and simulated percentages are reported; RAMP-mobility shares aligning with the reference data, hence representing well the mobility demand of night hours. Additionally, the same assessment used for Italian mobility in *Section 6.1* through petrol consumption is adopted to compare regional outputs with measured data. Regional oil bulletins [27] and number of vehicles [30] are considered to determine the regional yearly petrol consumption. For most of the regions differences are limited, with simulated annual values close to measured ones; exceptions are found for *Lombardia* and *Campania* for which significant gaps are highlighted in *Figure 7.6*.

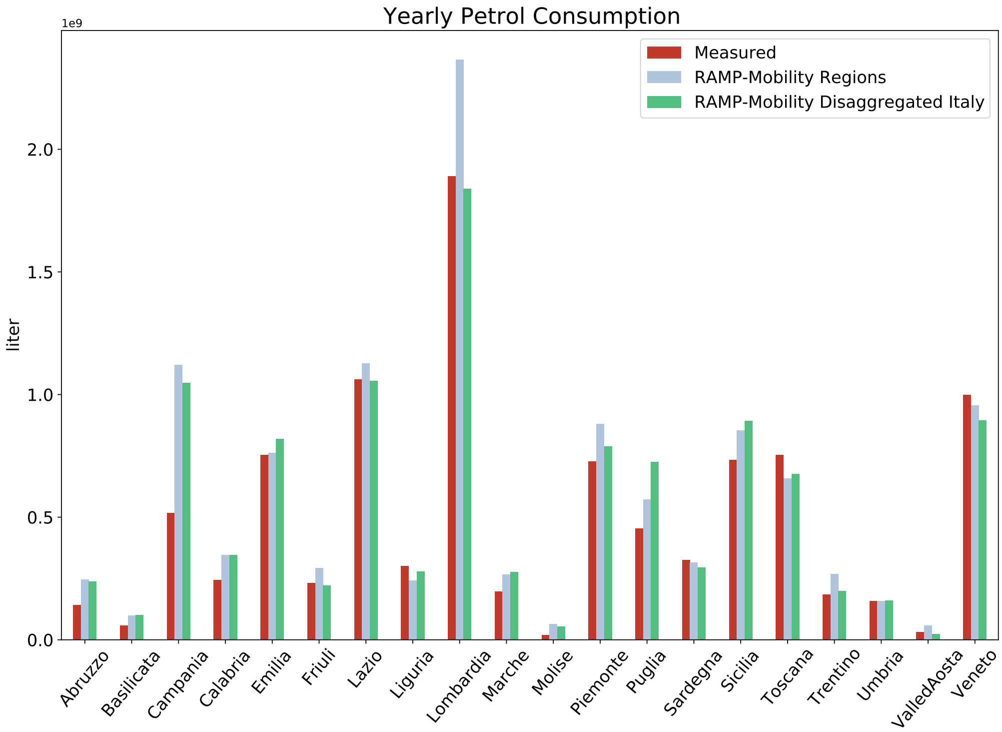

Figure 7.6: Comparison of annual petrol consumption between measured data, estimated ones from regional RAMP-mobility simulations, and distributed national consumption.

Furthermore, the national value of consumed liters has been disaggregated on population basis to compute regional consumption, and the results are showed in *Figure 7.6* together with measured data, derived from oil bulletin, and simulated regional consumption. Globally the two methods used to characterize regional mobility lead to similar values, meaning that the allocation based on population weights does not affect the breakdown. The approach here introduced produces regional results which are closer to the measured consumption for some regions as *Lombardia*, while for others the regional simulations represent a better estimation. Globally the disaggregation leads to a lower relative error of about 12%, while the single region simulations has a higher total error of 19% mainly due to *Lombardia* and *Campania*.

The regional values have been aggregated according to the Italian electricity market zones [12] for both the estimation approaches. Six groups are identified and reported in *Table 7.4* comparing with measured data through relative percentage errors. Except for *Sud* and *Centro Sud*, which have a consistent error around 40% with both approaches, all the other zones are characterized by a more precise estimation allowing for errors lower than 20%. Some zones are represented better by the redistributed values as for *Nord* and *Centro Nord*, whereas regions simulations of *Sud* and *Sicilia* are closer to reference consumption.

	Measured [$*10^6$ **liter**]	**RAMP** [$*10^6$ **liter**]	**Error** [%]	**RAMP Disaggregated** [$*10^6$ **liter**]	**Error Disaggregated** [%]
Nord	5117	5827	13.9	5063	-1.1
Centro Nord	1108	1083	-2.0	1113	0.4
Centro Sud	1720	2493	45.0	2340	36.0
Sud	775	1079	39.3	1226	58.3
Sicilia	733	855	16.6	893	21.8
Sardegna	326	314	-3.6	295	-9.6

Table 7.4: Comparison of annual petrol consumption aggregated in electricity market zones.

To determine the utility of regional simulations another comparison is carried on in terms of annual transport energy demand. National value obtained with aggregated regional inputs, and the one derived from aggregated regional outputs, considering population weights, are reported in *Table 7.5*. Even though stochasticity could influence significantly the differences of the results, no effect is highlighted with a relative error lower than 1%. Also the comparison based on the generated mobility time-series brings to the same consideration.

	Energy [MWh]	Weighted Energy [MWh]
Italy aggregated		3549.2
Italy	3518.9	
Error [%]	-	0.86

Table 7.5: Comparison between mobility demand of Italy and the weighted demand derived from the regional characterization.

In conclusion, a limited utility of the regional characterization of RAMP-mobility to simulate mobility demand specific for each region is found. Considering national inputs obtained from regional databases, and aggregating them to describe the whole Italian population is enough detailed, and the mobility demand is as accurate as the aggregated regional profiles, without requiring regional simulations. Higher differences could be obtained considering region-specific temperatures instead of adopting the same thermal demand for all of them. This aspect has not been analyzed since no region-specific temperature time-series have been found to characterize the regions. However, the weight of the thermal energy on the annual demand has been computed and the percentage is lower than 8%, hence no major differences are expected.

8 | Conclusions and future work

This thesis makes a step forward in the realistic modelling of electric mobility, improving the already existing RAMP-mobility framework with structural enhancements and resolution assessments. The result is a model able to produce mobility and charging time-series with a physical detail of consumption, based on the vehicle dynamic simulator VCAM. Moreover, important insights about the directions to be followed to improve modelling aspects of this framework have been provided. The refinement of the outputs of this model is crucial in the context of energy system modelling to provide realistic demand curves, which are necessary for reliable future scenarios. Since electric mobility is still in an early adoption phase, profiles of EVs power demand are highly uncertain, but the rapid development of this technology makes them essential for capacity planning and operational optimization.

Aside of this main outcome, there is the successful development of a *real-world* Driving Cycle Generator, able to produce realistic driving patterns from a standard reference cycle. This tool goes beyond the modelling of electric mobility, is independent from RAMP-mobility model, and is flexible in the choice of the reference cycle. The methodology followed in its development could be applied to produce synthetic driving cycles from key trip parameters for consumption estimations or even emission evaluations.

Conclusions

The research question that guided this thesis work is focused on the impact of a more accurate vehicle consumption estimation specific for the single trip. It has been assessed that introducing VCAM and solving RAMP-mobility inconsistencies, cause an increase of the annual transport demand of 27% with respect to the selected *Reference* case. The quality of the model is clearly increased by these enhancement, and the result highlights the influence of vehicle consumption estimation on the output mobility time-series. Seen the significant variation of simulated annual energy, the vehicle power consumption should be carefully modelled. Since measured mobility profiles are not available, this approach can not be assessed compared to *real-world* time-series, but only with aggregated mobility data. The improved RAMP-mobility is validated with a satisfying degree of accuracy thanks to the introduction of different charging functions in relations to the day-type, and to the tuning of their parameters. This is translated into mobility and charging profiles which, given reliable input data, can replicate effectively the *real-world* profiles.

An additional analysis has been made to exploit the potentiality of the model in the analysis of grid connection time-series. This additional output has great importance in the assessment of Vehicle to Grid potentialities, since it gives an estimation of the connected battery capacity exploitable for flexibility purposes. This future concept could become a great opportunity in the context of energy transition, but energy models have to consider V2G dependence from mobility behaviours to exploit its strengths. User behaviour has been proven to highly affect the connections more than infrastructure availability, even though the modelling of charging probability functions is covered by high uncertainty. Infrastructure availability and charging user choices are a great challenge since these aspects are not easily measurable. This work has highlighted the importance they have in shaping the charging profiles, influencing the accuracy of the output, and making hard to assess the quality of the model.

Another important conclusion is related to the model resolution and the impact of a more detailed geographical characterization. The generated regional profiles represent well the aggregated mobility demand, however the difference with the disaggregated national output are not appreciable. For this reason, the country detail is a good trade-off between output accuracy and the required characterization of input data. Concerning the detail of the input data, in particular those of the vehicle fleet composition, an important modelling insight is derived from its analysis. To the careful analysis of the vehicles in a country, aiming to increase the number of reference segments, does not correspond an equal increment of the output precision. Seen the actual vehicle share, which is mainly composed by smaller and medium vehicles, describing a country with only one reference medium vehicle does not produce significant differences, with errors lower than 5%. For future vehicle fleets even if the share of larger vehicles will increase, two reference vehicles will be enough, since the consumption of different segments can be clustered in only two main groups.

Future work

Different possible improvements can be introduced as future development of the model described in this thesis. These are mainly related to the charging module as some limits have been found during its analysis. Modelling the probability of finding a ready charging point when parking is at the same time complex and impactful; moreover it is not implemented with a country specificity. Efforts to improve this feature would be certainly necessary in future works, and a country detailing should be considered adopting a common method to determine these probabilities from empirical sources. Even the user charging behaviour, proved to be incisive on connections and V2G applicability, has not been largely investigated; the reduction of its uncertainty should be a priority in next improvements. These probabilities strongly affects the quality assessment of charging time-series, which is also limited by the lack of accessible data. Lastly, input dataset has been proven to have great leverage on RAMP-mobility output, thus finding reliable sources and refining their processing enriches the quality of the outputs.

Bibliography

[1] A. Alemanno, D. Fiorello, A. Martino, G. Pasaoglu, G. Scarcella, C. Thiel, C. Zubaryeva, and E. Commission. *Driving and parking patterns of European car drivers a mobility survey.* Technical report, Joint Research Centre (JRC). Institute for Energy and Transport., 2012. URL https://publications.jrc.ec.europa.eu/repository/handle/JRC77079.

[2] M. André. *The ARTEMIS European driving cycles for measuring car pollutant emissions.* *Science of the Total Environment*, 334-335:73–84, Dec. 2004. doi: 10.1016/j.scitotenv.2004.04.070.

[3] A. Beltramo, A. Julea, N. Refa, Y. Drossinos, C. Thiel, and S. Quoilin. *Using electric vehicles as flexible resource in power systems: a case study in the Netherlands*. *International Conference on the European Energy Market, EEM*, July 2017. doi: 10.1109/EEM.2017.7982006.

[4] BloombergNEF and Transport & Environment. *Hitting the EV Inflection Point*. Technical report, BNEF, May 2021. URL https://www.transportenvironment.org/wp-content/uploads/2021/08/2021_05_05_Electric_vehicle_price_parity_and_adoption_in_Europe_Final.pdf.

[5] A. Deschênes, J. Gaudreault, K. Rioux-Paradis, and C. Redmont. *Predicting electric vehicle consumption: A hybrid physical-empirical model*. *World Electric Vehicle Journal*, 11, Mar. 2020. doi: 10.3390/WEVJ11010002.

[6] Directorate-General for Mobility and Transport . *EU Transport in figures*. Technical Report URL https://op.europa.eu/s/t8OP, European Commission, Apr. 2020.

[7] European Commission. *The European Green Deal (COM(2019) 640 final)*, Dec. 2019. Accessed: 2021-11-7.

[8] European Commission. *European Green Deal: Commission proposes transformation of EU economy and society to meet climate ambitions*, July 2021.

[9] Eurostat. *Average passenger car occupancy for urban mobility on all days*. URL

https://ec.europa.eu/eurostat/statistics-explained/index.php?title=File:Average_passenger_car_occupancy_for_urban_mobility_on_all_days_fig_3.PNG&oldid=514830#filelinks, 2021. Accessed: 2021-10-31.

[10] D. Fischer, A. Harbrecht, A. Surmann, and R. McKenna. *Electric vehicles' impacts on residential electric local profiles – A stochastic modelling approach considering socio-economic, behavioural and spatial factors*. *Applied Energy*, 233-234:644–658, Jan. 2019. doi: 10.1016/j.apenergy.2018.10.010.

[11] C. Gaete-Morales, H. Kramer, W.-P. Schill, and A. Zerrahn. *An open tool for creating battery-electric vehicle time series from empirical data – emobpy*. *Scientific Data*, Apr. 2020. doi: 10.1038/s41597-021-00932-9. URL http://arxiv.org/abs/2005.02765#.

[12] Gestore Mercati Energetici. *Italian electricity market zones*. URL https://www.mercatoelettrico.org/it/mercati/mercatoelettrico/Zone.aspx, 2021. Accessed: 2021-10-31.

[13] Q. Gong, S. Midlam-Mohler, V. Marano, G. Rizzoni, and Y. Guezennec. *Statistical analysis of PHEV fleet data*. *2010 IEEE Vehicle Power and Propulsion Conference, VPPC 2010*, 2010. doi: 10.1109/VPPC.2010.5729224.

[14] G. Gruosso. *Analysis of impact of electrical vehicle charging on low voltage power grid*. *2016 International Conference on Electrical Systems for Aircraft, Railway, Ship Propulsion and Road Vehicles and International Transportation Electrification Conference, ESARS-ITEC 2016*, Feb. 2017. doi: 10.1109/ESARS-ITEC.2016.7841365.

[15] Istituto Nazionale di Statistica (Istat). *Database: attività quotidiane, punti orari*. URL http://dati.istat.it/Index.aspx?QueryId=24538, 2011. Accessed: 2021-11-7.

[16] Istituto Nazionale di Statistica (Istat). *Database: popolazione per condizione professionale*. URL http://dati.istat.it/index.aspx?queryid=42536, 2011. Accessed: 2021-11-7.

[17] Istituto Nazionale di Statistica (Istat). *Nota tecnica per l'elaborazione della matrice delle distanze tra comuni*. URL https://www.istat.it/it/files/2015/04/Nota_Tecnica_MatriciDistanza.pdf, 2011.

[18] Istituto Nazionale di Statistica (Istat). *Matrici di contiguità, distanza e pendolarismo*. URL https://www.istat.it/it/archivio/157423, 2011. Accessed: 2021-11-7.

[19] Istituto Nazionale di Statistica (Istat). *Principali statistiche geografiche sui comuni:*

superfici delle unità amministrative. URL https://www.istat.it/it/archivio/156224, 2011. Accessed: 2021-11-7.

[20] Istituto Superiore di Formazione e Ricerca per i Trasporti. *17° Rapporto sulla mobilità degli italiani tra gestione del presente e strategie per il futuro.* Technical Report URL https://www.isfort.it/wp-content/uploads/2020/12/RapportoMobilita2020.pdf, ISFORT, Nov. 2020.

[21] A. Lajunen. *Energy Efficiency and Performance of Cabin Thermal Management in Electric Vehicles. SAE Technical Paper*, Mar. 2017. doi: 10.4271/2017-01-0192.

[22] F. Lombardi, S. Balderrama, S. Quoilin, and E. Colombo. *Generating high-resolution multi-energy load profiles for remote areas with an open-source stochastic model. Energy*, 177:433–444, June 2019. doi: 10.1016/j.energy.2019.04.097.

[23] P. D. Lund, J. Lindgren, J. Mikkola, and J. Salpakari. *Review of energy system flexibility measures to enable high levels of variable renewable electricity. Renewable and Sustainable Energy Reviews*, 45:785–807, 2015. doi: 10.1016/j.rser.2015.01.057. Accessed: 2021-11-7.

[24] A. Mangipinto. *Development of electric vehicles load profiles for sector coupling in European energy system models.* Master's thesis, Politecnico di Milano, 2020.

[25] A. Mangipinto, F. Lombardi, F. Sanvito, S. Quoilin, M. Pavičević, and E. Colombo. *RAMP-mobility: time series of electric vehicle consumption and charging strategies for all European countries.* doi: 10.13140/RG.2.2.29560.26880, 2020. *Unpublished.*

[26] Ministero delle Infrastrutture e dei Trasporti (MIT). *Parco circolante dei veicoli.* URL http://dati.mit.gov.it/catalog/dataset/dataset-parco-circolante-dei-veicoli, 2019. Accessed: 2021-11-7.

[27] Ministero dello Sviluppo Economico. *Bollettino petrolifero.* URL https://dgsaie.mise.gov.it/bollettino-petrolifero?anno=2019, 2019. Accessed: 2021-11-7.

[28] Mobilität in Deutschland. URL https://www.bmvi.de/SharedDocs/DE/Artikel/G/mobilitaet-in-deutschland.html, 2021. Accessed: 2021-10-27.

[29] M. Muratori, M. J. Moran, E. Serra, and G. Rizzoni. *Highly-resolved modeling of personal transportation energy consumption in the United States. Energy*, 58:168–177, Sept. 2013. doi: 10.1016/j.energy.2013.02.055.

[30] U. Nazionale and R. A. Esteri. *UNRAE Book 2020 Analisi del mercato autoveicoli*

in Italia, XXI edizione. Technical Report URL http://www.unrae.it/files/Book%20UNRAE%202020_6038d7a7636d9.pdf, UNRAE, Feb. 2021.

[31] G. Pasaoglu, C. Thiel, A. Martino, A. Zubaryeva, D. Fiorello, L. Zani, and E. Commission. *Projections for electric vehicle load profiles in Europe based on travel survey data.* Technical report, Joint Research Centre (JRC). Institute for Energy and Transport., 2013. URL https://publications.jrc.ec.europa.eu/repository/handle/JRC82307.

[32] M. Pavičević, A. Mangipinto, W. Nijs, F. Lombardi, K. Kavvadias, J. P. J. Navarro, E. Colombo, and S. Quoilin. *The potential of sector coupling in future European energy systems: Soft linking between the Dispa-SET and JRC-EU-TIMES models. Applied Energy*, 267, June 2020. doi: 10.1016/j.apenergy.2020.115100.

[33] F. Sanvito, M. Ferraro, R. Mereu, and E. Colombo. *Improving electric vehicle consumption representation in energy system modelling: the impact of temperature in all European countries.* doi: 10.13140/RG.2.2.26325.35046, Oct. 2020. *Unpublished.*

[34] Transport & Environment. *Car CO_2 standards.* Technical Report URL https://www.transportenvironment.org/wp-content/uploads/2021/08/TE-cars-CO2-reaction-2-pager-2.pdf, European Federation for Transport and Environment, Aug. 2021.

[35] Transport & Environment. *Break-up with combustion engines.* Technical Report URL https://www.transportenvironment.org/discover/hitting-the-ev-inflection-point/, European Federation for Transport and Environment, May 2021.

[36] M. Tutuianu, P. Bonnel, B. Ciuffo, T. Haniu, N. Ichikawa, A. Marotta, J. Pavlovic, and H. Steven. *Development of the World-wide harmonized Light duty Test Cycle (WLTC) and a possible pathway for its introduction in the European legislation. Transportation Research Part D: Transport and Environment*, 40:61–75, Oct. 2015. doi: 10.1016/j.trd.2015.07.011.

[37] K. Uddin, M. Dubarry, and M. B. Glick. *The viability of vehicle-to-grid operations from a battery technology and policy perspective. Energy Policy*, 113:342–347, Feb. 2018. doi: 10.1016/j.enpol.2017.11.015.

[38] UnipolSai. *Presentati i risultati dell'Osservatorio UnipolSai sulle abitudini di guida degli italiani nel 2018 in seguito all'analisi dei dati delle scatole nere installate nelle automobili.* URL https://www.unipolsai.com/sites/corporate/

files/pages_related_documents/cs_osservatorio-unipolsai-2019.pdf, Dec. 2019. Accessed: 2021-11-7.

[39] N. Wulff, F. Miorelli, H. C. Gils, and P. Jochem. *Vehicle energy consumption in python (Vencopy): Presenting and demonstrating an open-source tool to calculate electric vehicle charging flexibility*. *Energies*, 14, July 2021. doi: 10.3390/en14144349.

[40] Y. Yang, Q. Zhang, Z. Wang, Z. Chen, and X. Cai. *Markov chain-based approach of the driving cycle development for electric vehicle application*. *Energy Procedia*, 152: 502–507, 2018. doi: 10.1016/j.egypro.2018.09.201.

List of Figures

List of Tables

Acronyms

AC+PTC Air Conditioning and Positive Temperature Coefficient heater.

ATUS The American Time Use Survey.

BEV battery electric vehicle.

BTMS Battery Thermal Management System.

COP coefficient of performance.

CP charging point.

DC Driving Cycles.

EV Electric Vehicle.

GHG greenhouse gasses.

GIS Geographic Information System.

HEV hybrid electric vehicle.

HP+PTC Heat Pump and Positive Temperature Coefficient heater.

HVAC Heating Ventilation and Air Conditioning.

ICEV internal combustion engine vehicle.

ISFORT Istituto Superiore di Formazione e Ricerca per i Trasporti.

JRC Joint Research Center.

LF Load Factor.

MID Mobilität in Deutschland.

MISE Ministero dello Sviluppo Economico.

MIT Ministero delle Infrastrutture e dei Trasporti.

MPE Mean Perecentage Error.

NRMSE Normalized Root Mean Square Error.

PHEV plug in hybrid electric vehicle.

RES renewable energy sources.

SOC State of Charge.

SUV Sport-Utility-Vehicle.

TPM Transition Probability Matrix.

TSO Transmission System Operator.

TV-tab Time-Velocity tables.

UNRAE Unione Nazionale Rappresentanti Autoveicoli Esteri.

US Urban Share.

USA United States of America.

V2G Vehicle to Grid.

VCAM Vehicle Consumption Assessment Model.

VencoPy Vehicle Energy Consumption in Python.

WLTC World-wide harmonized Light duty Test Cycle.

A | Appendix

Thermal model comparison

The key improvement introduced in RAMP-mobility with this work is the coupling with the vehicle dynamic simulator VCAM for the estimation of consumption values. In this section a comparison between the thermal consumption module of VCAM and the one of *Emobpy* [11] is presented. The literature analysis performed on both models in *Section 2.2* inspired this comparison with the goal of selecting the most physically accurate. While the dynamic module is similar in both models, the thermal load estimation follows different approaches. VCAM uses external temperature functions determined by Lajunen [21], instead *Emobpy* performs a heat balance to estimate heat transfer mechanisms between the vehicle cabin and the environment. *Emobpy* implementation seems more complex and potentially more precise seen the introduction of variables related to vehicle characteristics, as the cabin volume, and driving cycle features, as the actual velocity for the computation of heat transfer coefficients. A first assessment has been performed to investigate the effective impact of this two external variables which are reported in *Figure A.1*.

(a) Cabin volume dependence

(b) Driving speed dependence

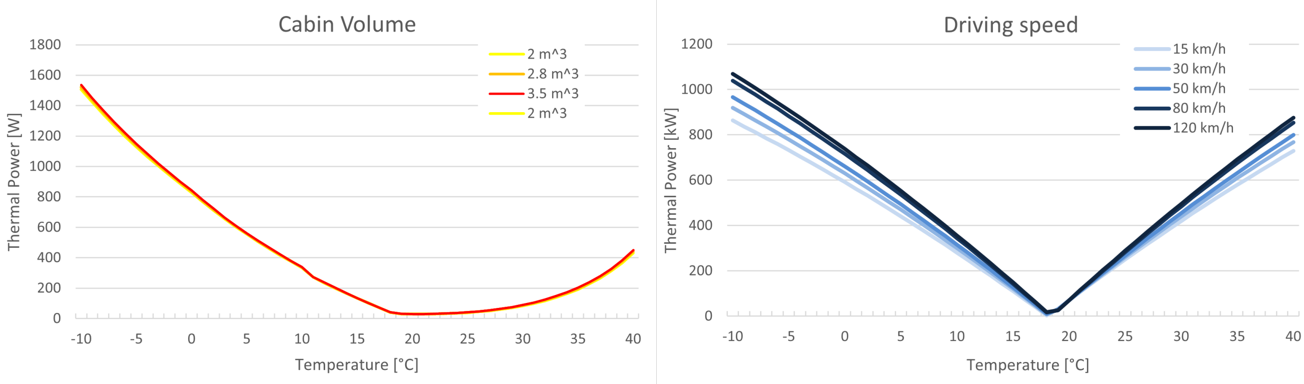

Figure A.1: Variables dependence of *Emobpy* thermal model.

As showed in *Figure A.1a* the influence of the cabin volume on the thermal demand required to the HVAC system is negligible in the range of possible vehicle dimensions, set between 2 and 3.5 m^3. Even the impact of driving cycles, displayed in *Figure A.1b* for different speed profiles, increase the thermal demand of only small fractions in a range of typical temperatures. Consumption are higher at larger average velocities due to the enhanced thermal interaction with the environment, however the rise is significant only for extreme values, uncommon for Italian temperature variations.

A comparison between the HVAC electric demand of the two models is reported in *Figure A.2*. It must be noticed that VCAM models the thermal dependence of the COP for a Heat Pump and Positive Temperature Coefficient heater using a function proposed by Lajunen [21], whereas *Emobpy* considers a constant value of COP set at 2.

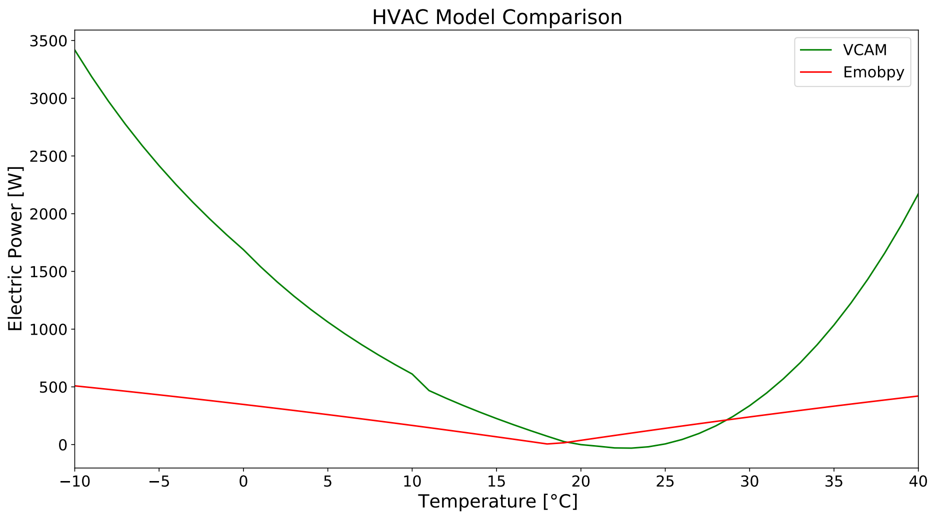

Figure A.2: Electric demand of HVAC system as function of external temperature.

The plot shows consistent differences between the two models: *Emobpy* estimates much lower consumption for most of temperature values and is generally less sensible to temperature variation than VCAM. Despite *Emobpy* model seems to have a more physically based structure considering also dependencies on variables other then external temperature, its final estimation is considered less accurate, since the thermal demand is underestimated and no quality assessments have been reported in literature. Since the thermal consumption represent only few percentage of the total annual energy demand, and the refinement of the thermal model brought only marginal changes of the consumption values, the potential improvement of the thermal module is neglected and the original VCAM structure is adopted.

B | Appendix

In this Appendix the detailed description of the improvements introduced to RAMP-mobility is reported. These are grouped considering the type of change, the assumptions introduced and the section of the model in which they are implemented. In *Data changes* the updated input variables and formal corrections are highlighted, whereas *country input file changes* refers to new variables introduced in the country definition section. *Model changes* instead deals with structural improvements which affect the core of the model.

Model	Tag	Data Changes	Country Input file changes	Model changes	Assumptions	Where
Reference	0	Free time occasional_use, pop_share_Italia.csv, vehicle_share_Italia.csv, windows_Italia.csv	Extending the number of Appliances (car segments)		occasional use: WD = 1/5 (20%) WE = WD+15% (35%)	Database + Input_file
	1	Deleting d_min from input file	Using directly v_mean as input data***	• Rename t_func as t_avg * • Introducing variability on t_avg (App.r_t_avg)** • Rename App.vel as v_mean • Splitting variability on v_mean in positive (r_v_pos) and negative (r_v_neg) instead of single r_v****	*New data from regional analysis **Assumed 20% ***New data from v_mean regional analysis ****New data from regional analysis	Input_file + Core + Stochastic process
	2	Daily driven distance: d_tot.csv*	• New file of d_tot already includes the breakdown of distance between functioning windows • Deleting trips distribution by time and perc_usage variables		*New data from regional analysis	Database + Input_file
Mobility behaviour	2 A	Setting variability of functioning windows only on free time*		• Inverting the sequence of the appliances • Main FW as complementary of Free Time ones • Increasing probability of picking central Free Time window in case of 3 of them** • Anticipating FW definition before occasional use	*Assigned value: 10% linked to custom windows definition **Assumed: 60% (central), 20% (lateral)	Input_file + Stochastic process
	2 B			• Adding App.kind to track the type ('ft' or 'm') • Introducing miss_dist local variable to transfer not-driven km to the next appliance		Input_file + Core + Stochastic process
Trip specific cons.	2 C	• Include JRC-Consumption tables in database • Include T-V distribution table in database** • Set Power randomicity (r_P) to 5%***		• Add import_tables module to import data required* • Compute trip average speed (v local variable) from table with trip lenght (duration local variable) • Compute App.power using imported table	*New data computed externally applying JRC function to DCs **Tables region-specific ***Value obtained from the analysis of power tables	Database + Stochastic process
Vehicle cons. model	V C A M	Include VCAM-Consumption tables in database		• Compute App.power using VCAM imported table • Change temperature correction function to include VCAM thermal model		Stochastic process + Post process

Figure B.1: Detailed explanation of the improvements introduced in RAMP-mobility for each Italian step.

Model	Tag	Data Changes	Country Input file	Model changes	Assumptions	Where
Reference	0	Free time occasional_use			occasioanl use: WD = 1/5 (20%) - WE = WD+15% (35%)	Input_file
	1	Deleting d_min from input file	Using directly v_mean as input data***	• Rename t_func as t_avg * • Introducing variability on t_avg (App.r_t_avg)** • Rename App.vel as v_mean • Splitting variability on v_mean in positive (r_v_pos) and negative (r_v_neg) instead of single r_v****	*Kept values from JRC **Assumed 20% ***Computed as d_min/t_func (JRC data) ****Assuming the same variability of Italy case (data anlysis)	Input_file + Core + Stochastic process
	2	Daily driven distance: d_tot.csv*			*Rescaling JRC according to the ratio computed for the Italy case	Database
Mobility behaviour	2 A	Setting variability of functioning windows only on free time*		• Inverting the sequence of the appliances • Main FW as complementary of FT ones • Increasing probability of picking central FT window in case of 3 of them** • Anticipating FW definition before occasional_use	*Default value: 20% **Assumed: 60% (central), 20% (lateral)	Input_file + Stochastic process
	2 B			• Adding App.kind to track the type ('ft' or 'm') • Introducing miss_dist local variable to transfer not-driven km to the next appliance		Input_file + Core + Stochastic process
Trip specific cons.	2 C	• Include JRC-Consumption tables in database • Include T-V distribution table in database** • Set Power randomicity (r_P) to 5%***		• Add import_tables module to import data required* • Compute trip average speed (v local variable) from table with trip lenght (duration local variable) • Compute App.power using imported table	*New data computed externally applying JRC function to DCs **Tables for IT extended to all countries ***Value obtianed from the analysis of power tables	Database + Stochastic process
Vehicle cons. model	V C A M	Include VCAM-Consumption tables in database		• Compute App.power using VCAM imported table • Change temperature correction function to include VCAM thermal model		Stochastic process + Post process

t_avg: Mean trip duration, required as input, previously called t_func

d_min: Mean trip lenght, used only in default RAMP for computing the first guess speed used to estimate driving time from driving distance (input), cancelled from step 1

v_mean: first guess trip velocity (only for converting daily km into daily min), previously computed as d_min/t_func inside the process, previously called App.vel

r_t_avg: variability on t_avg, added

Figure B.2: Detailed explanation of the improvements introduced in RAMP-mobility for each Dutch step.